EUROPEAN COMMISSION
Directorate General Joint Research Centre
Institute for Energy - HFR Unit

19 March 2007
D(07)5909

TECHNICAL MEMORANDUM
HFR / 07 / 4827

HFR-EU1:
Irradiation Progress Report

Cycles 06-08, 06-09, 06-10, 07-01

Project n° 337.1

rev. A

Alain Marmier

	Author	Verified by	Approved by Unit Head
Name	A. Marmier	M. A. Fütterer	R. May
Date	19.3.07	19.3.07	23/03/07
Signature			

Distribution List

JRC-IE	**NRG**
K. Törrönen R. May M. A. Fütterer R. Moss A. Marmier G. Berg	S. de Groot H. G. Thesingh P. J. M. Thijssen J. A. Waard F. J. Wijtsma
JRC-IE Electronic Archive – 1 copy	
HTR-F Fuel Database – 1 copy	
HTR-F/F1 Partners • S. Lansiart, M. Phélip CEA Cadarache, France • H. Werner Forschungszentrum Jülich, Germany • E. Toscano JRC-ITU, Germany • T. Abram Nexia Solutions, United Kingdom • P. Guillermier AREVA NP, France • K. Bakker NRG, The Netherlands	
Tsinghua University, Beijing, China **Institute for Nuclear Energy Technology (INET)** • Chunhe Tang	

Revision	Date	Description
A	19.03.07	initial release
B		
C		

Abstract

The HFR-EU1 irradiation in the HFR Petten is performed in cooperation between the European FP5 project consortium HTR-F/F1 and the Institute of Nuclear Energy Technology (INET) of the Tsinghua University in Beijing, China.

The experiment consists in irradiating 3 German AVR pebbles and 2 INET pebbles to very high burn-up with fission gas release measurements. After irradiation, the pebbles will undergo post-irradiation examination and safety testing in the KÜFA facility at JRC.ITU.

This is the first progress report on this experiment combining the results of the first four irradiation cycles.

The irradiation had started on 30 September 2006.

This document contains the history of the irradiation including significant special events, nuclear data as well as temperature and fission gas release measurements.

Some preliminary attempts were made to analyze and interpret the information obtained so far.

Further reports will contain a summary of the irradiation, new neutronics predictions including fission gas birth rates and burn-up, as well as more detailed analysis of experimental results.

Further data is available to INET and the HTR-F/F1 partners on request.

Table of Contents

1 Irradiation History

30.09.06 17:10 start cycle 06-08 **1 scrams and 3 gas samples taken per capsule** **29.10.06 09:00 end cycle 06-08**
02.11.06 4:40 start cycle 06-09 **2 scram and 3 gas samples taken per capsule** **29.11.06 08:00 end cycle 06-09**
2.12.06 18:40 start cycle 06-10 **No scram and 3 gas samples taken per capsule** **31.12.06 08:00 end cycle 06-10**
3.01.07 06:40 start cycle 07-01 **No scram but power perturbation from 14:20 to 17:10 on the 15th of January** **3 gas samples taken per capsule** **31.01.07 08:00 end cycle 07-01**

1.1 Special events

After the first start of the experiment, it was initially foreseen to keep it for one week at the lowest possible temperature to remove humidity from the sample holder. A long scram (06.10.06 20:10 to 11.10.06 4:50) prolonged this situation until 16.10.06 12:30. Unlike HFR-EU1bis, for which initial temperatures (meaning temperatures while purging containments with pure Helium at BOI) were matching the target conditions, HFR-EU1 had much lower initial temperatures due to two phenomena:

- Steel emissivity was not implemented in the thermal calculation model,
- HFR conversion from HEU to LEU caused a local thermal flux decrease.

To reach nominal temperatures, significant Ne fractions had to be used quite early thus decreasing the margin for burn-up compensation that would be required later in the irradiation.

Due to the HFR buckling and the high position of the Chinese capsule, the expected initial fission power of the highest INET pebble was also decreased. Therefore, the temperatures of the INET pebbles were very different and could not both reach the target values. To compensate this situation, it was decided in agreement with INET to increase the nominal temperature of the lower INET pebble to 940°C (instead of 900°C).

1.2 Modifications of installation

After three reactor cycles, a significant burn-up was reached leading to fission power depletion that could not be compensated anymore by increasing the Ne fraction in the gas. Therefore, from the 4th cycle, the experiment moved from position H2 to H4 where the thermal flux is approx. 15% higher.

2 Nuclear Data

The information in this section is extracted from post-cycle nuclear calculations of the HFR core.

2.1 Fluxes, fluences and other data cycle 06-08

Cycle 06-08, position H2, **orientation North**, data from [1]

	Flux Middle of Cycle $[10^{18}\ m^{-2}s^{-1}]$	Flux Cycle Averaged $[10^{18}\ m^{-2}s^{-1}]$	Fluence $[10^{24}\ m^{-2}]$
Φ_1 1) Fast	0.404	0.409	0.856
Φ_2 1)	0.602	0.612	1.281
Φ_3 1)	0.59	0.602	1.260
Φ_4 1) Thermal	0.685	0.697	1.459
$\Phi_{E > 1\ MeV}$		0.359	0.752
$\Phi_{E > 0.1\ MeV}$		0.777	1.627
Φ_{Co}		0.614	1.285
Φ_{Fe}		0.378	0.791
Φ_{Ni}		0.388	0.812

1) energy groups with boundaries: $0.82\times10^6 – 0.00553\times10^6 – 0.625 – 0$ eV

Table 1: Neutron fluxes and fluences cycle 06-08

full power days	24.23
dpa (stainless steel)	0.11
gamma heating in small graphite samples [W/g]	1.19 middle of cycle

Table 2: Nuclear characteristics for cycle 06-08

2.2 Fluxes, fluences and other data cycle 06-09

Cycle 06-09, position H2, **orientation South**, data from [2]

	Flux Middle of Cycle $[10^{18}\ m^{-2}s^{-1}]$	Flux Cycle Averaged $[10^{18}\ m^{-2}s^{-1}]$	Fluence $[10^{24}\ m^{-2}]$
Φ_1 [1)] Fast	0.416	0.412	0.957
Φ_2 [1)]	0.62	0.615	1.428
Φ_3 [1)]	0.608	0.603	1.400
Φ_4 [1)] Thermal	0.696	0.691	1.605
$\Phi_{E > 1\ MeV}$		0.391	0.908
$\Phi_{E > 0.1\ MeV}$		0.782	1.816
Φ_{Co}		0.609	1.414
Φ_{Fe}		0.381	0.885
Φ_{Ni}		0.39	0.906

[1)]energy groups with boundaries: $0.82\times10^6 - 0.00553\times10^6 - 0.625 - 0$ eV

Table 3: Neutron fluxes and fluences cycle 06-09

full power days	26.88
dpa (stainless steel)	1.21
gamma heating in small graphite samples [W/g]	1.19 middle of cycle

Table 4: Nuclear characteristics for cycle 06-09

2.3 Fluxes, fluences and other data cycle 06-10

Cycle 06-10, position H2, **orientation North**, data from [3]

	Flux Middle of Cycle $[10^{18}\ m^{-2}s^{-1}]$	Flux Cycle Averaged $[10^{18}\ m^{-2}s^{-1}]$	Fluence $[10^{24}\ m^{-2}]$
Φ_1 1) Fast	0.432	0.443	1.093
Φ_2 1)	0.643	0.645	1.592
Φ_3 1)	0.63	0.632	1.560
Φ_4 1) Thermal	0.727	0.73	1.801
$\Phi_{E > 1\ MeV}$		0.38	0.938
$\Phi_{E > 0.1\ MeV}$		0.821	2.026
Φ_{Co}		0.643	1.587
Φ_{Fe}		0.4	0.987
Φ_{Ni}		0.41	1.012

1) energy groups with boundaries: $0.82\times10^6 - 0.00553\times10^6 - 0.625 - 0$ eV

Table 5: Neutron fluxes and fluences cycle 06-10

full power days	28.56
dpa (stainless steel)	0.137
gamma heating in small graphite samples [W/g]	1.24 middle of cycle

Table 6: Nuclear characteristics for cycle 06-10

2.4 Fluxes, fluences and other data cycle 07-01

Cycle 06-10, position H4, **orientation South**, data from [4]

	Flux Middle of Cycle $[10^{18}\ m^{-2}s^{-1}]$	Flux Cycle Averaged $[10^{18}\ m^{-2}s^{-1}]$	Fluence $[10^{24}\ m^{-2}]$
Φ_1 1) Fast	0.695	0.695	1.674
Φ_2 1)	0.926	0.927	2.233
Φ_3 1)	0.872	0.873	2.103
Φ_4 1) Thermal	0.863	0.866	2.086
$\Phi_{E > 1\ MeV}$		0.612	1.474
$\Phi_{E > 0.1\ MeV}$		1.266	3.050
Φ_{Co}		0.778	1.874
Φ_{Fe}		0.661	1.592
Φ_{Ni}		0.677	1.631

1)energy groups with boundaries: $0.82\times10^6 - 0.00553\times10^6 - 0.625 - 0$ eV

Table 7: Neutron fluxes and fluences cycle 07-01

full power days	27.88
dpa (stainless steel)	0.213
gamma heating in small graphite samples [W/g]	2.07 middle of cycle

Table 8: Nuclear characteristics for cycle 07-01

2.5 Analysis of nuclear data

From [1)]energy groups with boundaries: $0.82\times10^{6} - 0.00553\times10^{6} - 0.625 - 0$ eV

Table 1 through Table 8 the following can be concluded:

Cycle	efpd	Φ_1 [1)]	Φ_2 [1)]	Φ_3 [1)]	Φ_4 [1)]	Fluence_4	$\text{Fluence}_{E>0.1\,MeV}$
	[days]	Cycle Averaged [10^{18} $m^{-2}s^{-1}$]				[10^{24} m^{-2}]	
2006-08	24.23	0.409	0.612	0.602	0.697	1.459	1.627
2006-09	26.88	0.412	0.615	0.603	0.691	1.605	1.816
2006-10	28.56	0.443	0.645	0.632	0.73	1.801	2.026
2007-01	27.88	0.695	0.927	0.873	0.866	2.086	3.050
variation between 06-08 and 06-10	15.16%	41.15%	33.98%	31.04%	20.21%	30.05%	46.66%

[1)]energy groups with boundaries: $0.82\times10^{6} - 0.00553\times10^{6} - 0.625 - 0$ eV

Table 9: Comparison of fluxes and fluences

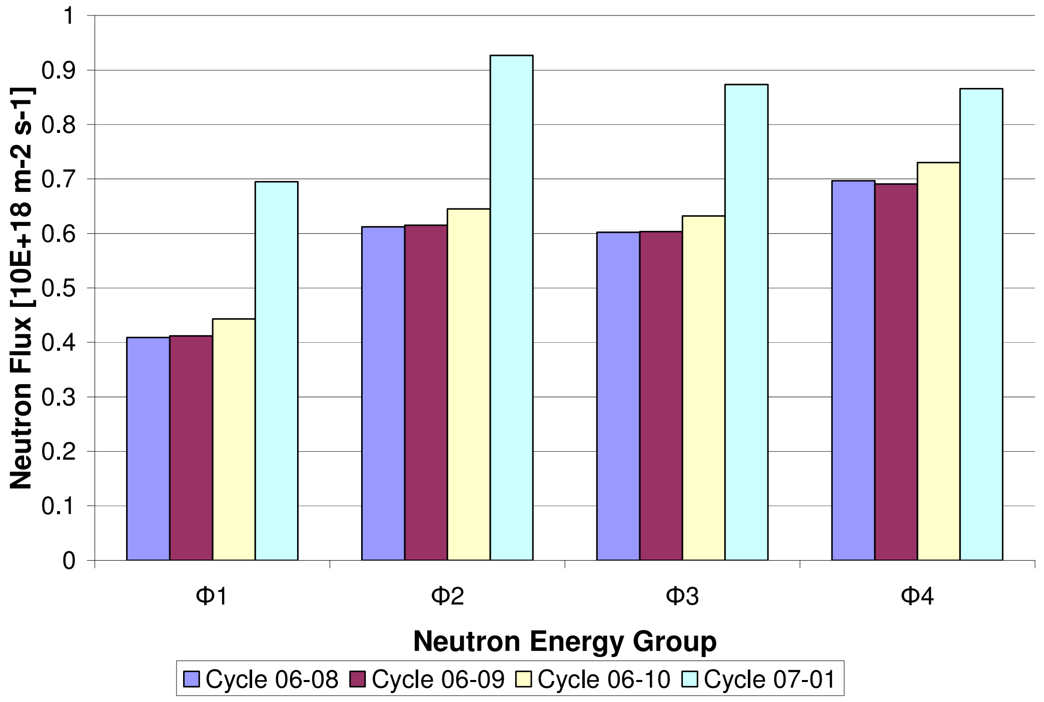

Energy groups with boundaries: $0.82\times10^6 - 0.00553\times10^6 - 0.625 - 0$ eV

Figure 1: Comparison of neutron fluxes per reactor cycle

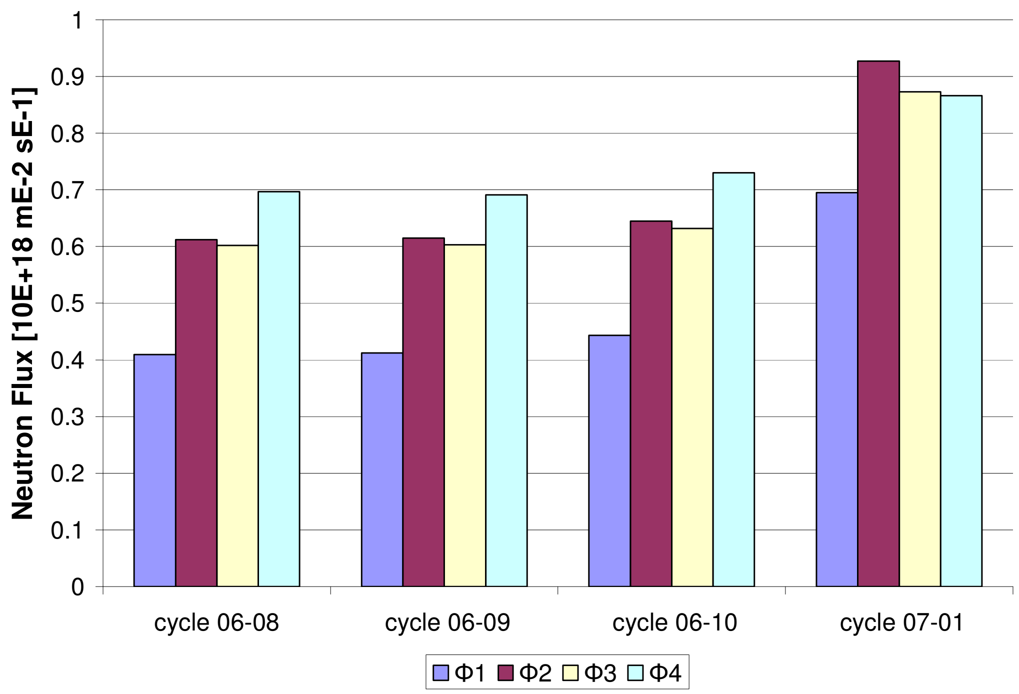

Energy groups with boundaries: $0.82\times10^6 - 0.00553\times10^6 - 0.625 - 0$ eV

Figure 2: Comparison of neutron fluxes per energy group

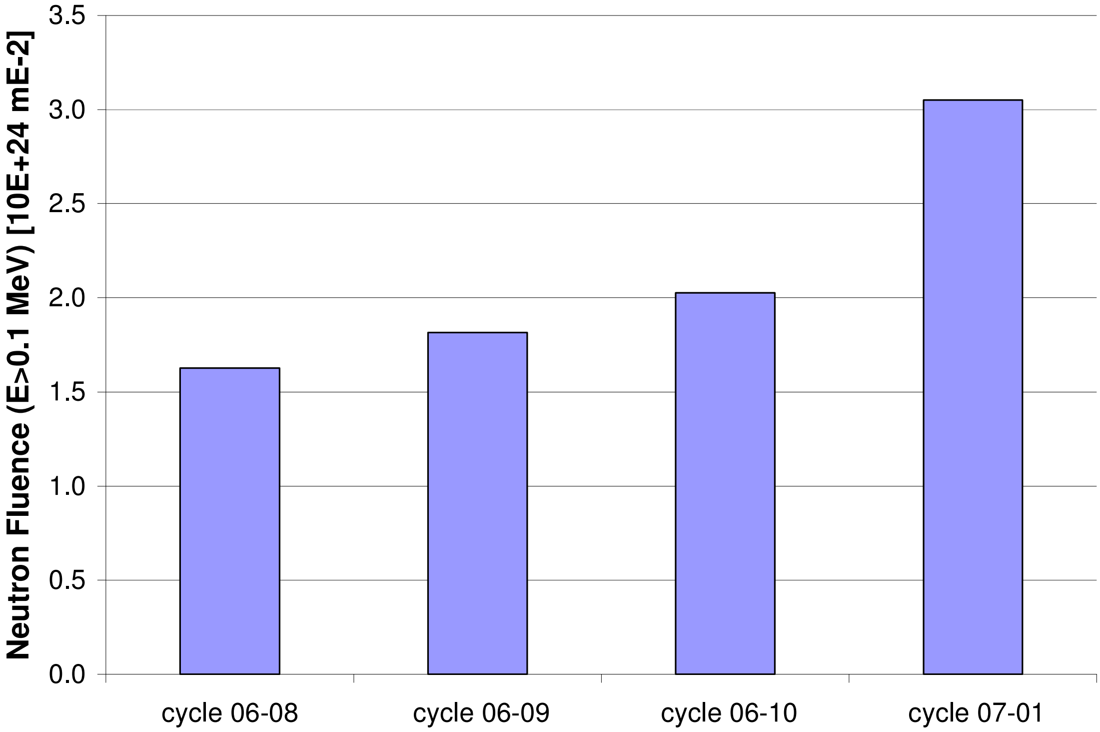

Figure 3: Comparison of fast fluences (E > 0.1 MeV) per reactor cycle

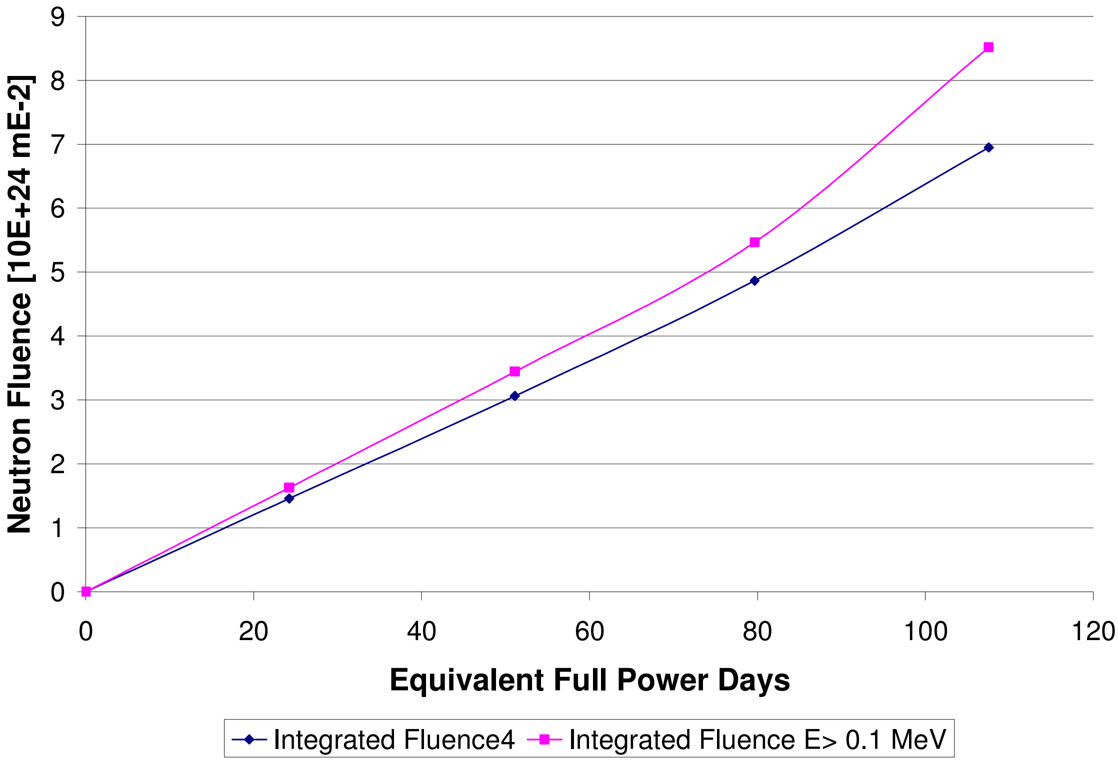

Figure 4: Incremental increase in fast (upper curve) and thermal fluence per reactor cycle

3 Reactor Power and Control Rod Positions

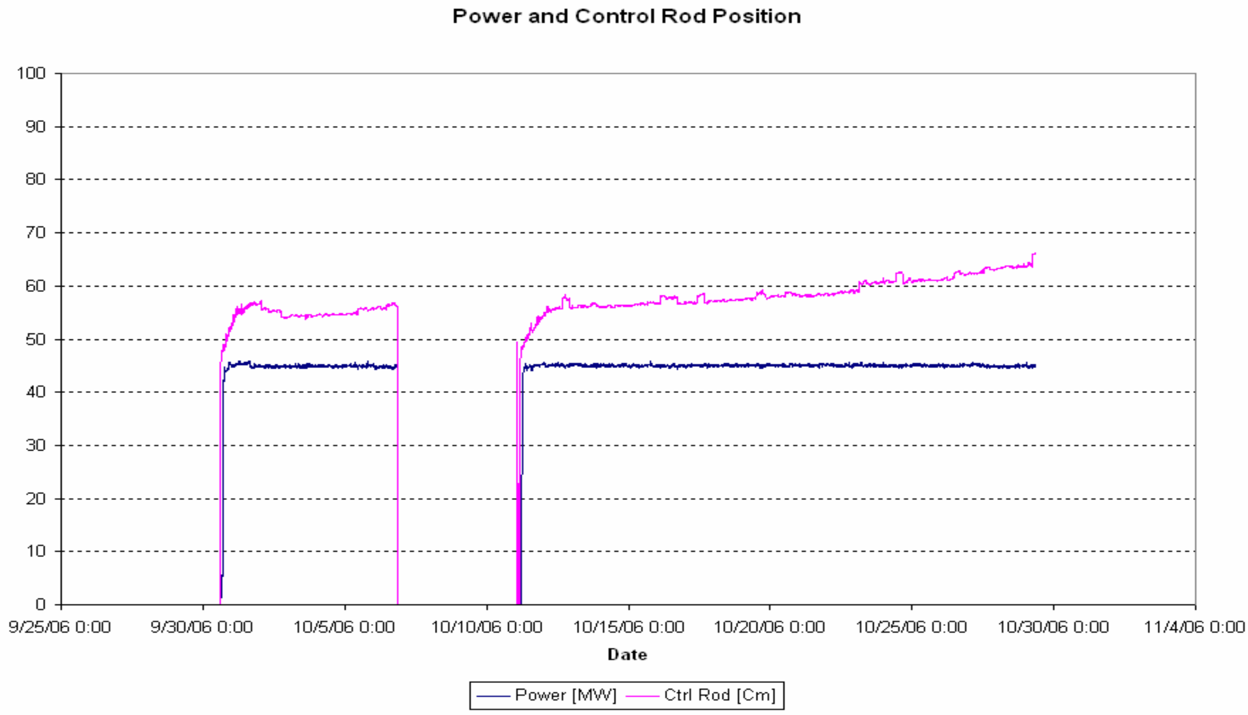

Figure 5: Reactor Power/Control Rod position cycle 06-08

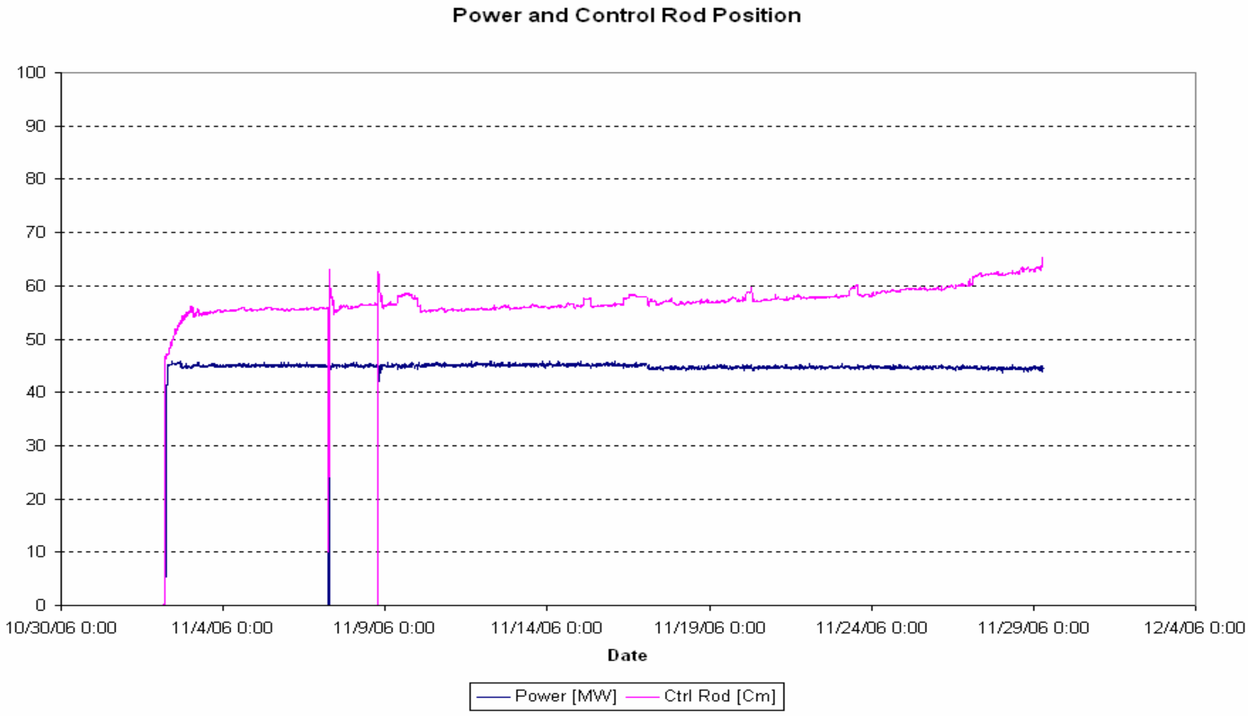

Figure 6: Reactor Power/Control Rod position cycle 06-09

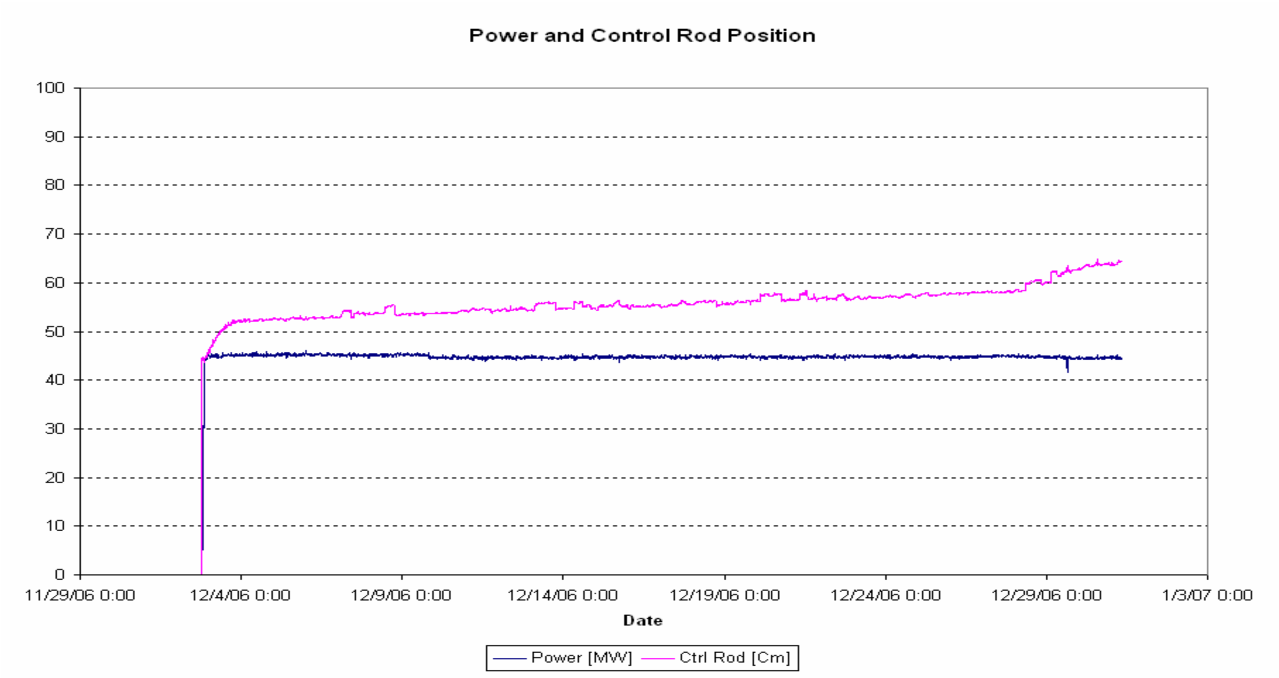

Figure 7: Reactor Power/Control Rod position cycle 06-10

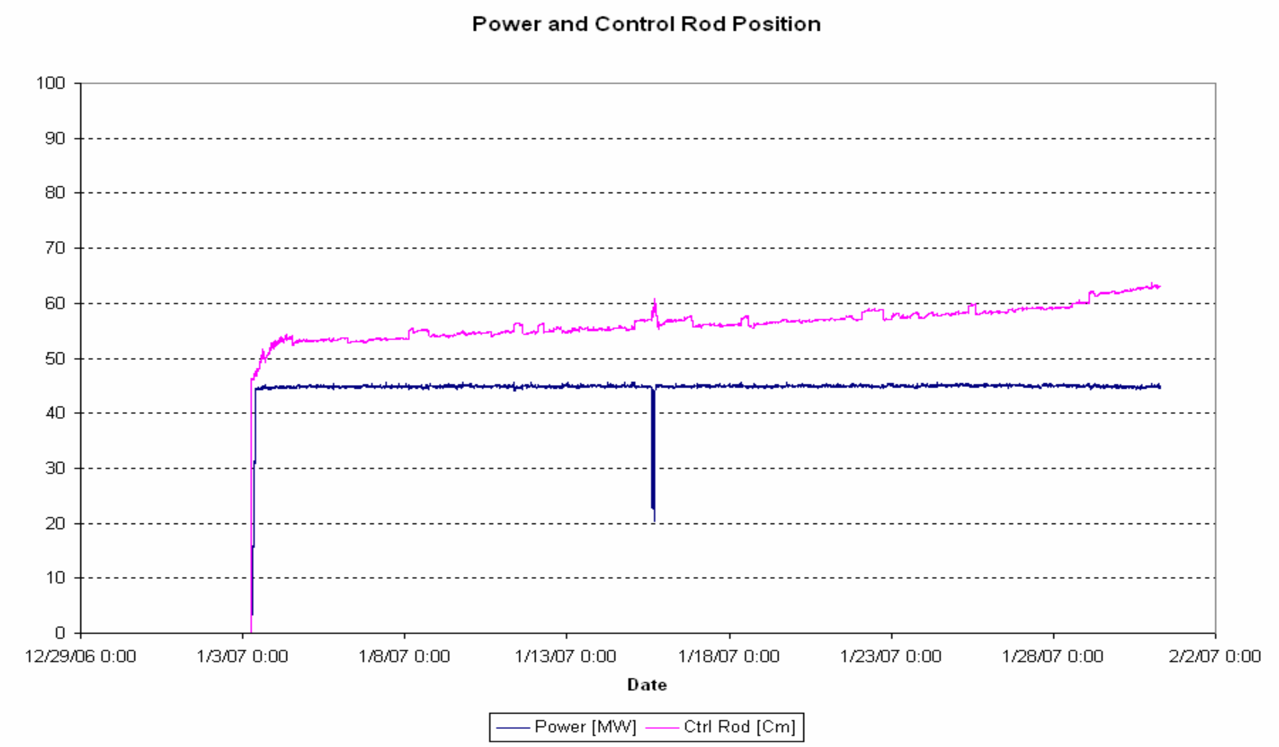

Figure 8: Reactor Power/Control Rod position cycle 07-01

4 Vertical Displacement Unit (VDU) Position

The VDU was not used since the beginning of the irradiation and was held in the lowest possible position. The very small measured differences are artifacts related to the data acquisition system.

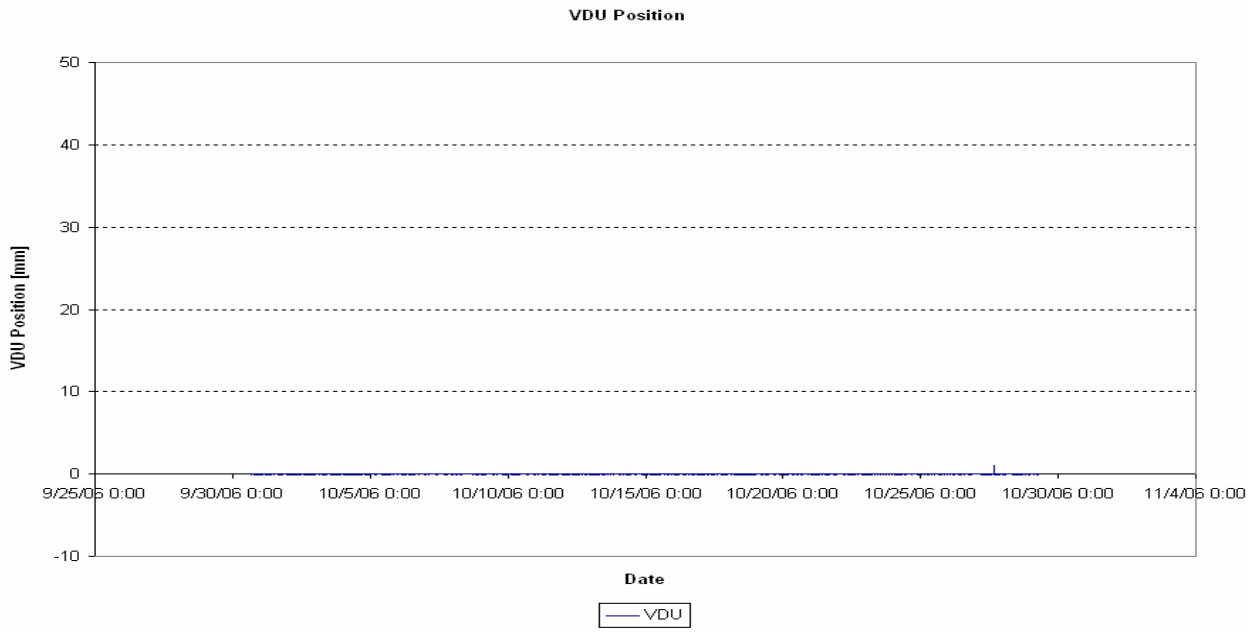

Figure 9: VDU position cycle 06-08

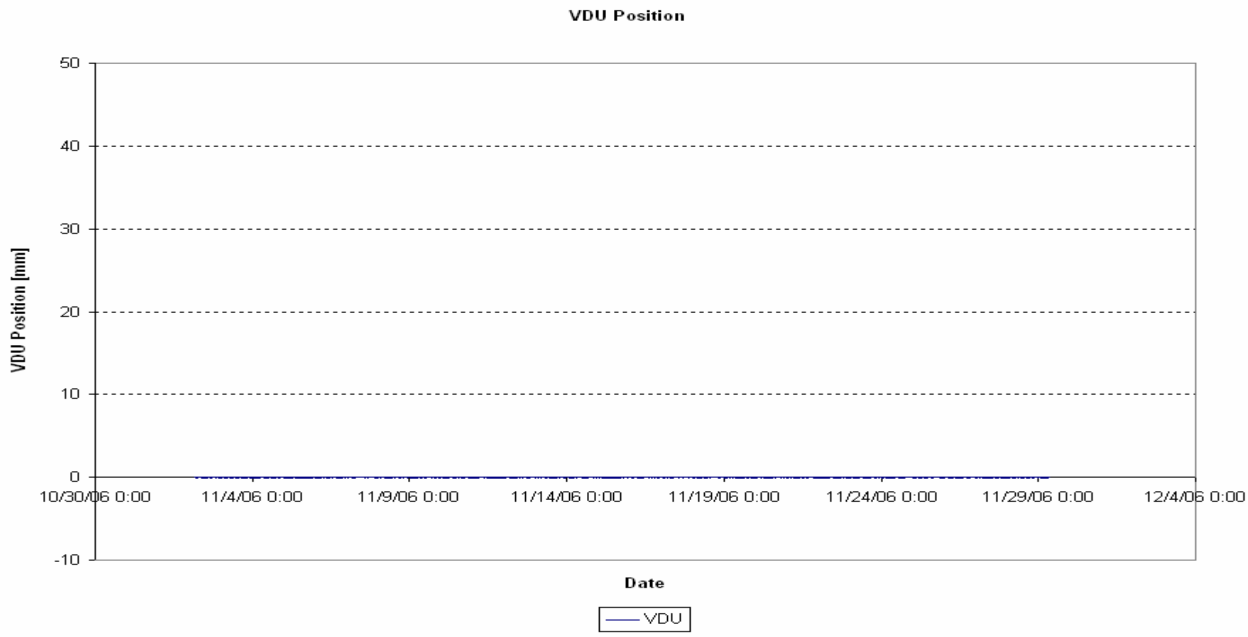

Figure 10: VDU position cycle 06-09

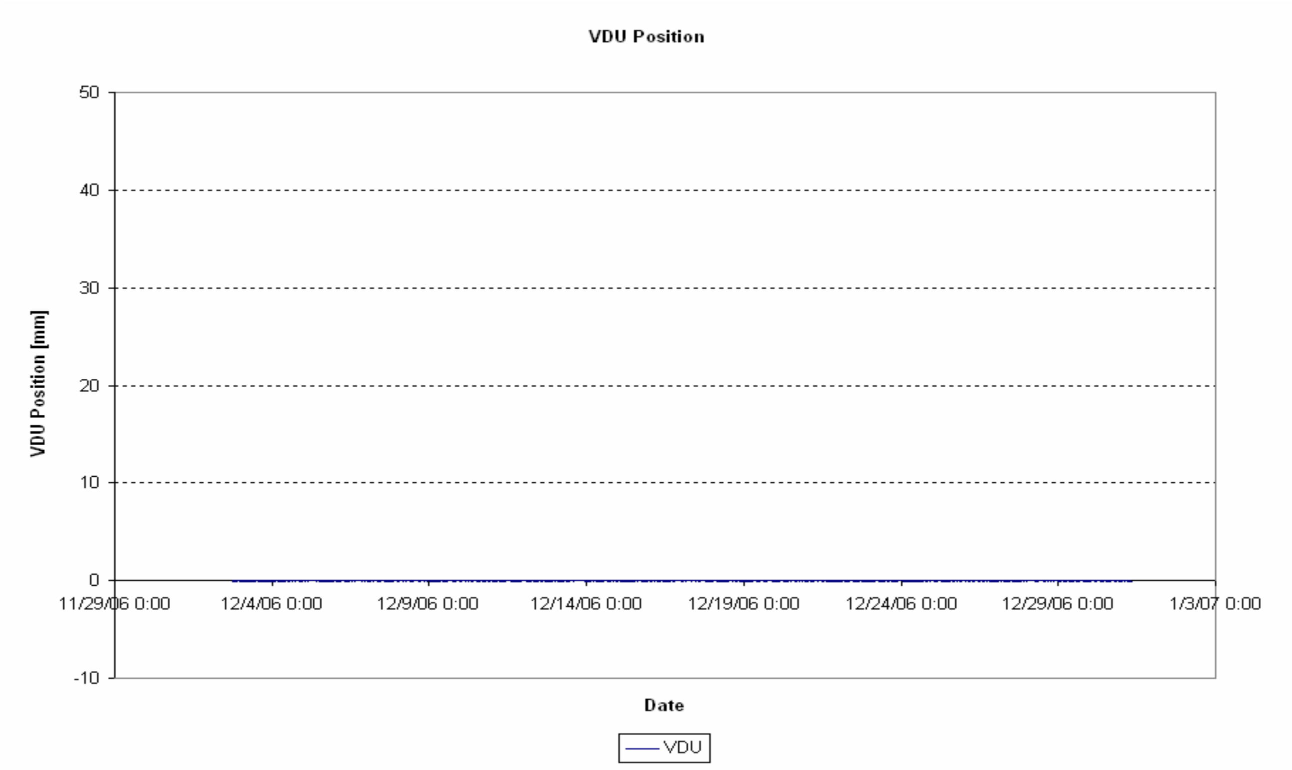

Figure 11: VDU position cycle 06-10

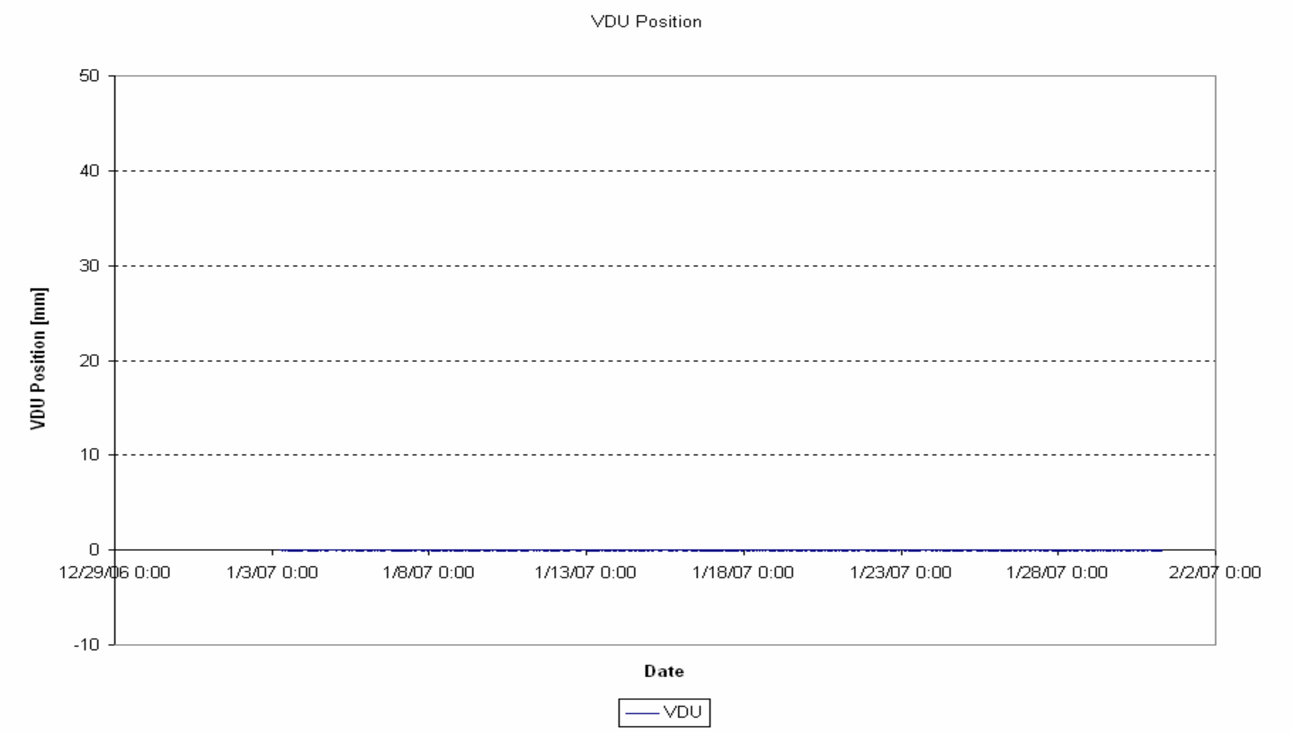

Figure 12: VDU position cycle 07-01

5 Counter Readings in Gas Panel (SPI.1-NaI and SPI.2-NaI)

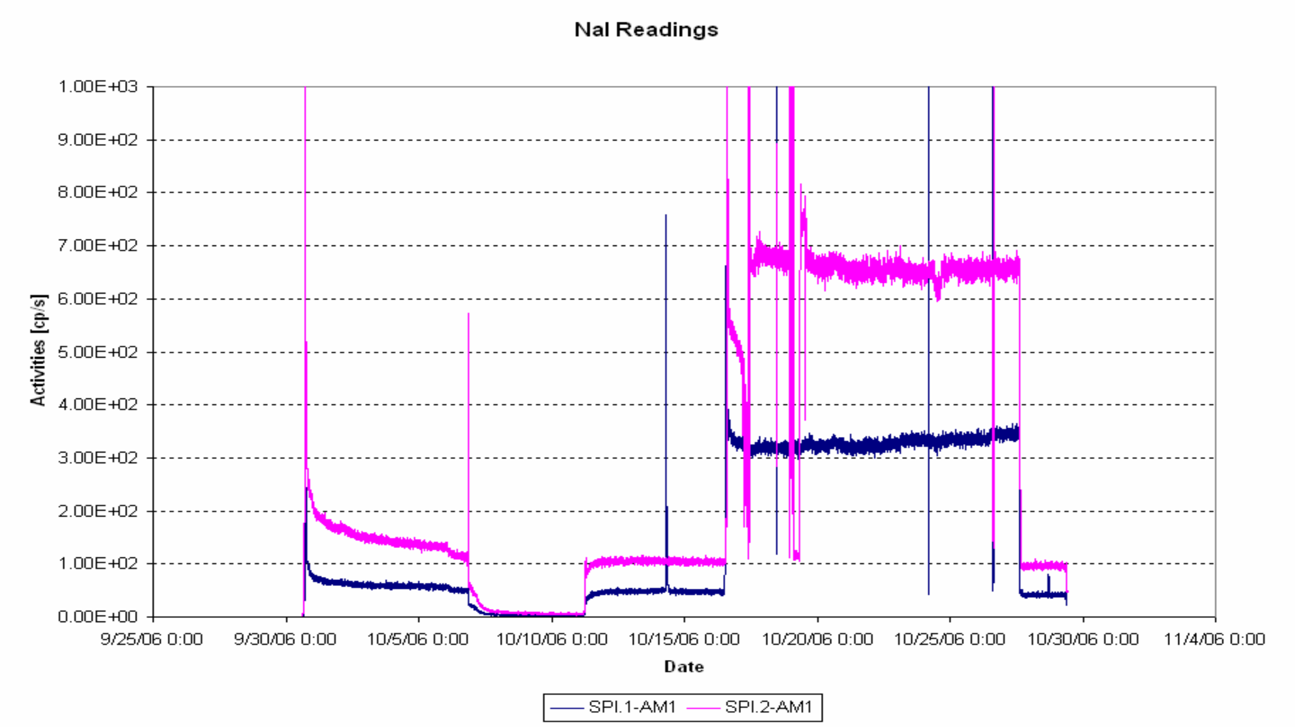

Figure 13: NaI readings cycle 06-08

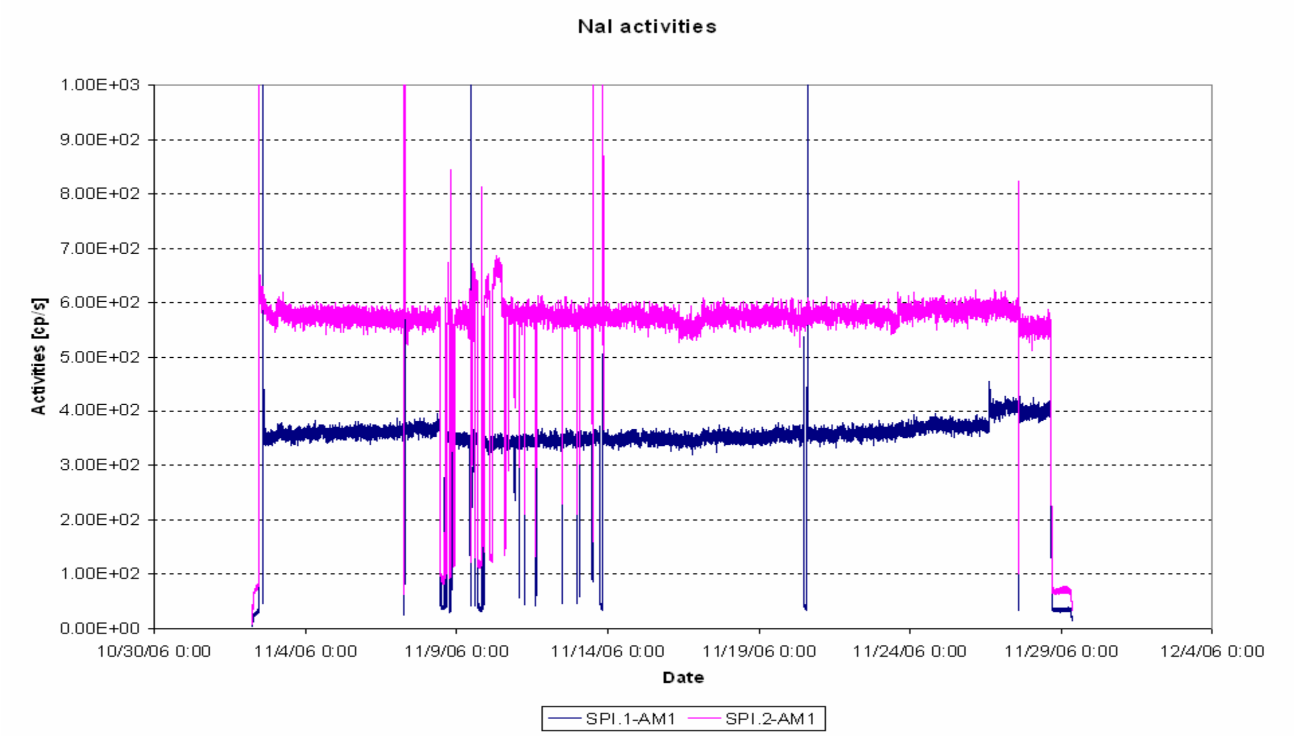

Figure 14: NaI readings cycle 06-09

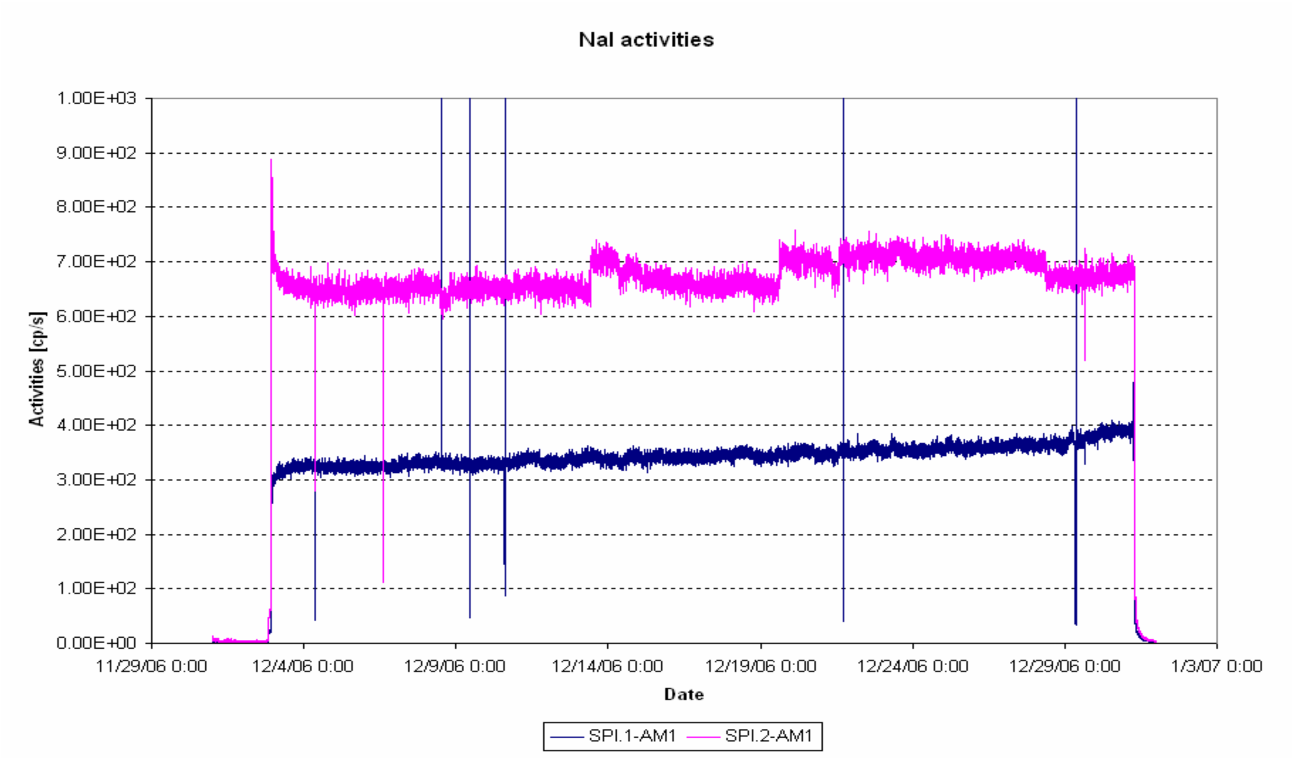

Figure 15: NaI readings cycle 06-10

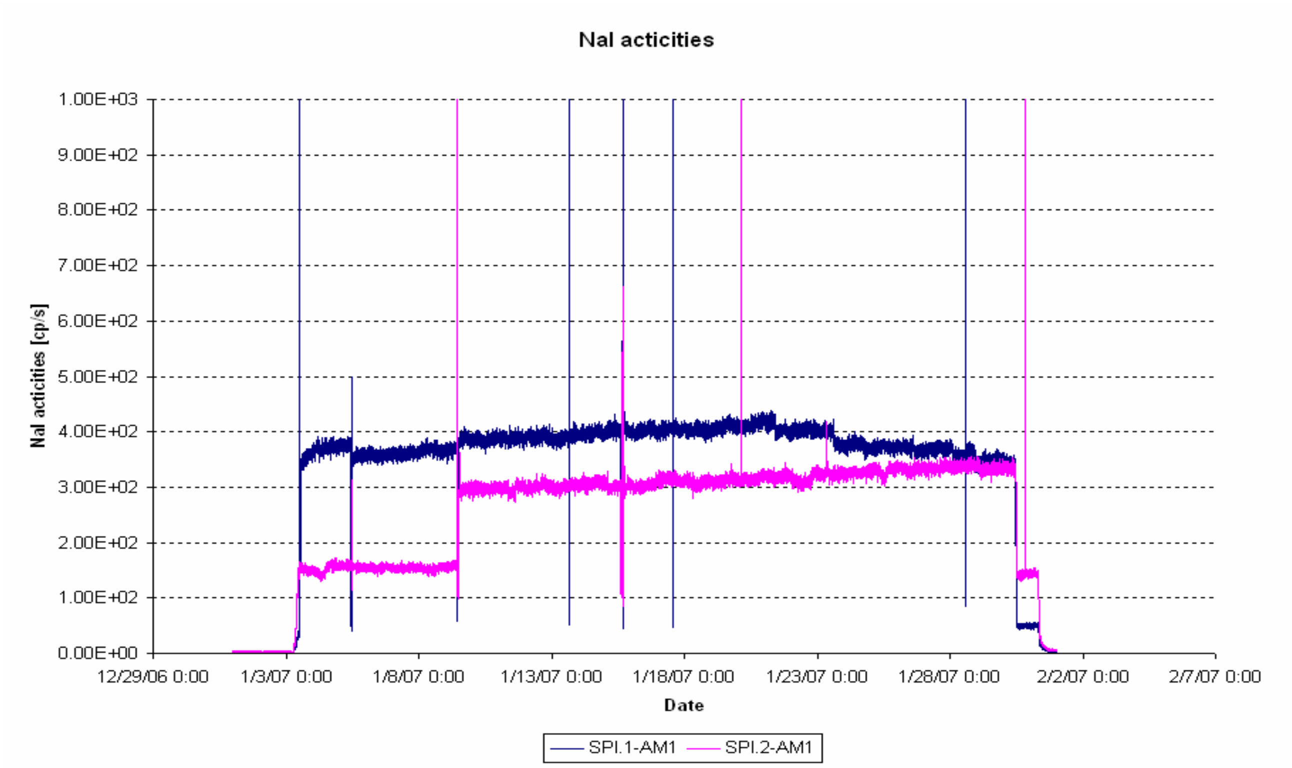

Figure 16: NaI readings cycle 07-01

6 Temperature Measurements

After the first 4 cycles, 3 out of 34 thermocouples provided wrong information. These thermocouples are all situated in high temperature areas between two pebbles.

Location	TC #	
Top Graphite INET	1, 2	
INET.1	3, 4, 5, 6	
Graphite between INET.1 and INET.2	7, 8	TC-08 some erratic values since cycle 06-09
INET.2	9, 10, 11, 12	
Bottom Graphite INET	13, 14	
Top Graphite INET	**15**, 16	TC-15 erroneous values since 10.11.2006 TC-16 some erratic values in cycle 06-09
AVR.1	17, 18, 19, 20	
Graphite between AVR.1 and AVR.2	**21, 22**	TC-21 showed hysteresis in cycle 06-10 TC-22 some erratic values since cycle 06-08 Both went completely down in cycle 07-01
AVR.2	23, 24, 25, 26	TC-25 some erratic values since cycle 06-08 TC-26 some erratic values since cycle 06-10
Graphite between AVR.2 and AVR.3	27, 28	TC-27 some erratic values since cycle 06-09
AVR.3	29, 30, 31, 32	
Bottom Graphite AVR	33, 34	TC-33 and 34 some erratic values since cycles 06-09 and 06-10

Table 10: Location of thermocouples

Malfunction is indicated in **bold red**

TC nr	axial position [mm]	Cycle 06-08	Cycle 06-09	Cycle 06-10	Cycle 07-01	Cycle 06-08	Cycle 06-09	Cycle 06-10	Cycle 07-01
1	236.24	**803.8**	**823.9**	**836.7**	**866.5**				
2	236.24	**804.4**	**825.5**	**836.1**	**863.3**				
3	228.19	**797.7**	**817.0**	**832.3**	**857.6**				
4	228.19	**801.3**	**821.2**	**833.8**	**850.2**				
5	228.19	**803.2**	**824.4**	**832.9**	**847.0**				
6	228.19	**799.4**	**815.6**	**829.0**	**851.2**				
7	172.81	**905.5**	**937.4**	**926.4**	**948.5**				
8	172.81	**905.4**	**934.7**	**911.7**	**943.9**		TC8 occasional drop-outs		
9	159.46	**906.7**	**935.6**	**924.7**	**943.8**				
10	159.46	**907.8**	**935.0**	**924.7**	**940.7**				
11	159.46	**892.8**	**919.0**	**919.2**	**934.2**				
12	159.46	**896.8**	**925.0**	**923.6**	**943.7**				
13	102.31	**900.5**	**925.9**	**919.5**	**963.0**				
14	102.31	**894.5**	**915.2**	**918.8**	**962.1**				
15	35.15	**962.7**	**192.8**	**323.6**	**0.5**		TC15 failed on 10.11.2006		
16	35.15	**961.4**	**953.5**	**938.9**	**960.0**				
17	-21.60	**948.4**	**943.3**	**911.6**	**926.6**				
18	-21.60	**943.6**	**935.6**	**936.3**	**945.1**				
19	-21.60	**954.0**	**944.5**	**951.6**	**949.8**				
20	-21.60	**936.4**	**933.5**	**904.1**	**892.8**				
21	-35.15	**963.4**	**867.5**	**936.9**	**131.9**			shows hysteresis	failed permanently
22	-35.15	**962.4**	**961.0**	**953.2**	**233.7**				failed permanently
23	-91.22	**973.0**	**952.6**	**954.9**	**950.7**				
24	-91.22	**981.7**	**961.5**	**966.1**	**974.1**				
25	-91.22	**959.5**	**950.7**	**944.8**	**946.5**	TC25 occasional drop-outs			
26	-91.22	**961.8**	**946.8**	**931.3**	**911.0**				
27	-104.87	**980.2**	**969.5**	**960.9**	**968.9**	TC27 occasional drop-outs			
28	-104.87	**987.2**	**973.9**	**971.6**	**979.9**	TC28 occasional drop-outs			
29	-160.24	**966.3**	**928.5**	**942.4**	**941.2**				
30	-160.24	**969.6**	**933.9**	**929.9**	**924.7**				
31	-160.24	**962.6**	**935.2**	**934.2**	**919.3**	TC31 occasional drop-outs			
32	-160.24	**960.8**	**925.6**	**944.0**	**936.5**				
33	-168.49	**969.8**	**936.6**	**945.2**	**957.5**				
34	-168.49	**968.0**	**939.3**	**931.7**	**953.3**	TC34 occasional drop-outs			

Table 11: Average temperatures and history of thermocouple behavior

In Table 11, the behavior of all 34 thermocouples was analyzed to obtain an idea about the reliability of the obtained data. The magenta lines indicate temperature measurements at pebble surfaces. Yellow boxes indicate suspicious behavior of the concerned thermocouple and thus potentially unreliable data.

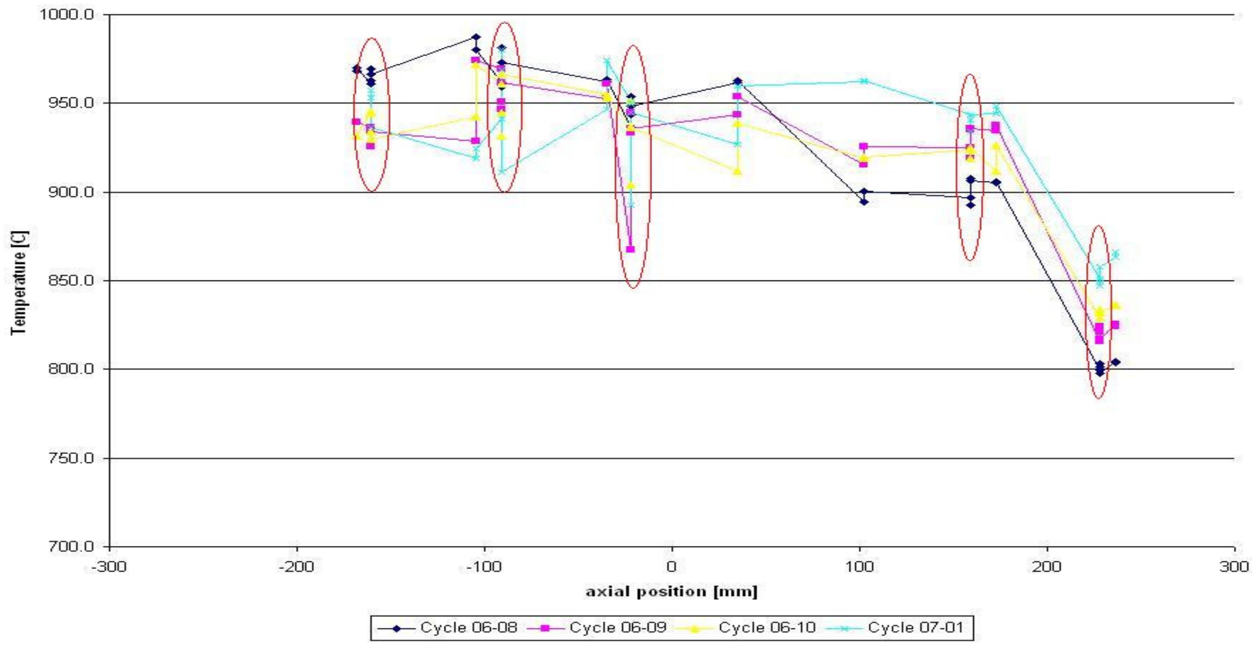

Figure 17: Average temperatures in irradiation rig for all 4 irradiation cycles

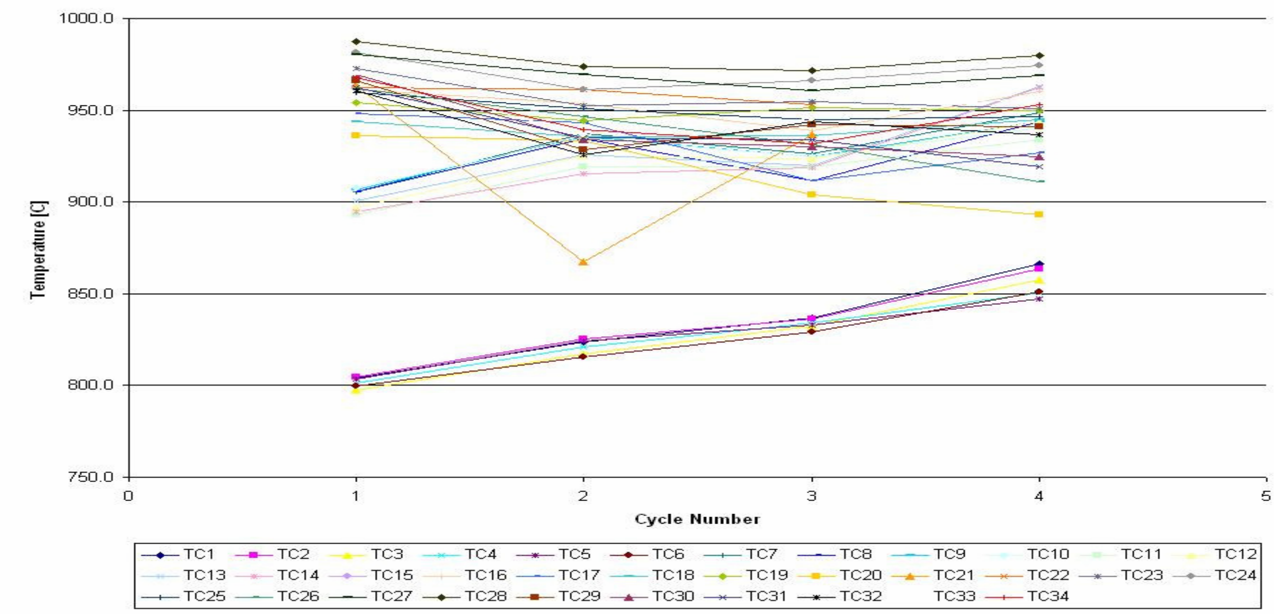

Figure 18: Evolution of average temperatures during irradiation

In comparison with HFR-EU1Bis, thermocouples 1 to 14 rose with time to compensate the experiment wrong design (i.e. the HFR buckling leads to a lower fission rate for INET 1, which then required an increase of the initial capsule temperature set point from 900°C to 940°C).

6.1 Temperatures during Cycle 06-08

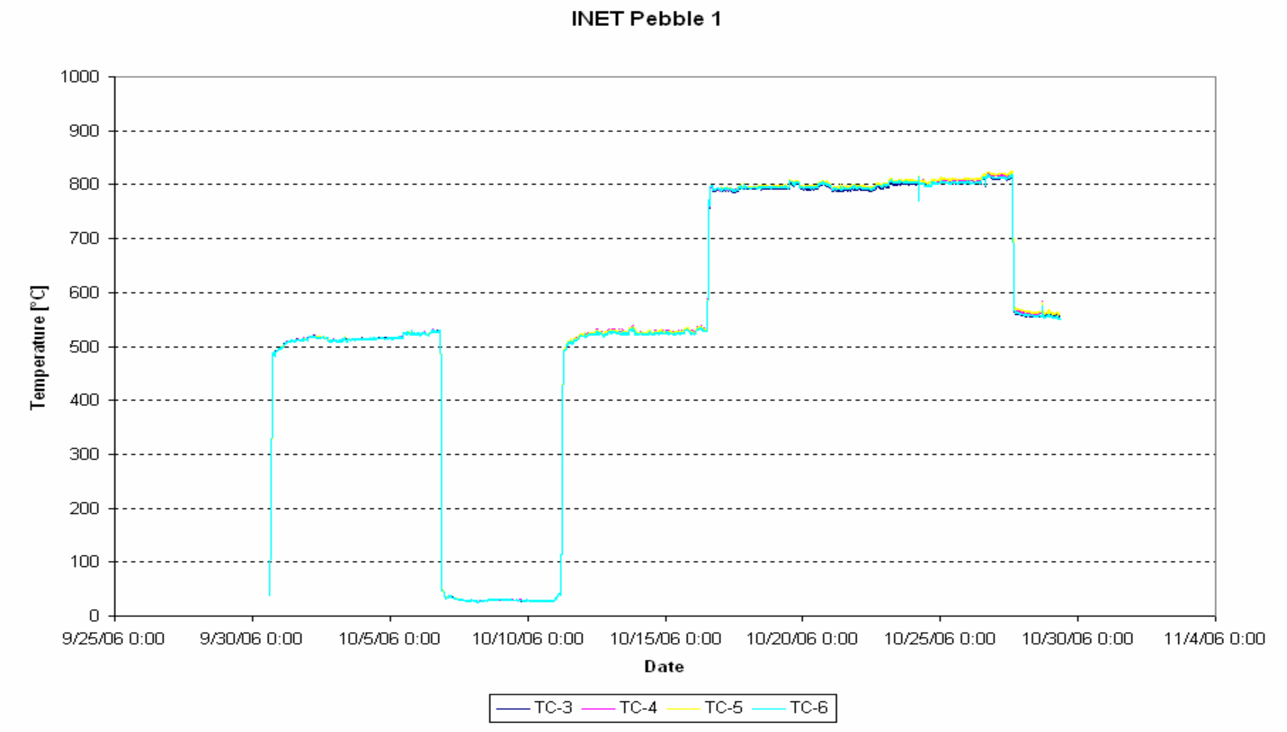

Figure 19: Temperatures pebble INET.1 (TC-03, TC-04, TC-05, TC-06)

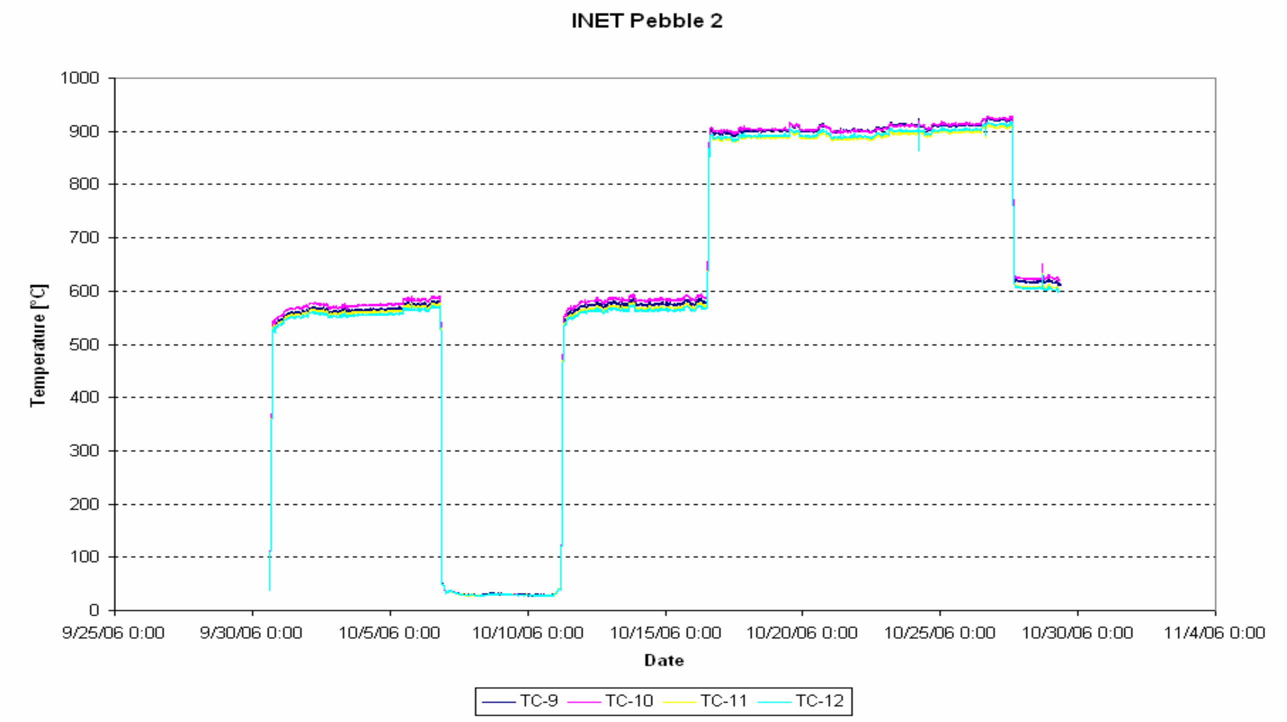

Figure 20: Temperatures pebble INET.2 (TC-09, TC-10, TC-11, TC-12)

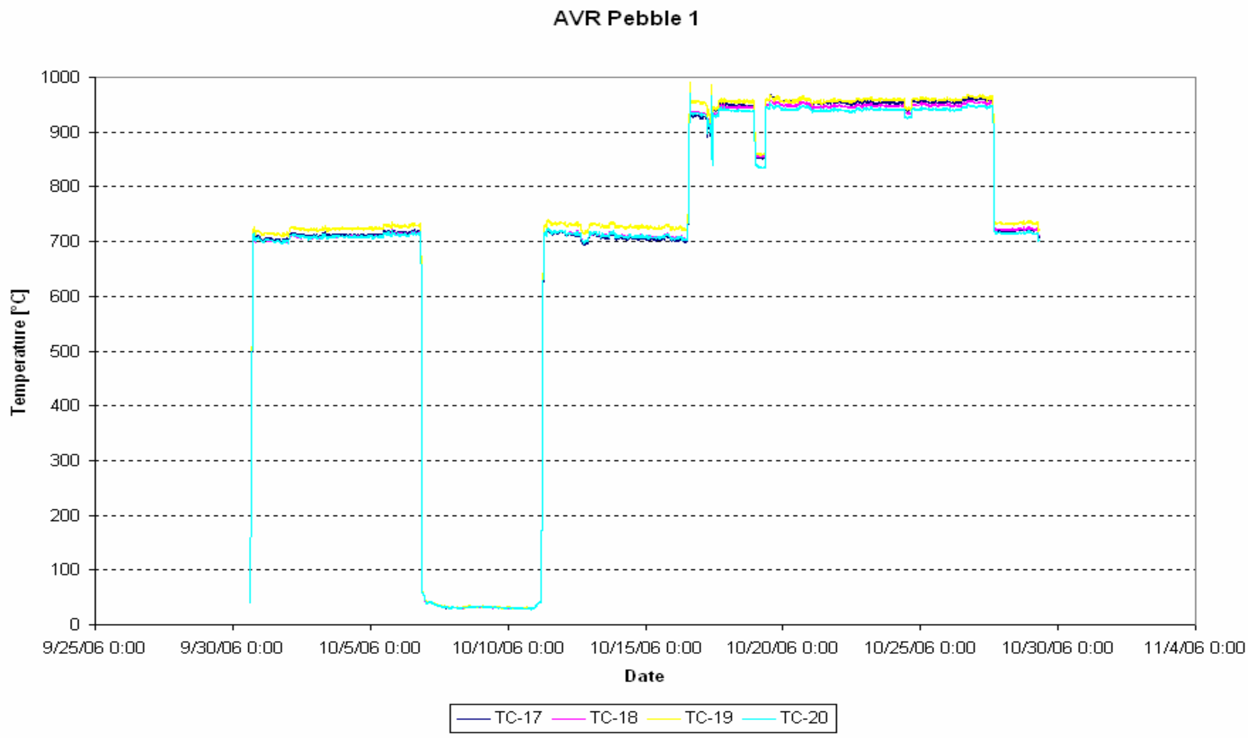

Figure 21: Temperatures pebble AVR.1 (TC-17, TC-18, TC-19, TC-20)

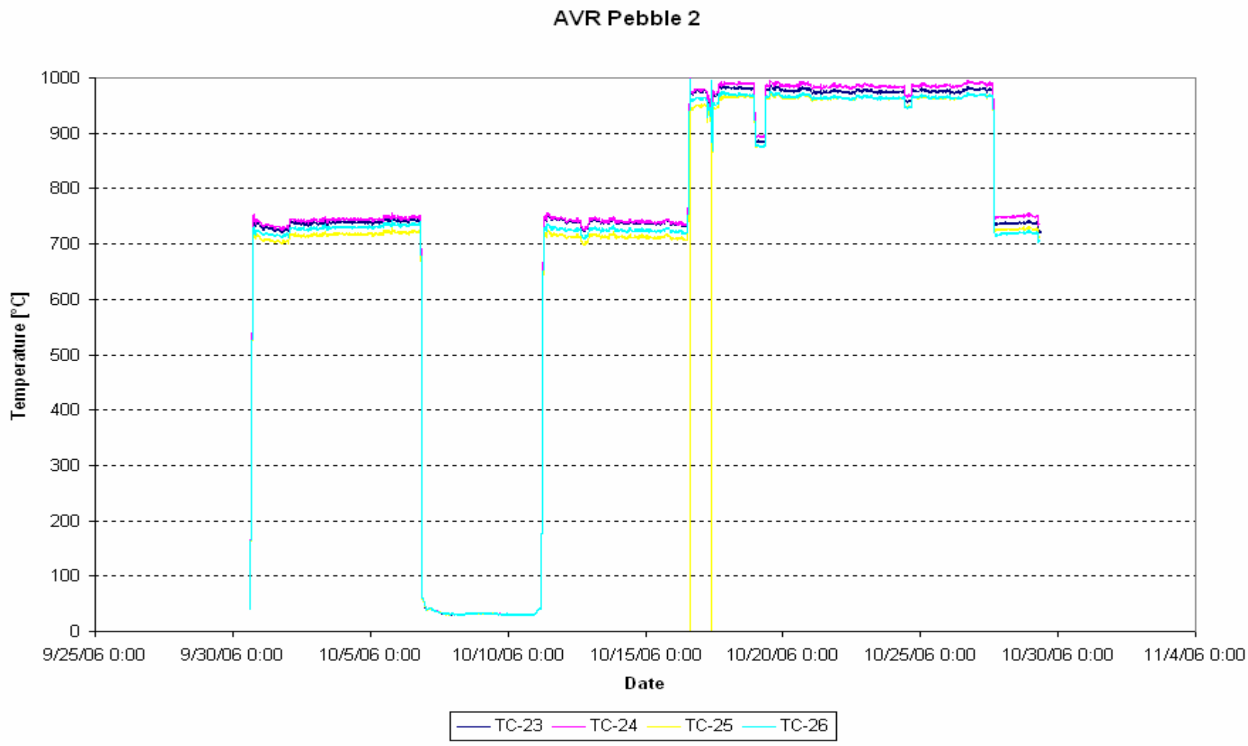

Figure 22: Temperatures pebble AVR.2 (TC-23, TC-24, TC-25, TC-26)

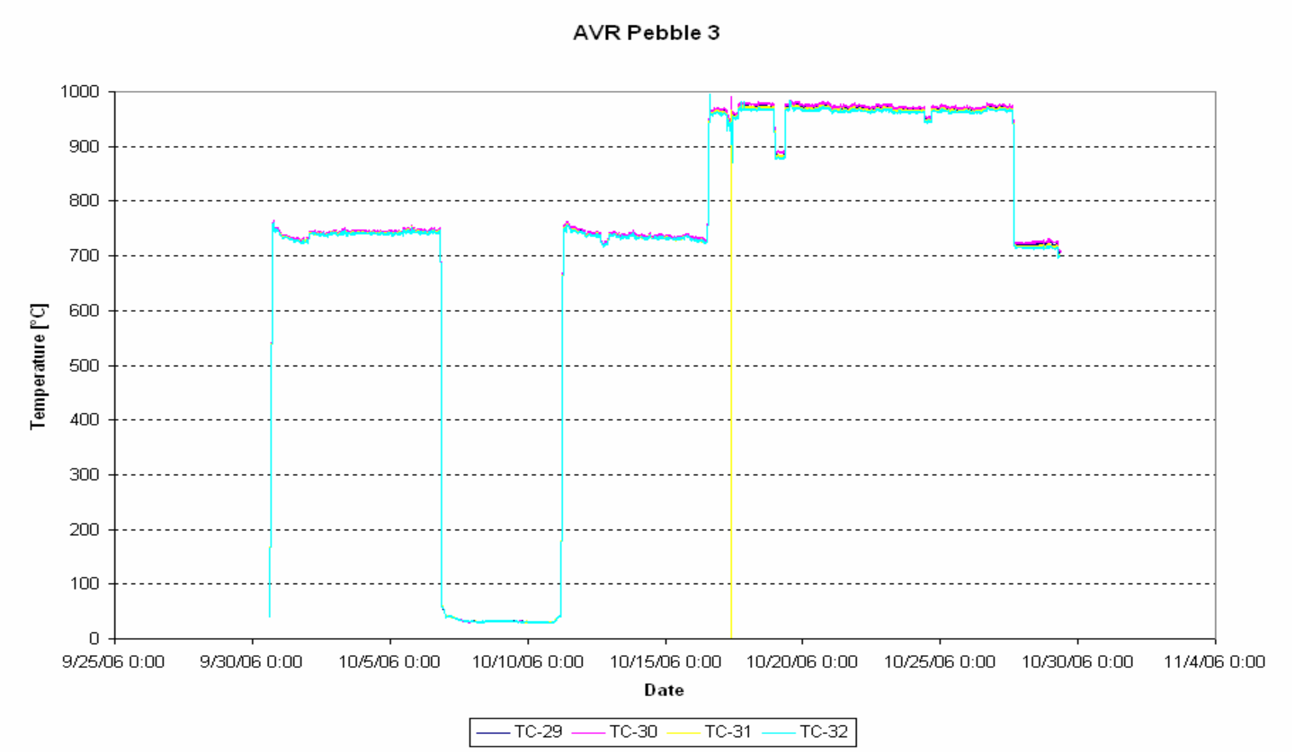

Figure 23: Temperatures pebble AVR.3 (TC-28, TC-29, TC-30, TC-31)

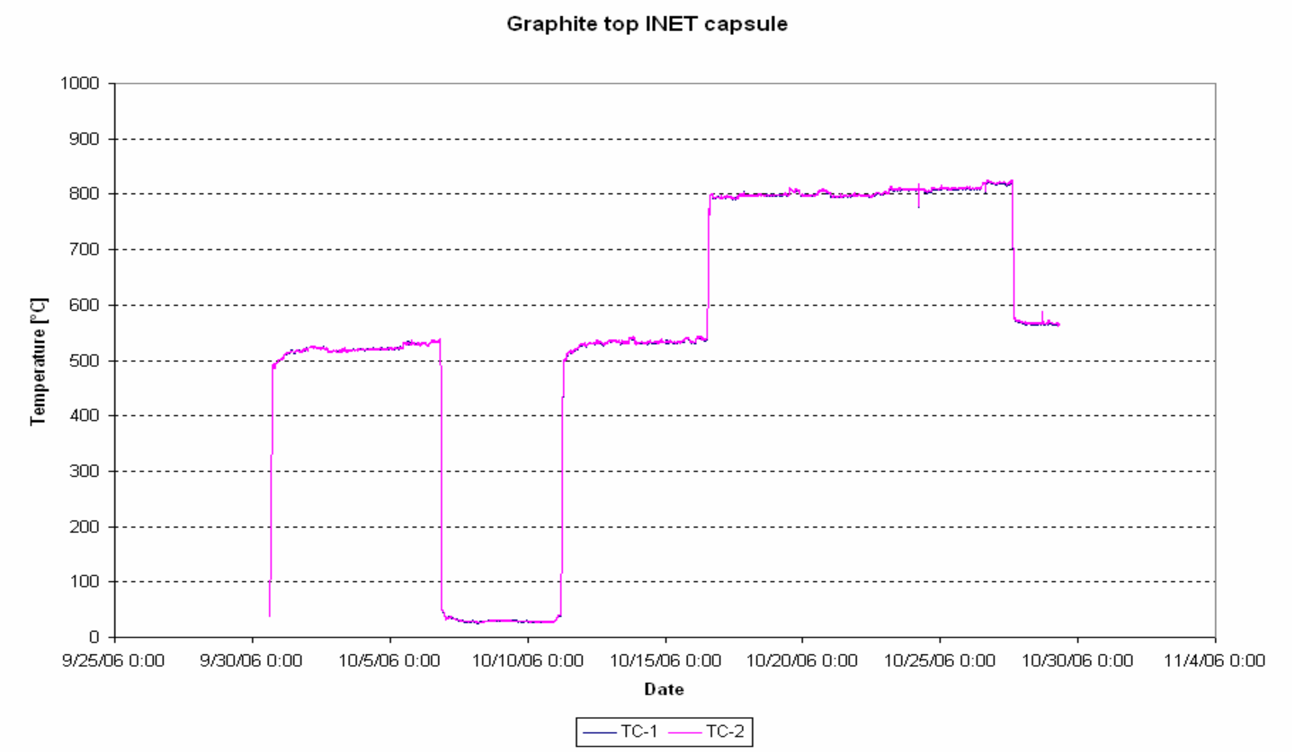

Figure 24: Temperatures top graphite INET capsule (TC-01, TC-02)

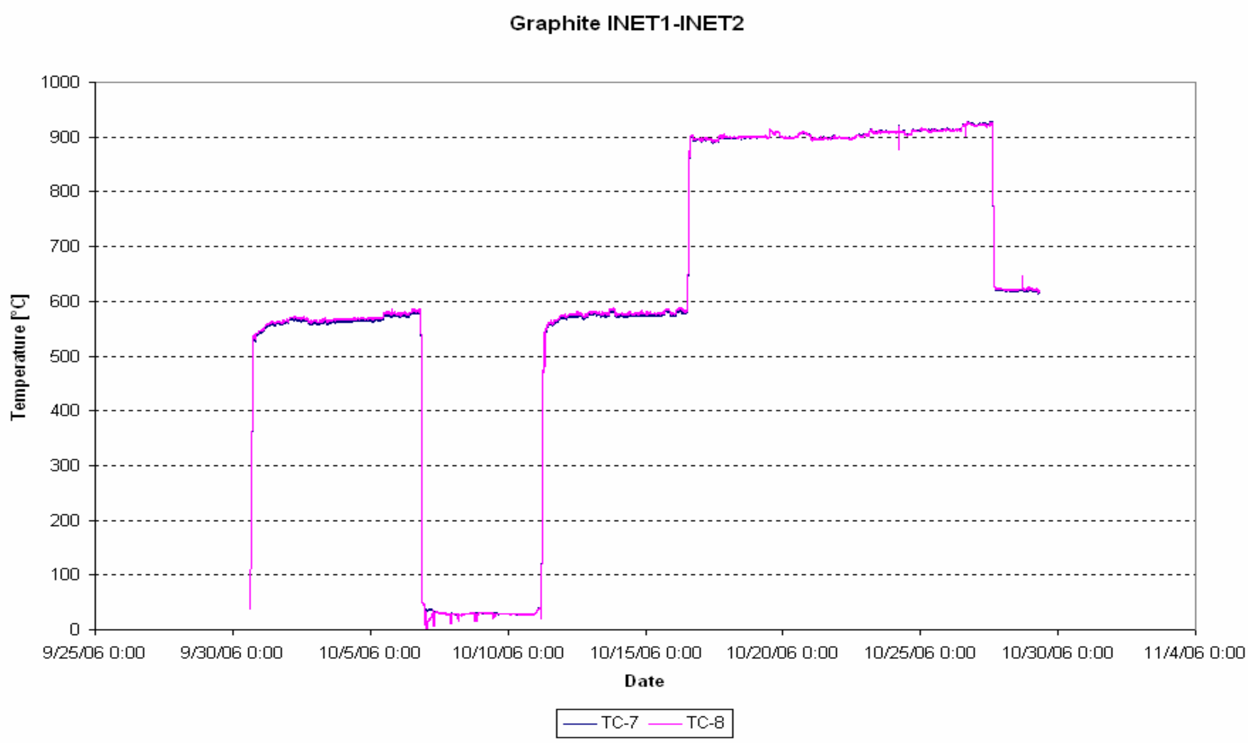

Figure 25: Temperatures graphite between INET.1 and INET.2 (TC-07, TC-08)

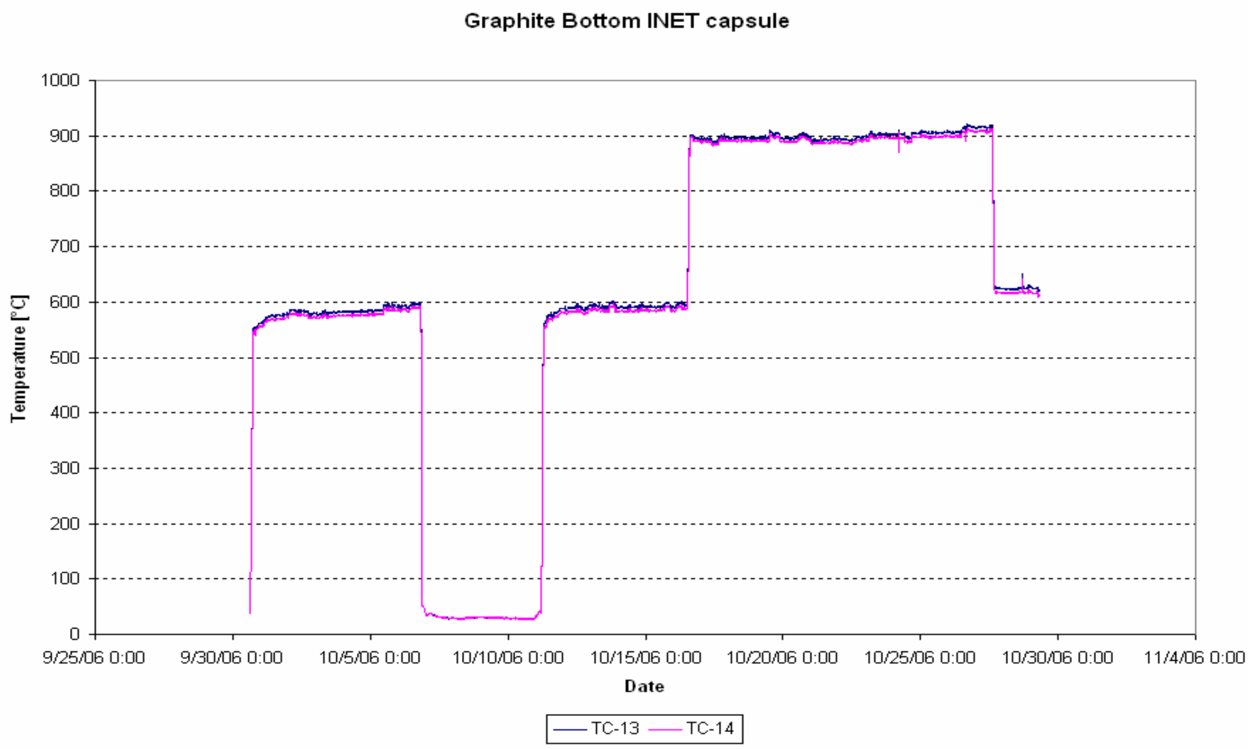

Figure 26: Temperatures bottom graphite INET Capsule (TC-13, TC-14)

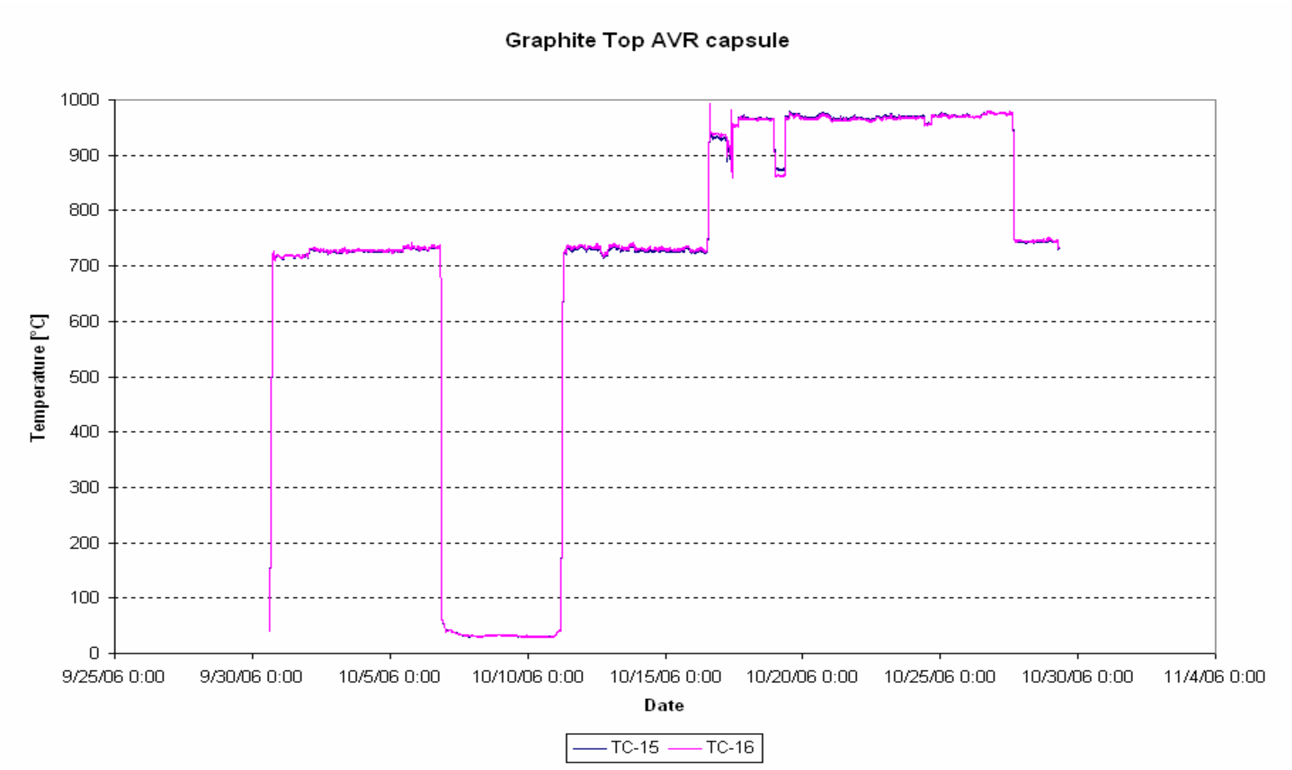

Figure 27: Temperatures top graphite AVR capsule (TC-15, TC-16)

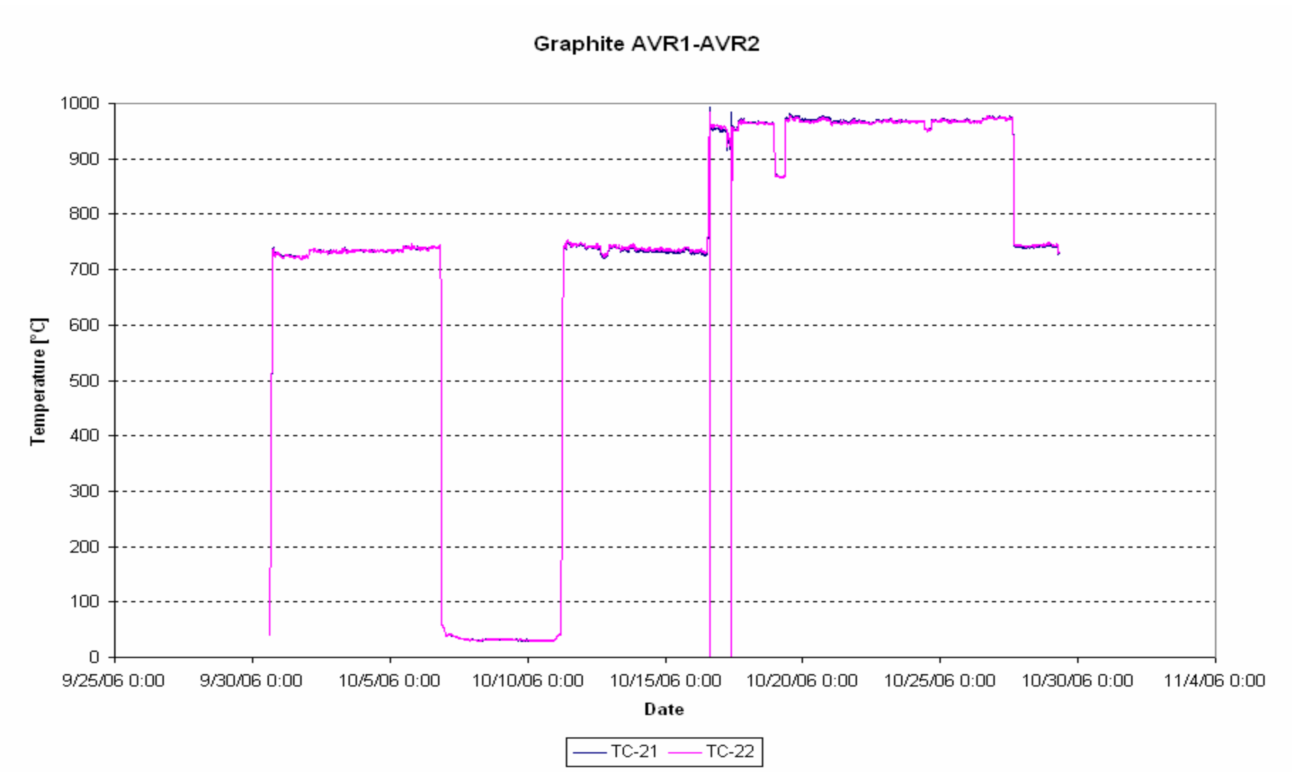

Figure 28: Temperatures graphite between AVR.1 and AVR.2 (TC-21, TC-22)

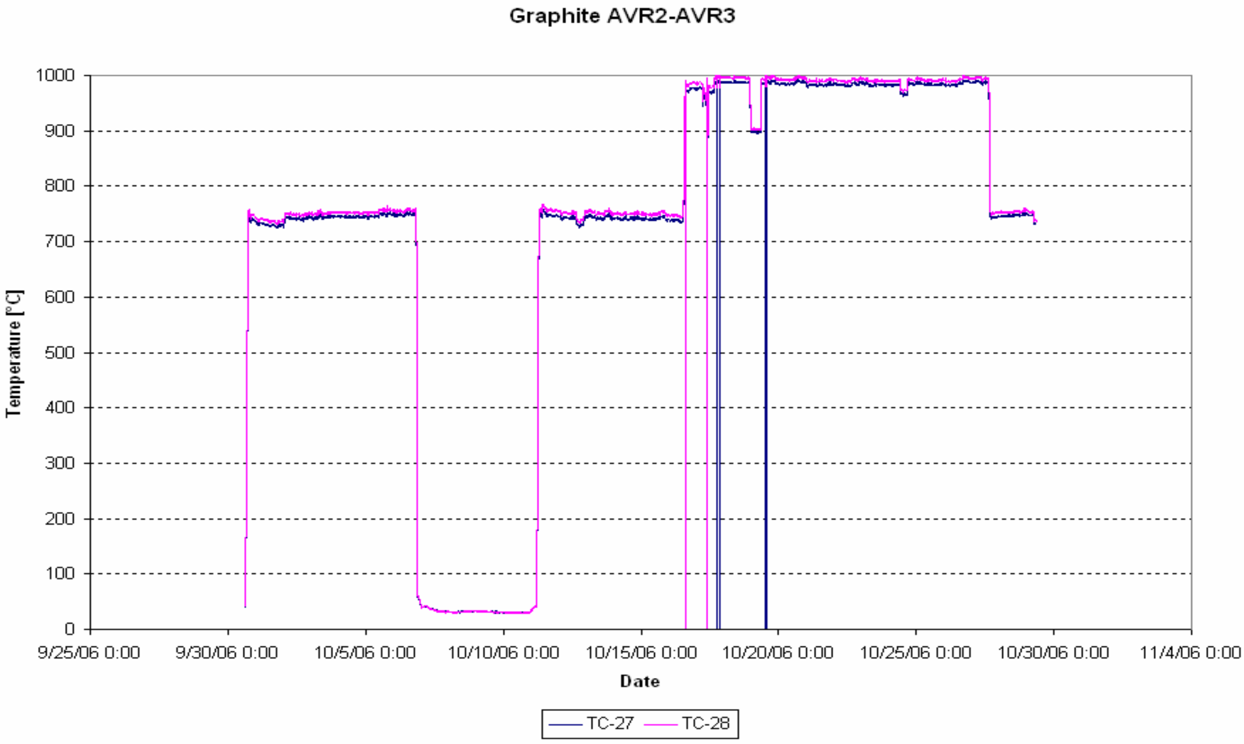

Figure 29: Temperatures graphite between AVR.2 and AVR.3 (TC-27, TC-28)

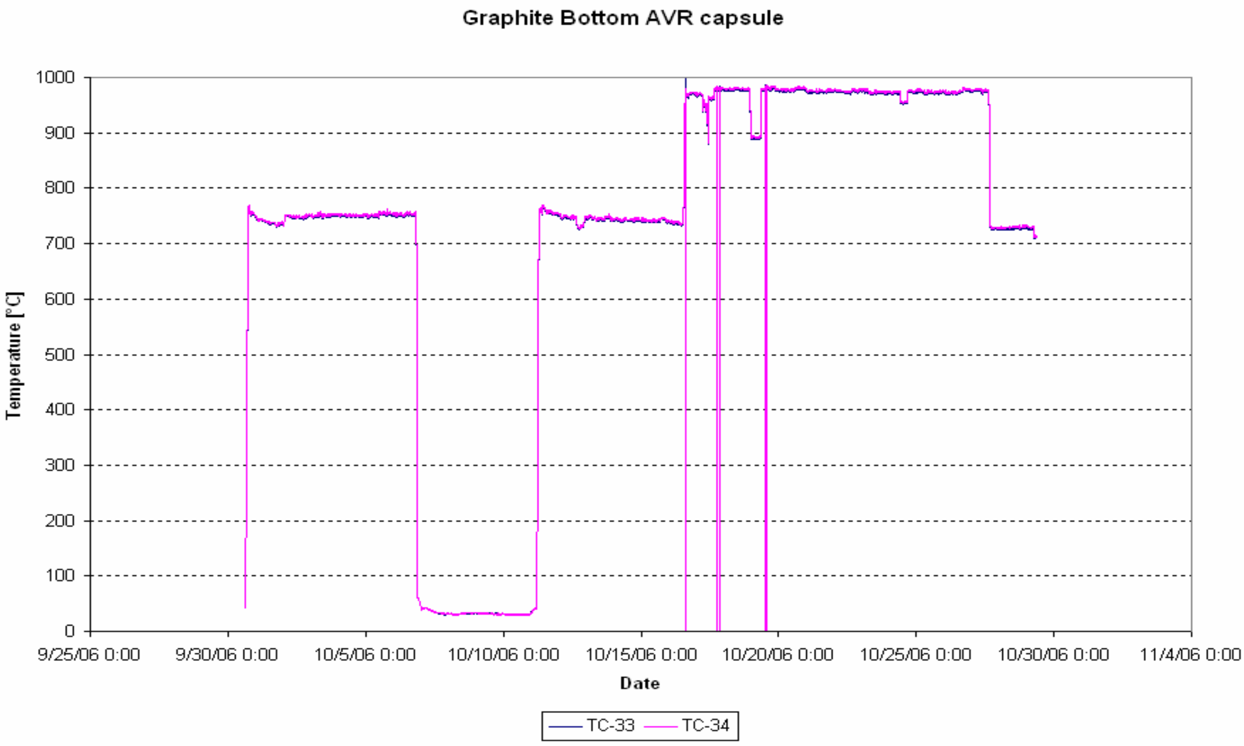

Figure 30: Temperatures bottom graphite (TC-33, TC-34)

TC number	Average temperature during full power operation [°C]	Average temperature during high temperature operation [°C]	Target temperature [°C]	Location
TC-01	656.4	803.8		Graphite
TC-02	656.9	804.4		
TC-03	650.0	797.7		INET 1
TC-04	652.4	801.3		
TC-05	653.2	803.2		
TC-06	650.3	799.4		
TC-07	726.8	905.5		Graphite
TC-08	728.6	905.4		
TC-09	727.8	906.7	900	INET 2
TC-10	732.7	907.8		
TC-11	718.2	892.8		
TC-12	717.7	896.8		
TC-13	733.4	900.5		Graphite
TC-14	726.9	894.5		
TC-15	836.6	962.7		Graphite
TC-16	837.0	961.4		
TC-17	820.2	948.4		AVR 1
TC-18	818.1	943.6		
TC-19	830.9	954.0	950	
TC-20	814.2	936.4		
TC-21	840.1	963.4		Graphite
TC-22	840.2	962.4		
TC-23	846.1	973.0		AVR 2
TC-24	852.5	981.7		
TC-25	827.9	959.5		
TC-26	834.2	961.8		
TC-27	851.6	980.2		Graphite
TC-28	859.1	987.2		
TC-29	841.8	966.3		AVR 3
TC-30	844.8	969.6		
TC-31	839.6	962.6		
TC-32	838.1	960.8		
TC-33	847.2	969.8		Graphite
TC-34	847.2	968.0		

Table 12: Time averaged temperature readings during cycle 06-08

6.2 Temperatures during Cycle 06-09

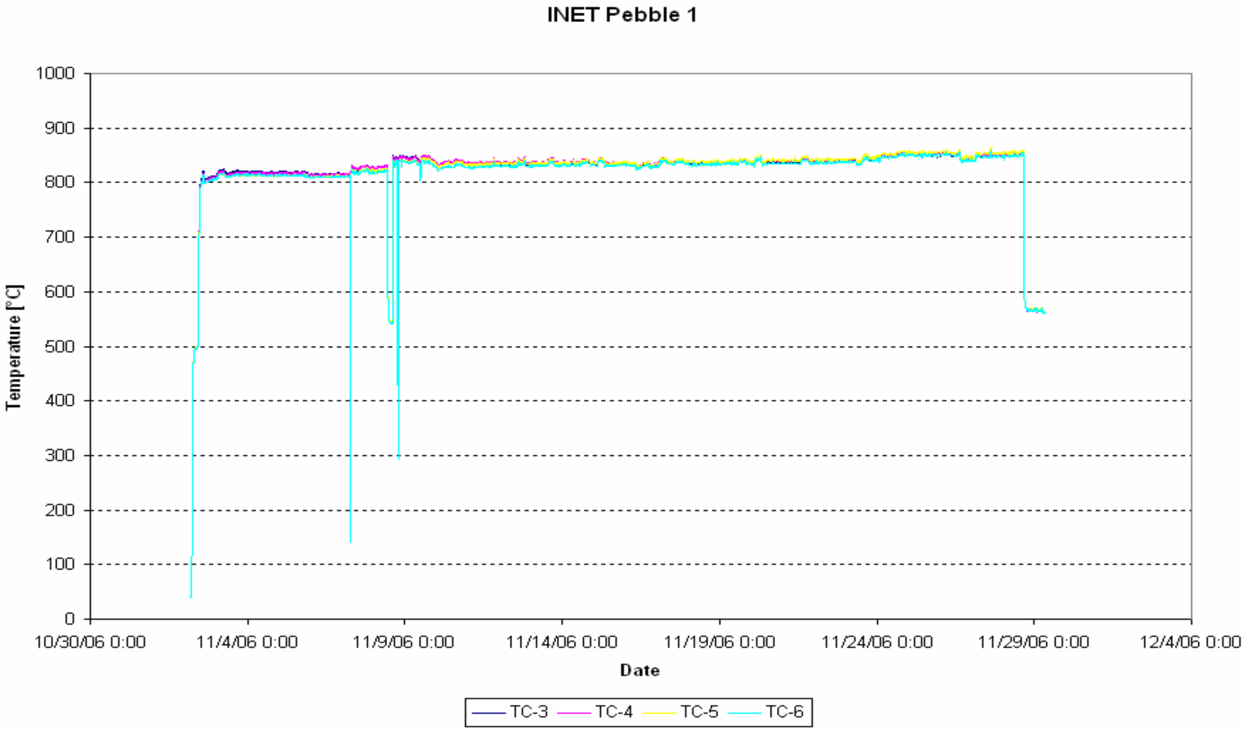

Figure 31: Temperatures pebble INET.1 (TC-03, TC-04, TC-05, TC-06)

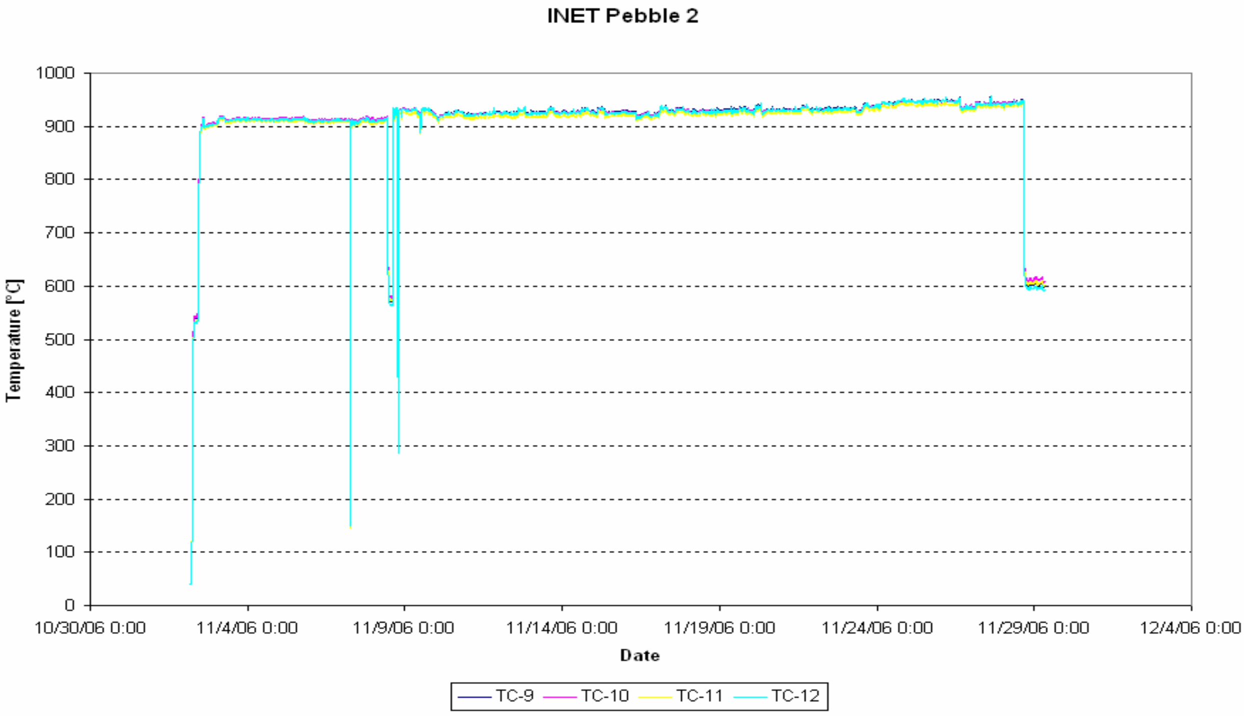

Figure 32: Temperatures pebble INET.2 (TC-09, TC-10, TC-11, TC-12)

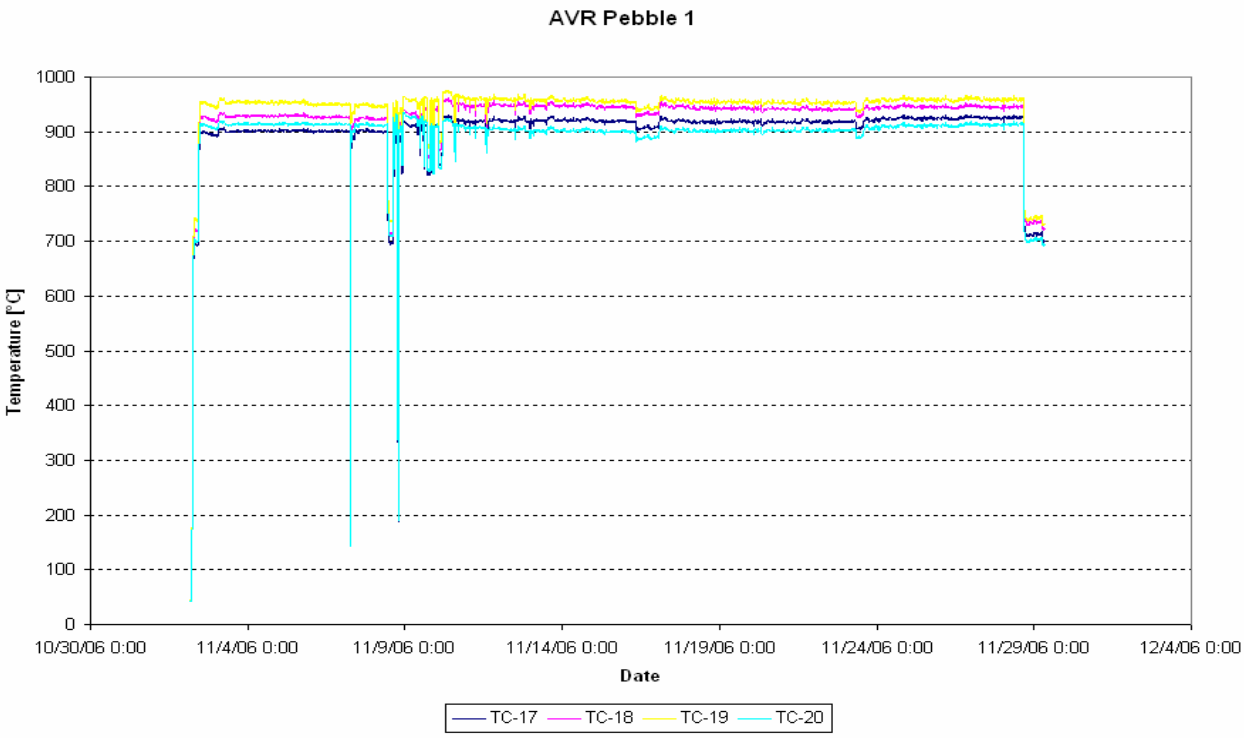

Figure 33: Temperatures pebble AVR.1 (TC-17, TC-18, TC-19, TC-20)

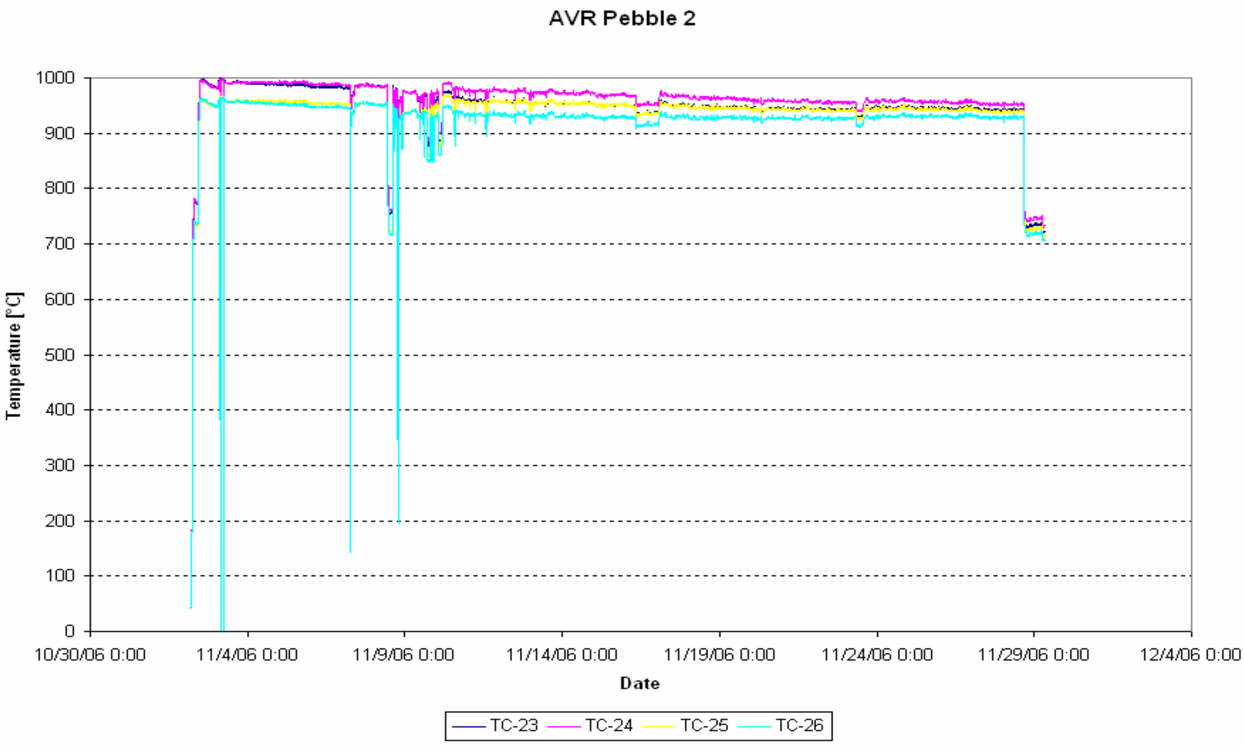

Figure 34: Temperatures pebble AVR.2 (TC-23, TC-24, TC-25, TC-26)

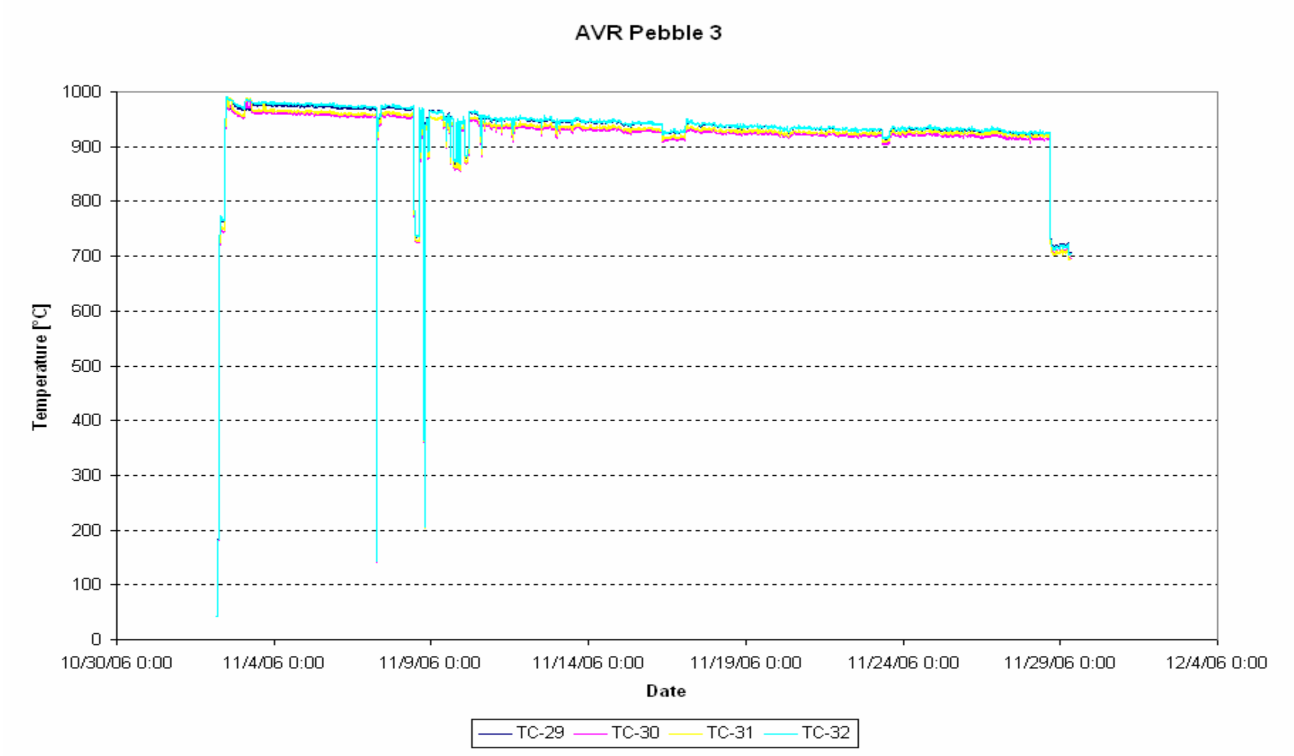

Figure 35: Temperatures pebble AVR.3 (TC-28, TC-29, TC-30, TC-31)

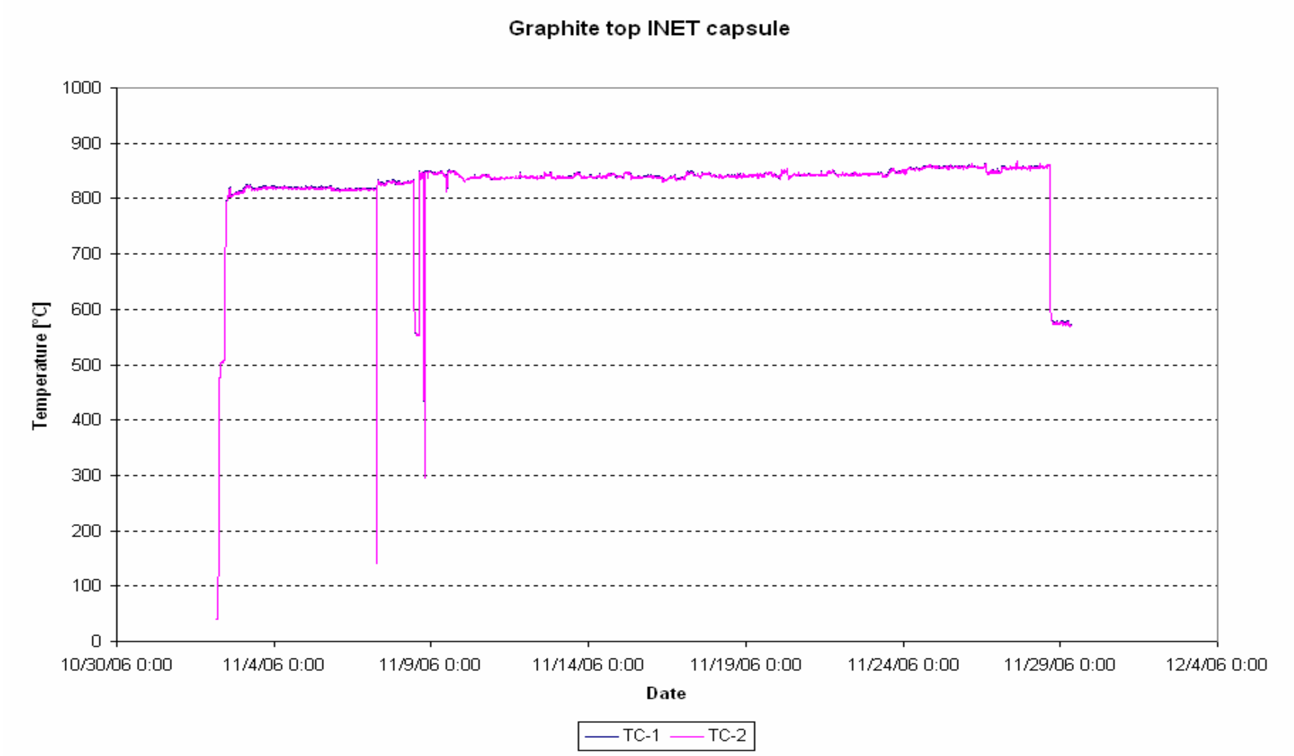

Figure 36: Temperatures top graphite INET capsule (TC-01, TC-02)

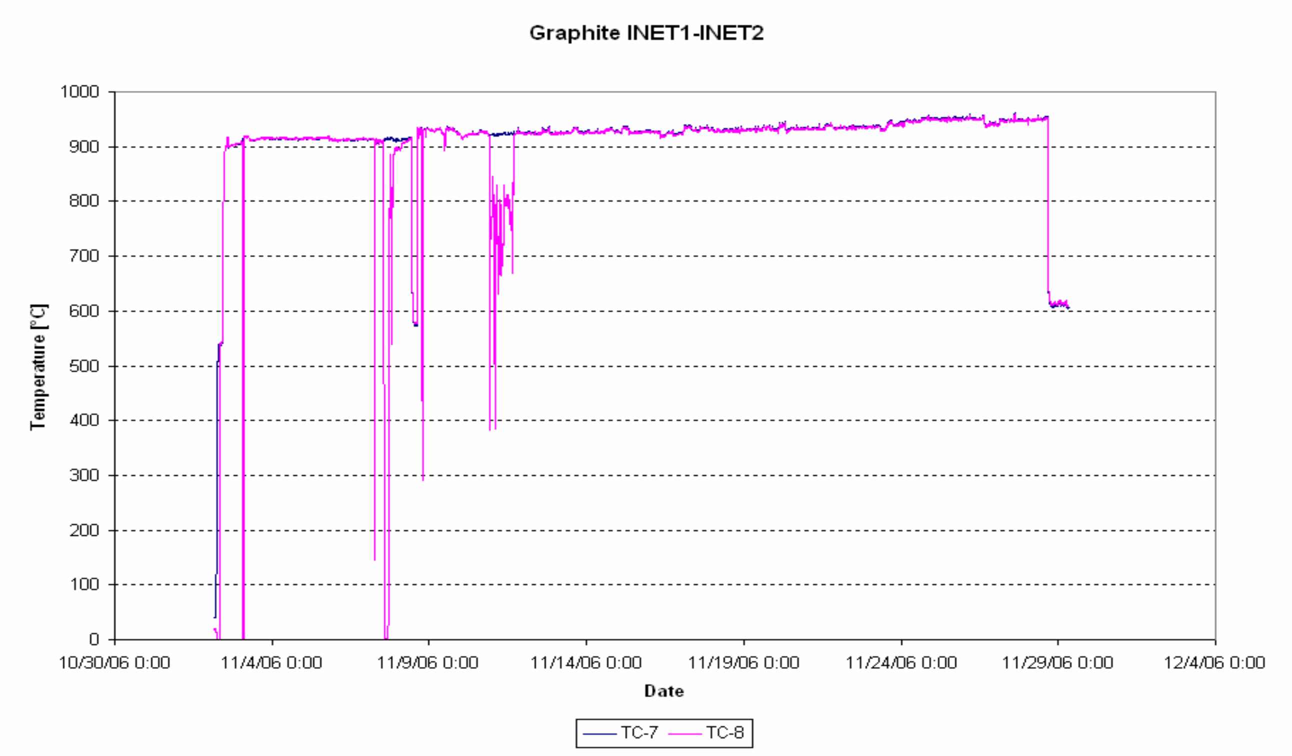

Figure 37: Temperatures graphite between INET.1 and INET.2 (TC-07, TC-08)

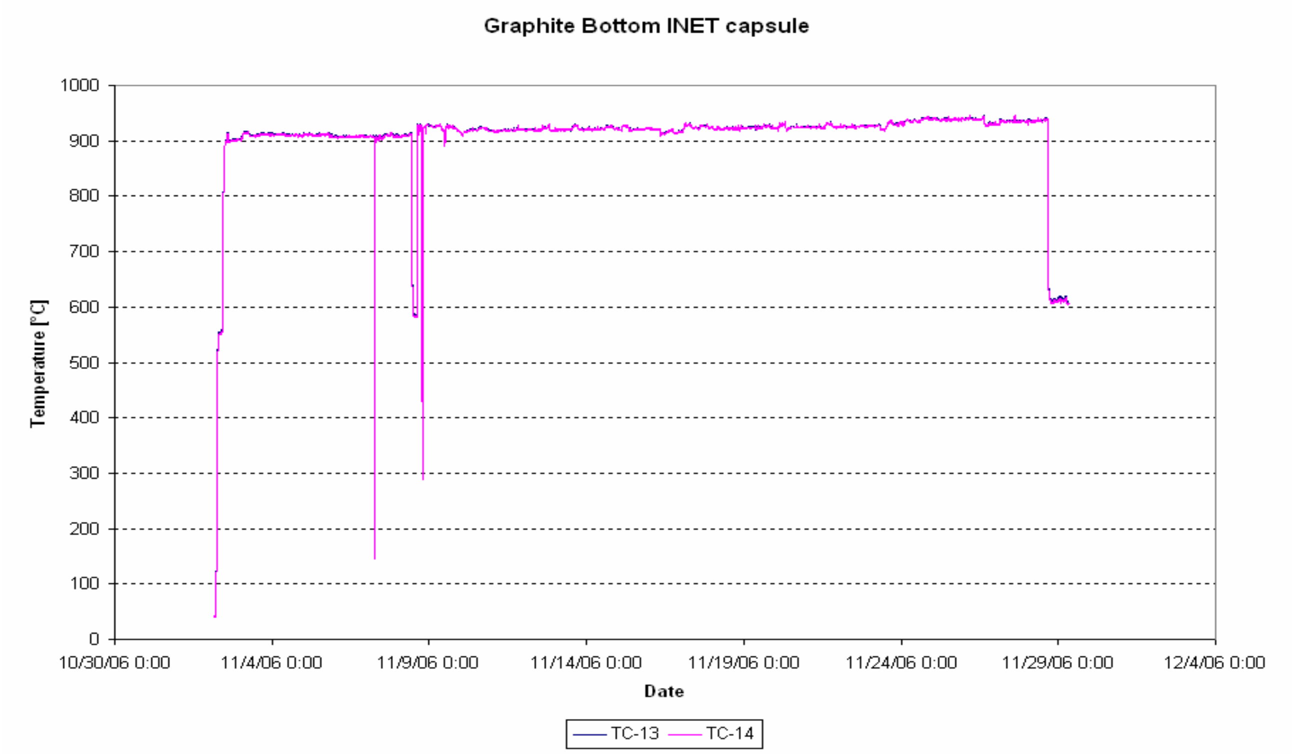

Figure 38: Temperatures bottom graphite INET Capsule (TC-13, TC-14)

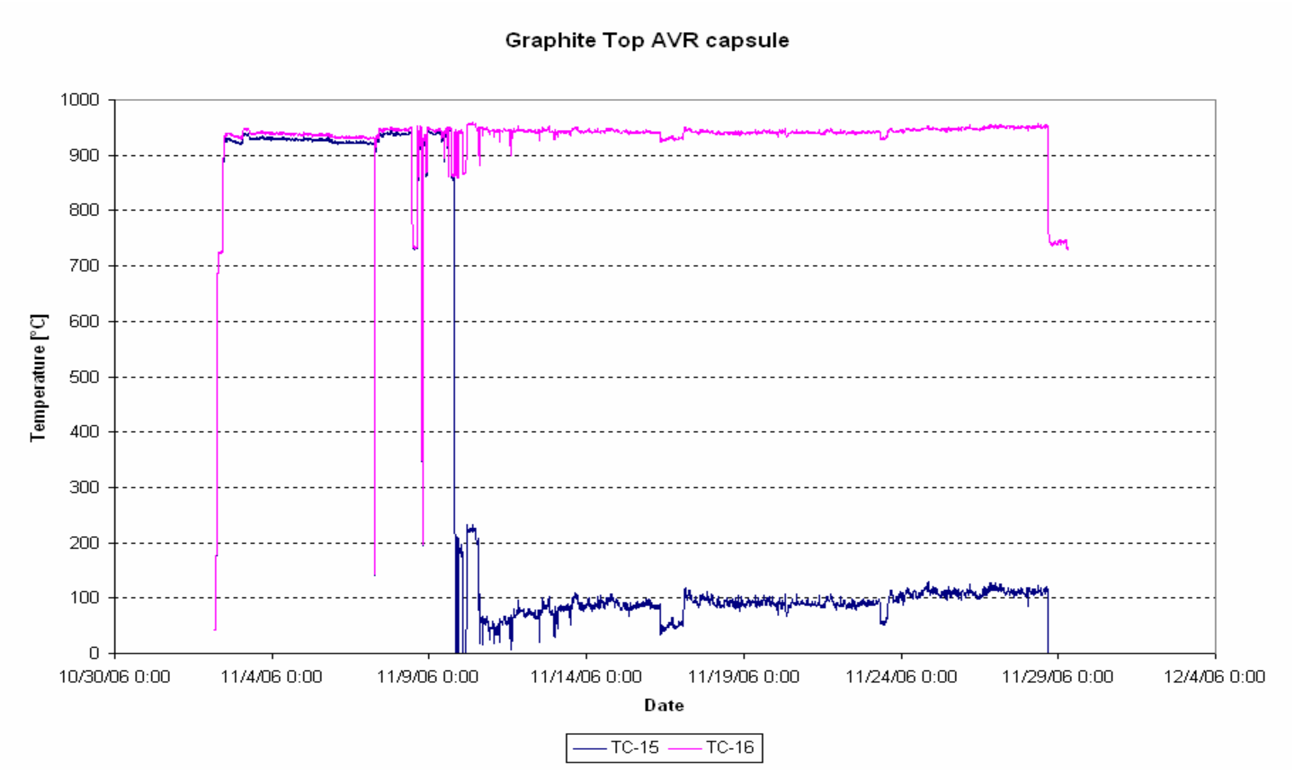

Figure 39: Temperatures top graphite AVR capsule (TC-15, TC-16)

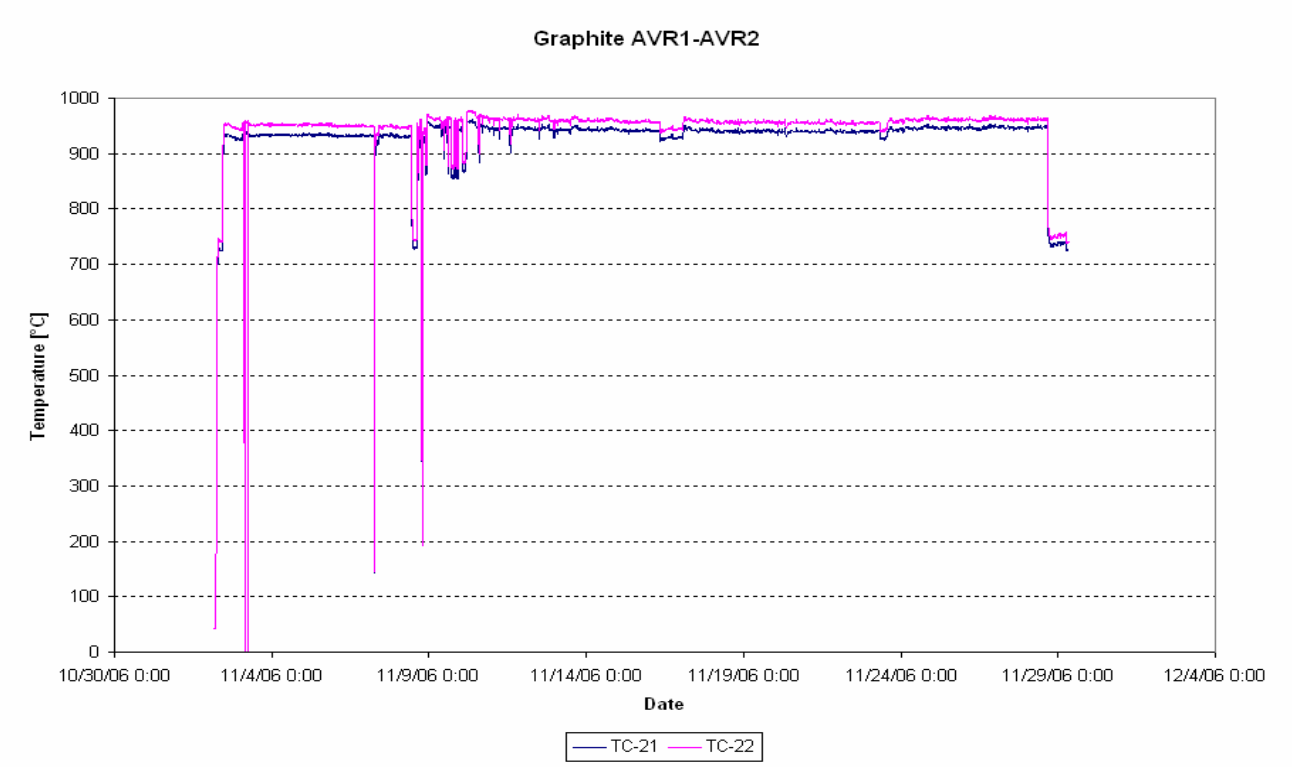

Figure 40: Temperatures graphite between AVR.1 and AVR.2 (TC-21, TC-22)

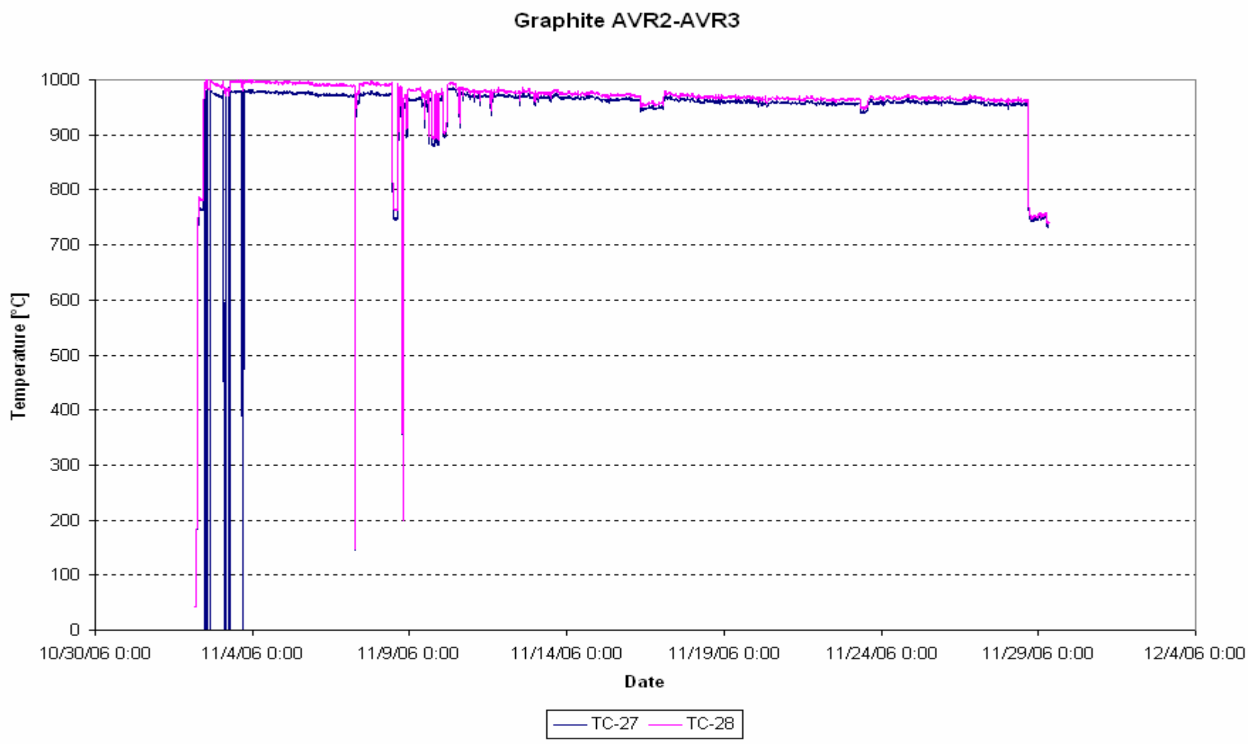

Figure 41: Temperatures graphite between AVR.2 and AVR.3 (TC-27, TC-28)

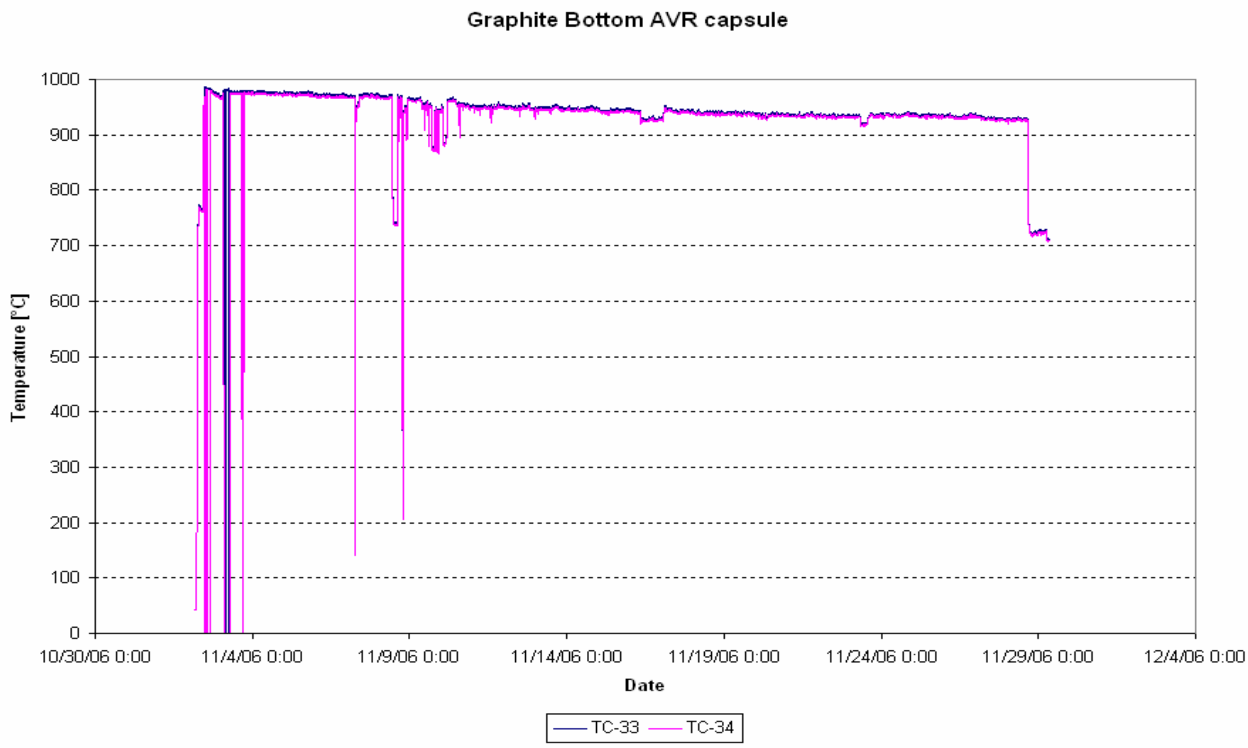

Figure 42: Temperatures bottom graphite (TC-33, TC-34)

TC number	Average temperature during full power operation [°C]	Average temperature during high temperature operation [°C]	Target temperature [°C]	Location
TC-01	823.0	823.9		Graphite
TC-02	824.6	825.5		
TC-03	816.1	817.0		INET 1
TC-04	820.3	821.2		
TC-05	823.5	824.4		
TC-06	814.7	815.6		
TC-07	936.3	937.4		Graphite
TC-08	932.8	934.7		
TC-09	934.5	935.6	900 ⇒ 940 (09/11/06)	INET 2
TC-10	934.0	935.0		
TC-11	917.9	919.0		
TC-12	923.9	925.0		
TC-13	924.8	925.9		Graphite
TC-14	914.2	915.2		
TC-15	192.2	192.8		Graphite
TC-16	952.9	953.5		
TC-17	942.7	943.3	950	AVR 1
TC-18	935.0	935.6		
TC-19	943.9	944.5		
TC-20	932.9	933.5		
TC-21	867.3	867.5		Graphite
TC-22	960.3	961.0		
TC-23	952.0	952.6		AVR 2
TC-24	960.8	961.5		
TC-25	950.0	950.7		
TC-26	946.1	946.8		
TC-27	968.9	969.5		Graphite
TC-28	973.2	973.9		
TC-29	927.9	928.5		AVR 3
TC-30	933.3	933.9		
TC-31	934.6	935.2		
TC-32	925.1	925.6		
TC-33	935.8	936.6		Graphite
TC-34	938.3	939.3		

Table 13: Time averaged temperature readings during cycle 06-09

6.3 Temperatures during Cycle 06-10

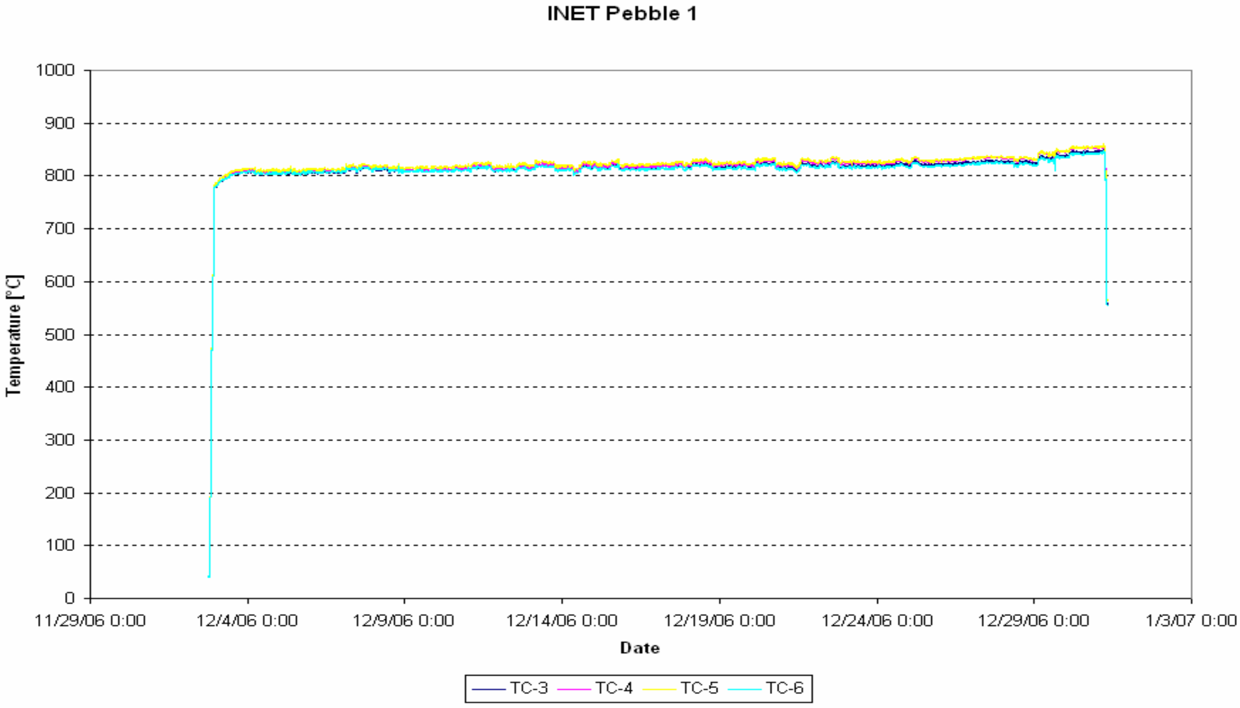

Figure 43: Temperatures pebble INET.1 (TC-03, TC-04, TC-05, TC-06)

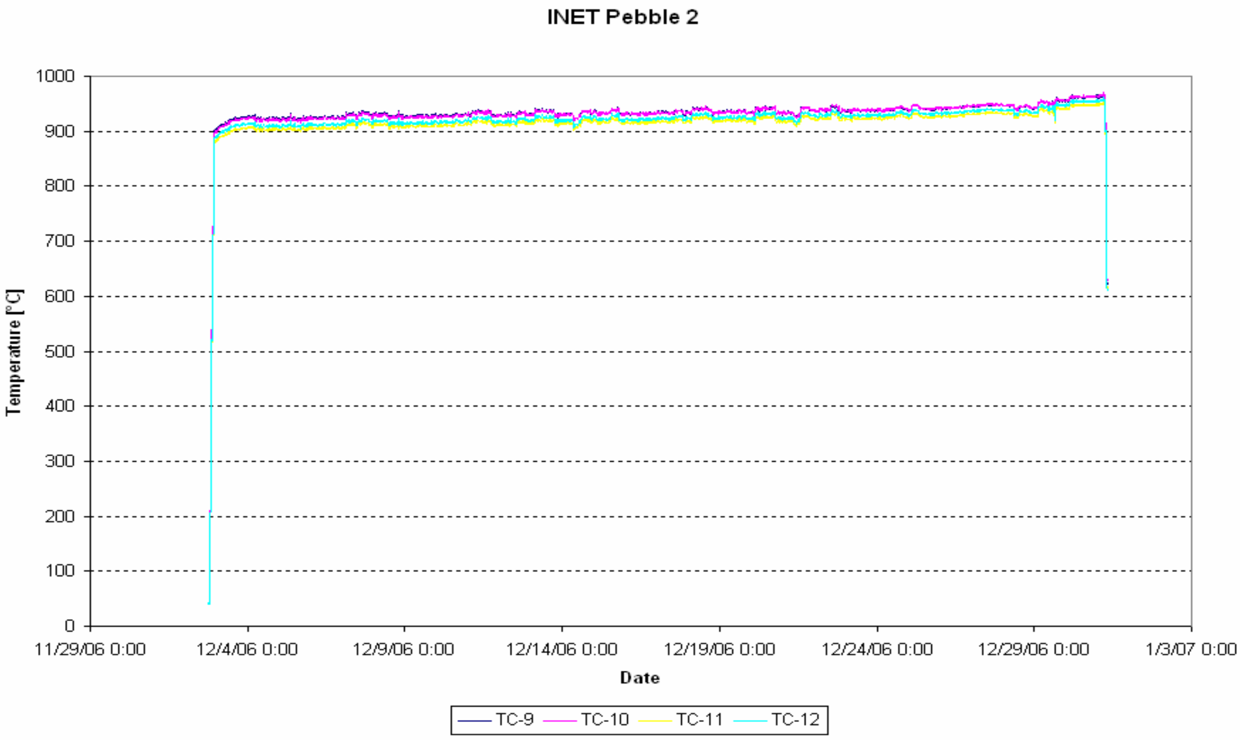

Figure 44: Temperatures pebble INET.2 (TC-09, TC-10, TC-11, TC-12)

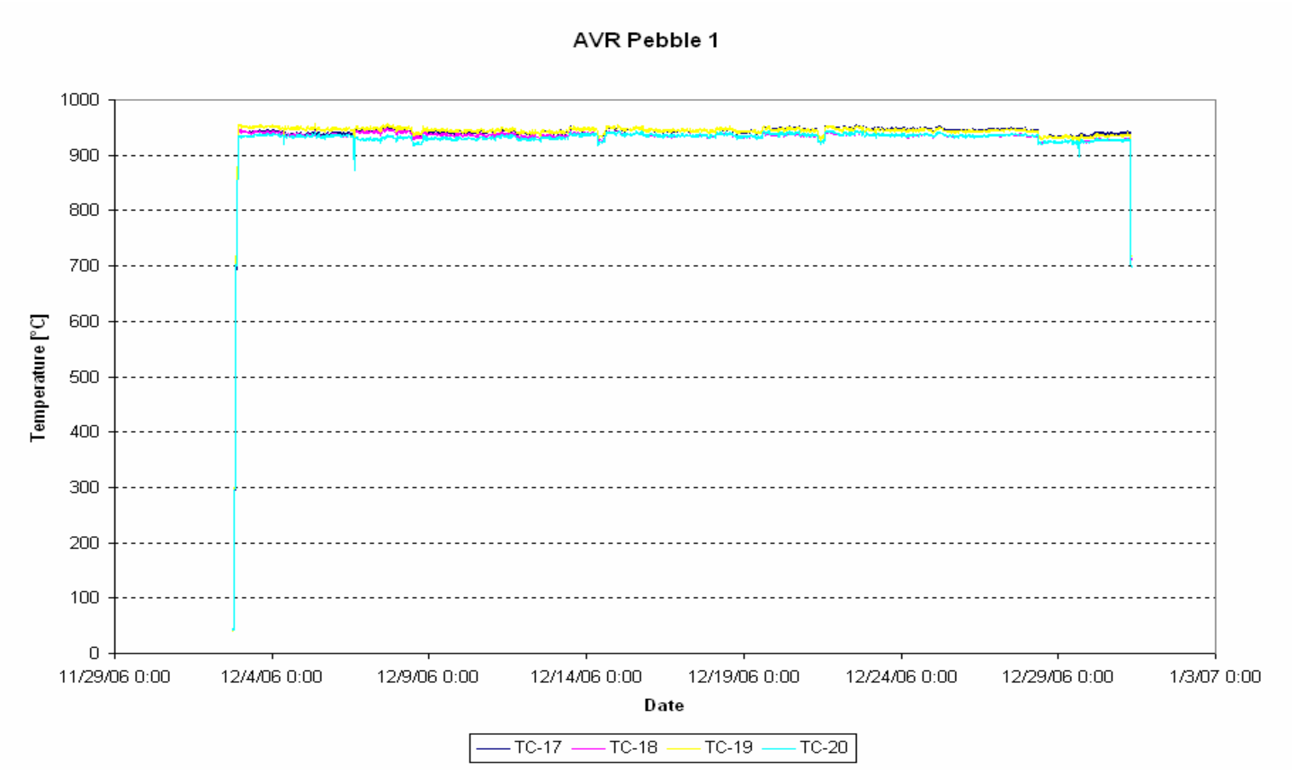

Figure 45: Temperatures pebble AVR.1 (TC-17, TC-18, TC-19, TC-20)

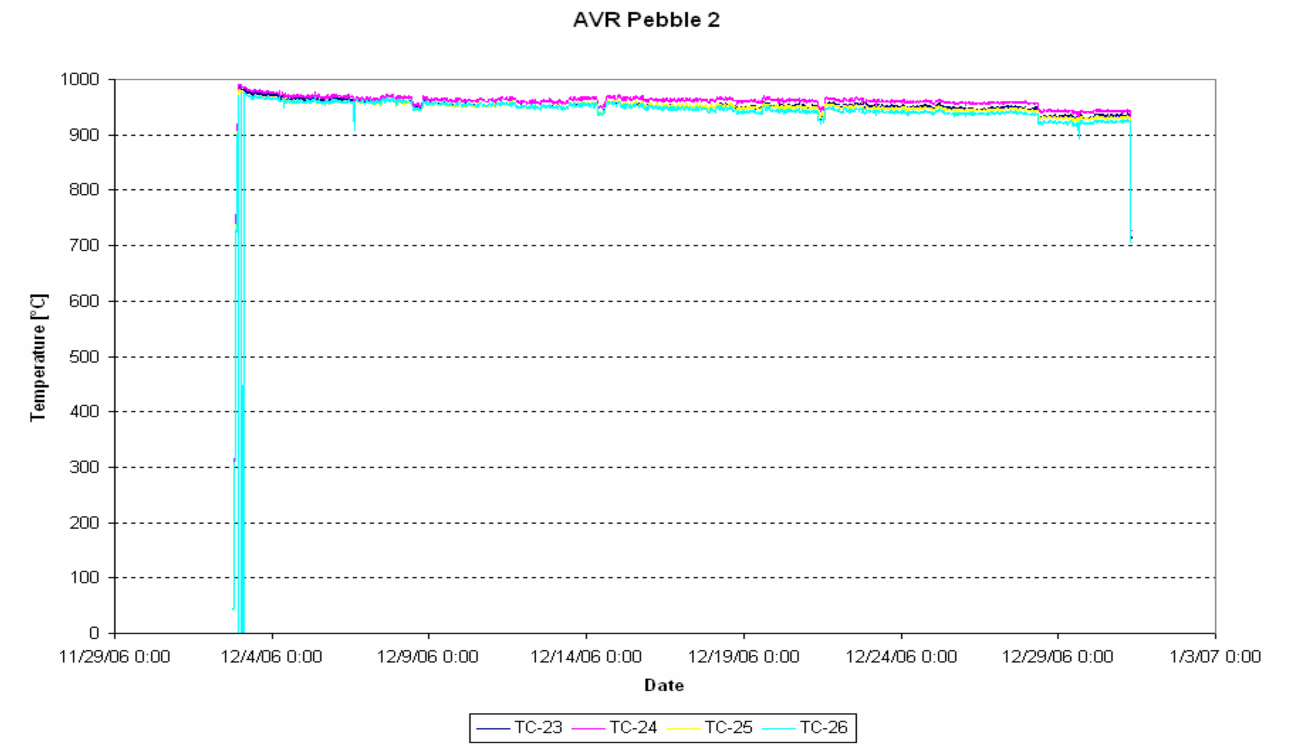

Figure 46: Temperatures pebble AVR.2 (TC-23, TC-24, TC-25, TC-26)

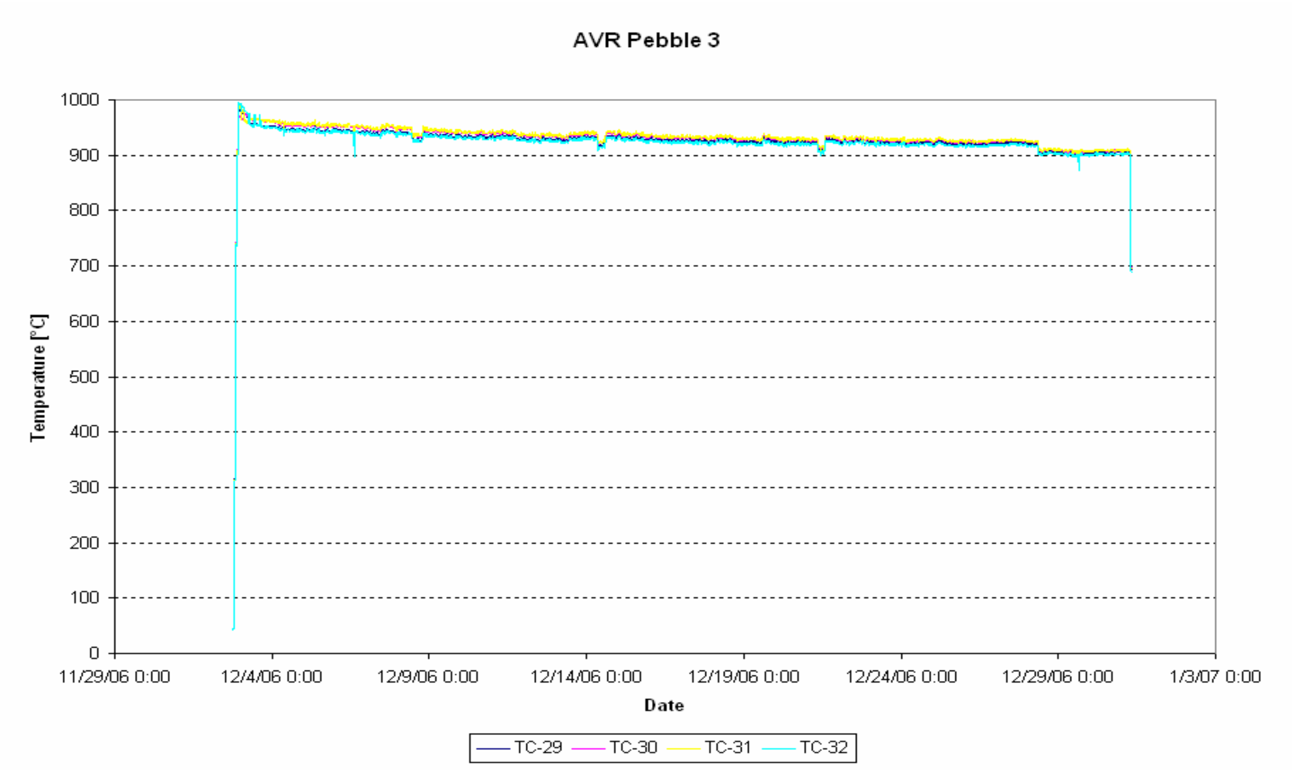

Figure 47: Temperatures pebble AVR.3 (TC-28, TC-29, TC-30, TC-31)

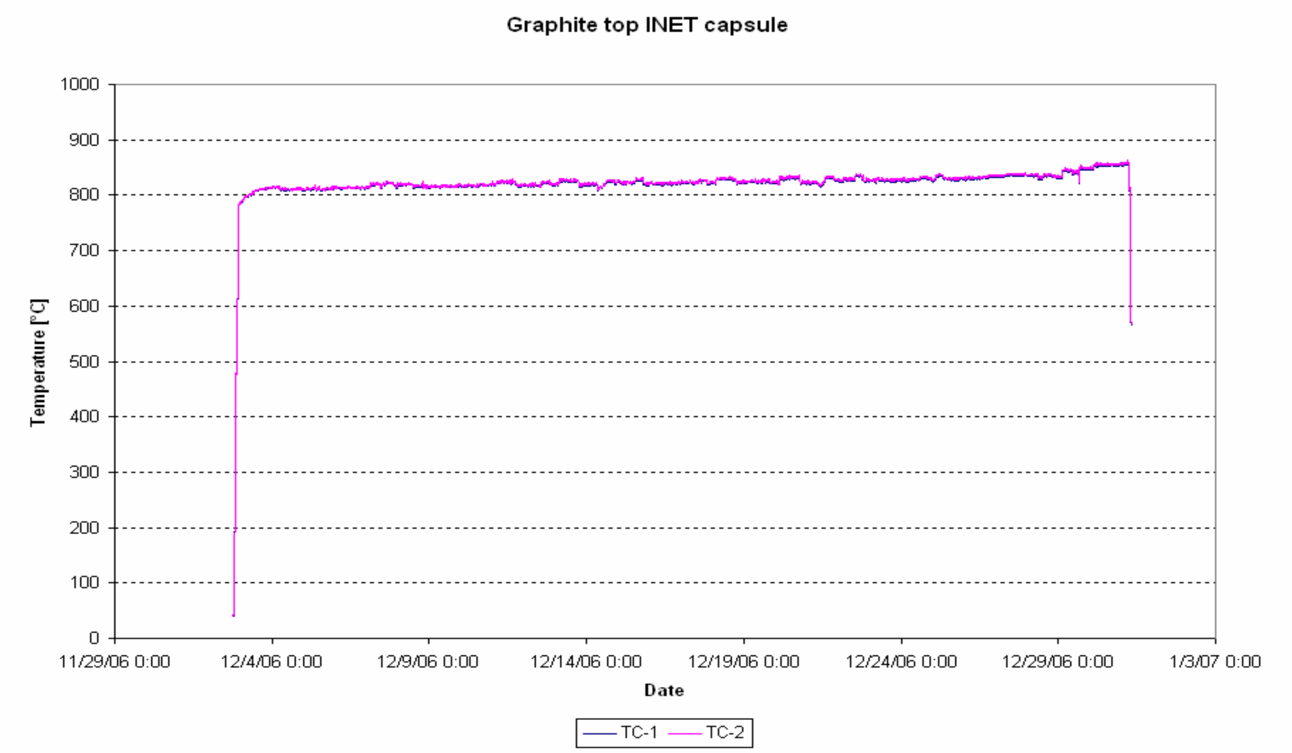

Figure 48: Temperatures top graphite INET capsule (TC-01, TC-02)

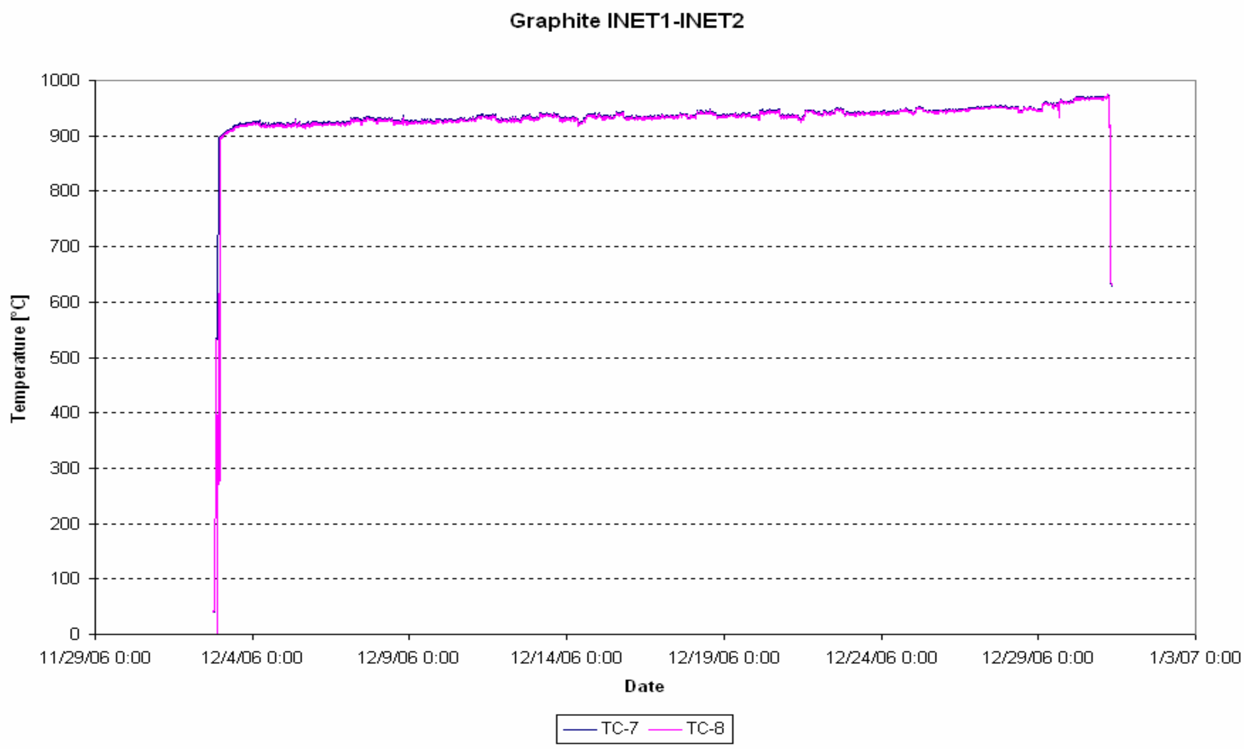

Figure 49: Temperatures graphite between INET.1 and INET.2 (TC-07, TC-08)

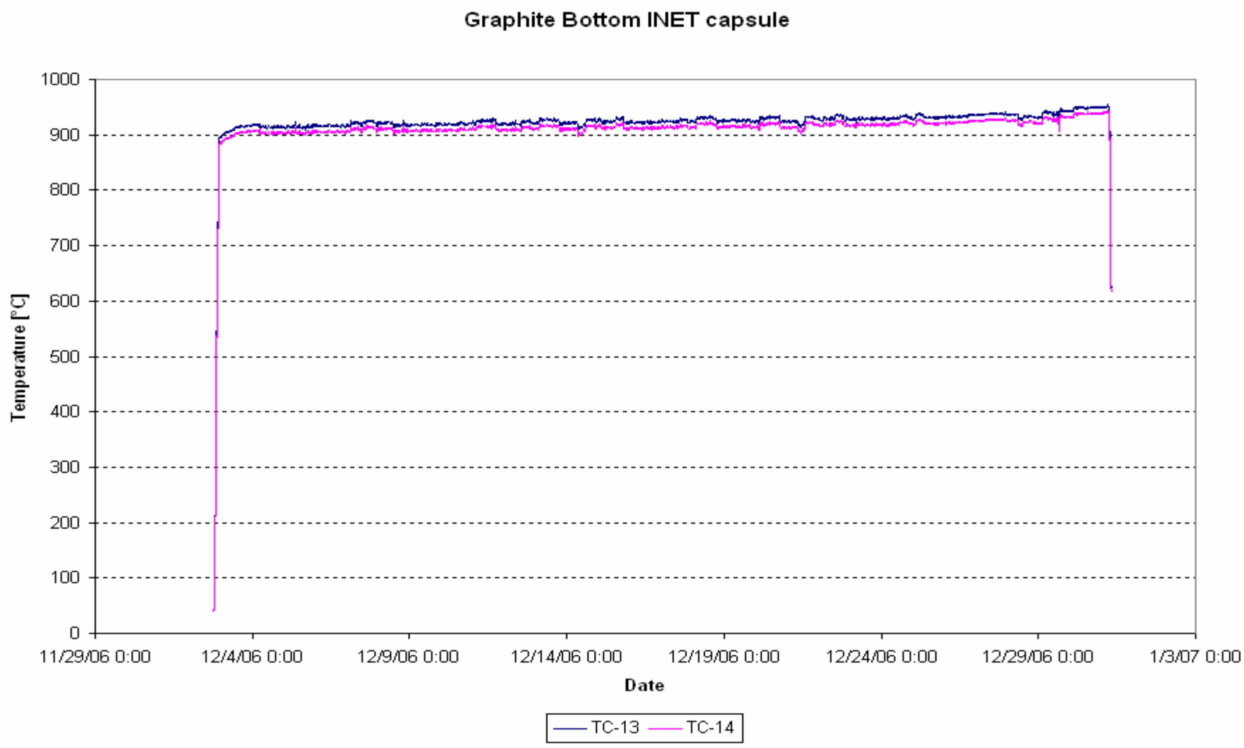

Figure 50: Temperatures bottom graphite INET Capsule (TC-13, TC-14)

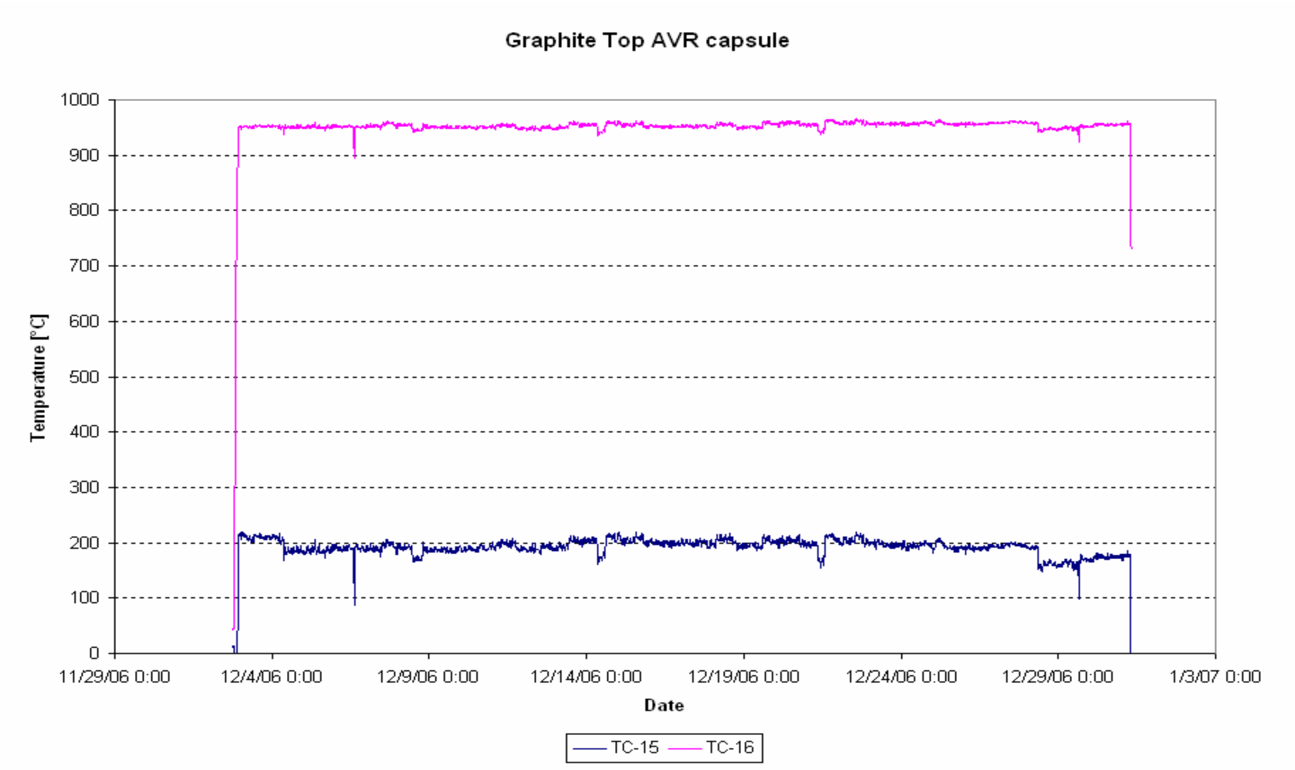

Figure 51: Temperatures top graphite AVR capsule (TC-15, TC-16)

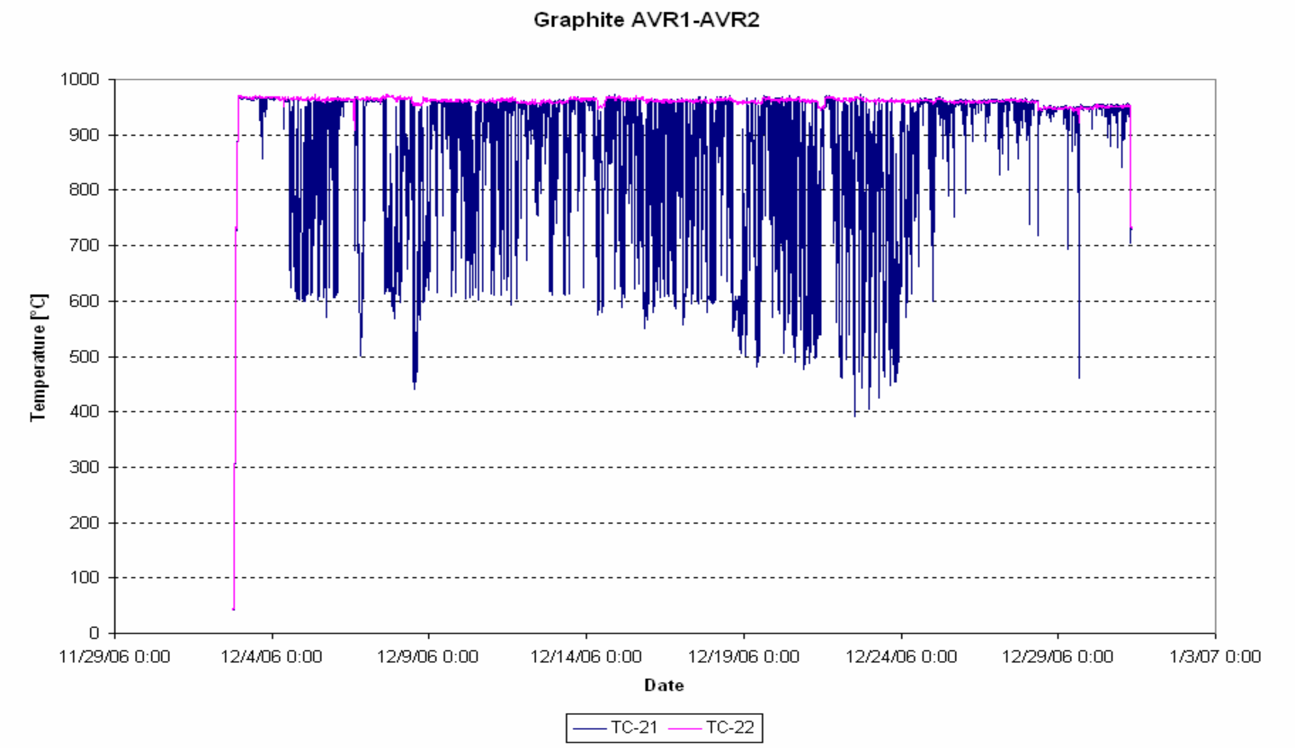

Figure 52: Temperatures graphite between AVR.1 and AVR.2 (TC-21, TC-22)

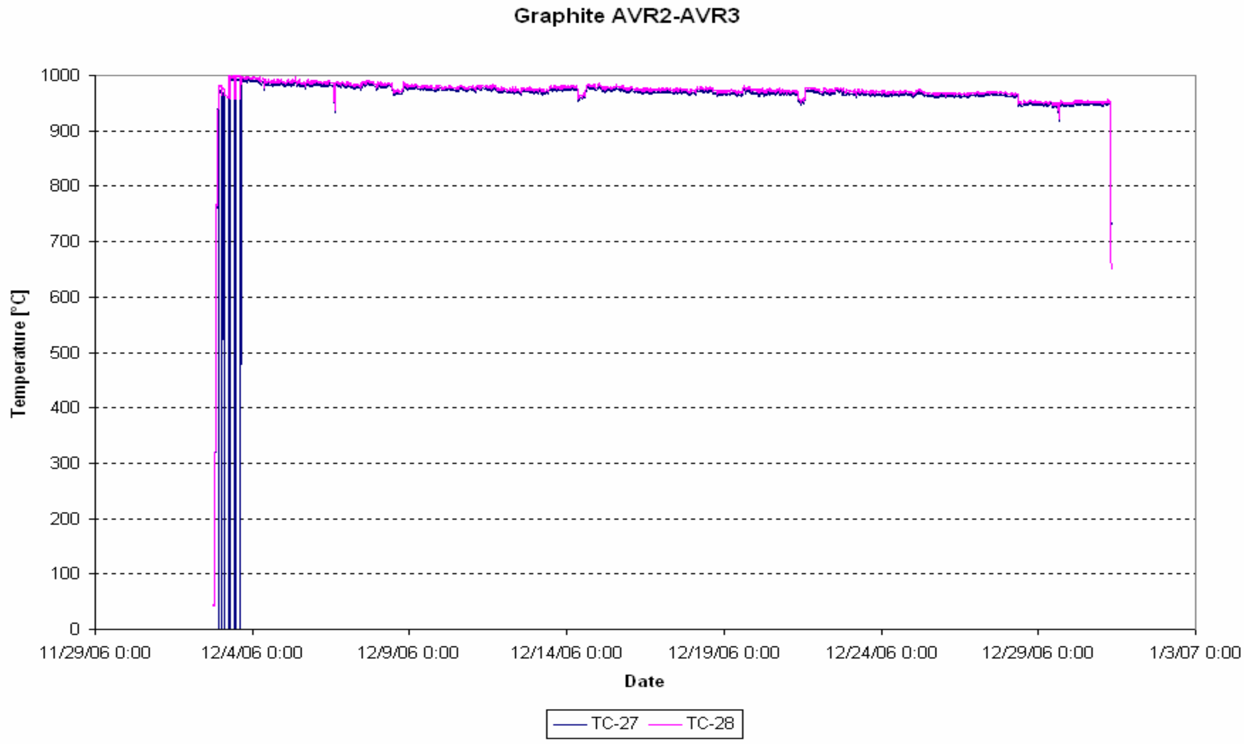

Figure 53: Temperatures graphite between AVR.2 and AVR.3 (TC-27, TC-28)

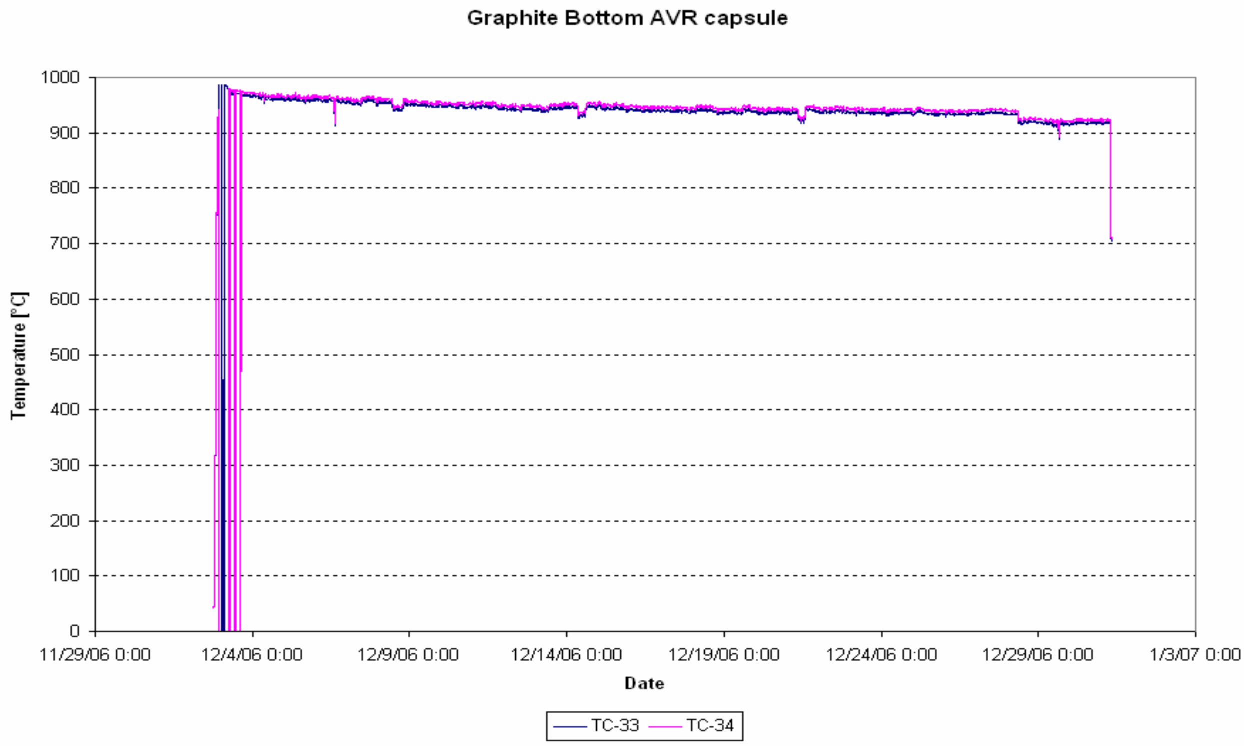

Figure 54: Temperatures bottom graphite (TC-33, TC-34)

TC number	Average temperature during full power operation [°C]	Average temperature during high temperature operation [°C]	Target temperature [°C]	Location
TC-01	828.2	836.7		Graphite
TC-02	827.5	836.1		
TC-03	823.6	832.3		INET 1
TC-04	825.1	833.8		
TC-05	824.2	832.9		
TC-06	820.5	829.0		
TC-07	916.2	926.4		Graphite
TC-08	901.1	911.7		
TC-09	914.4	924.7	940	INET 2
TC-10	914.6	924.7		
TC-11	909.0	919.2		
TC-12	913.1	923.6		
TC-13	909.8	919.5		Graphite
TC-14	908.9	918.8		
TC-15	319.7	323.6		Graphite
TC-16	932.7	938.9		
TC-17	905.4	911.6		AVR 1
TC-18	930.0	936.3		
TC-19	945.2	951.6	950	
TC-20	898.0	904.1		
TC-21	930.7	936.9		Graphite
TC-22	947.0	953.2		
TC-23	948.6	954.9		AVR 2
TC-24	959.6	966.1		
TC-25	938.2	944.8		
TC-26	925.0	931.3		
TC-27	954.4	960.9		Graphite
TC-28	965.2	971.6		
TC-29	935.9	942.4		AVR 3
TC-30	923.5	929.9		
TC-31	927.7	934.2		
TC-32	937.5	944.0		
TC-33	938.9	945.2		Graphite
TC-34	923.9	931.7		

Table 14: Time averaged temperature readings during cycle 06-10

6.4 Temperatures during Cycle 07-01

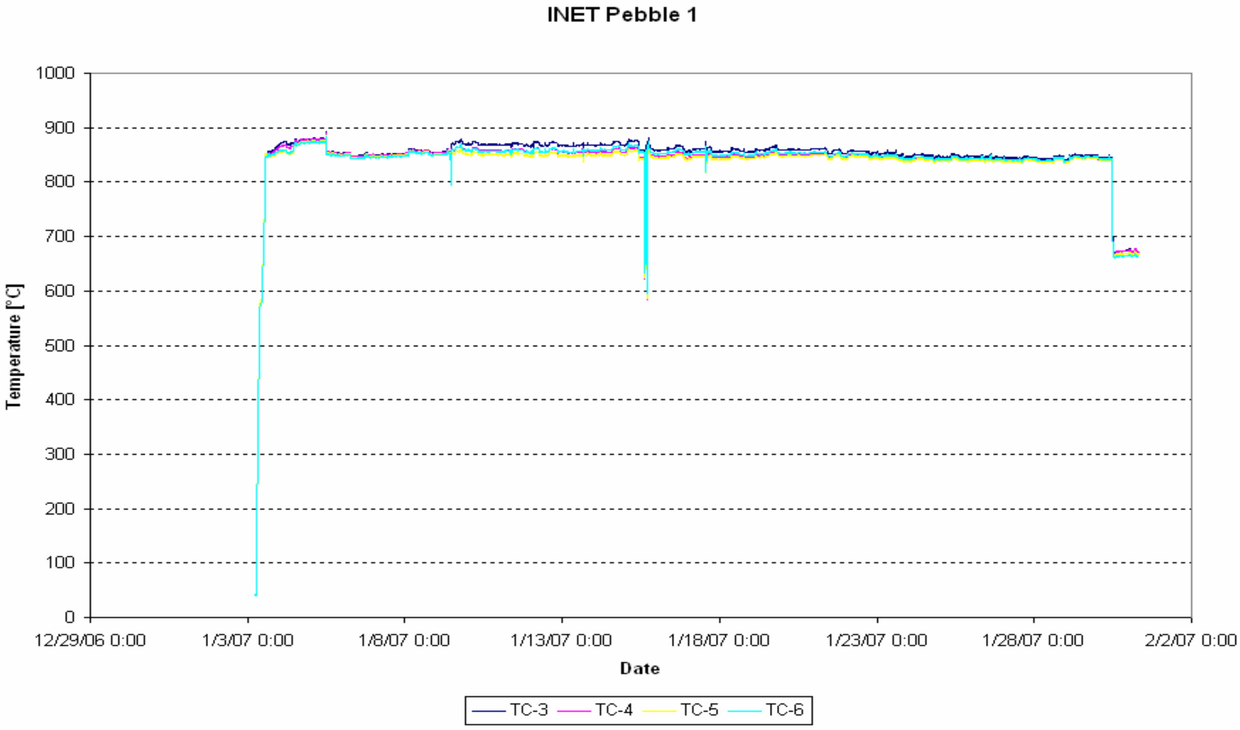

Figure 55: Temperatures pebble INET.1 (TC-03, TC-04, TC-05, TC-06)

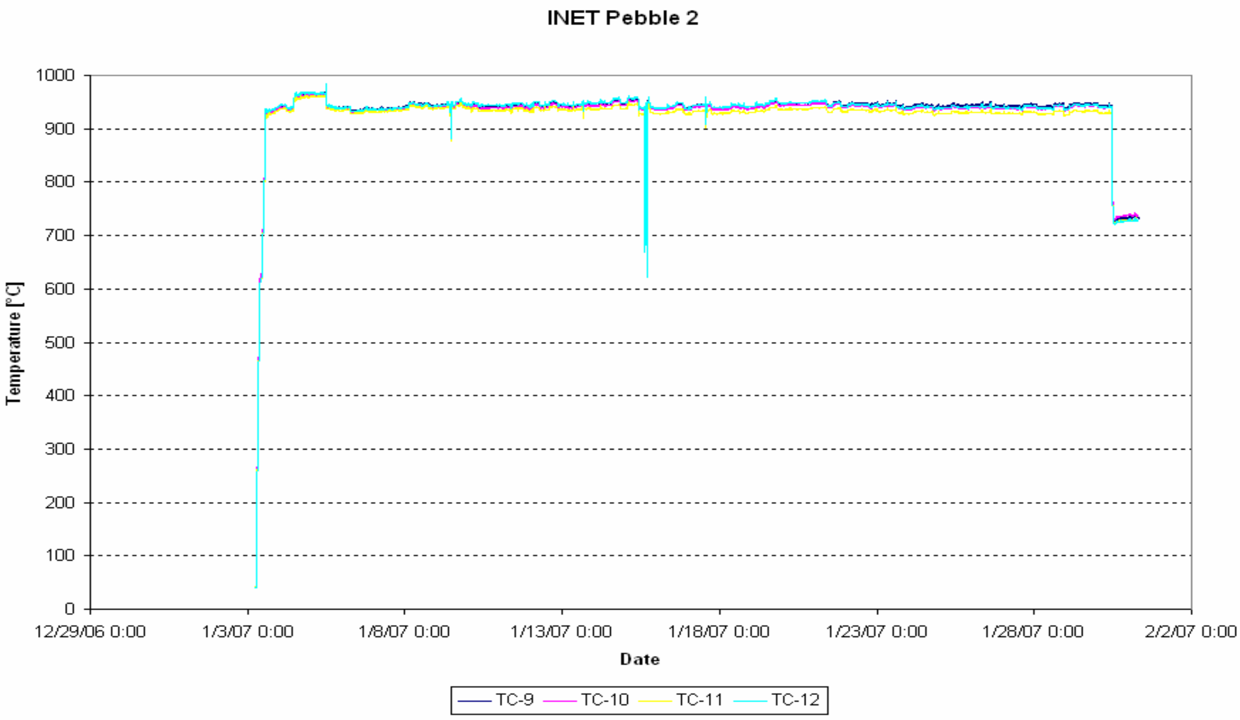

Figure 56: Temperatures pebble INET.2 (TC-09, TC-10, TC-11, TC-12)

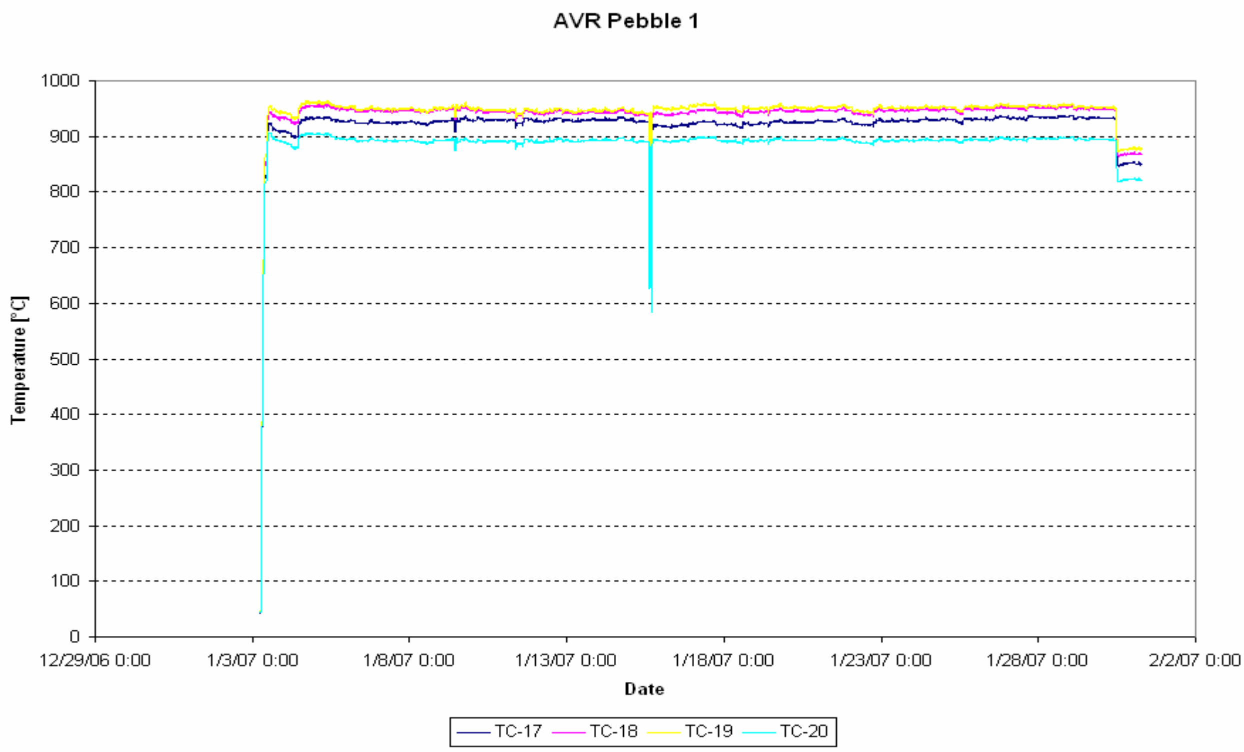

Figure 57: Temperatures pebble AVR.1 (TC-17, TC-18, TC-19, TC-20)

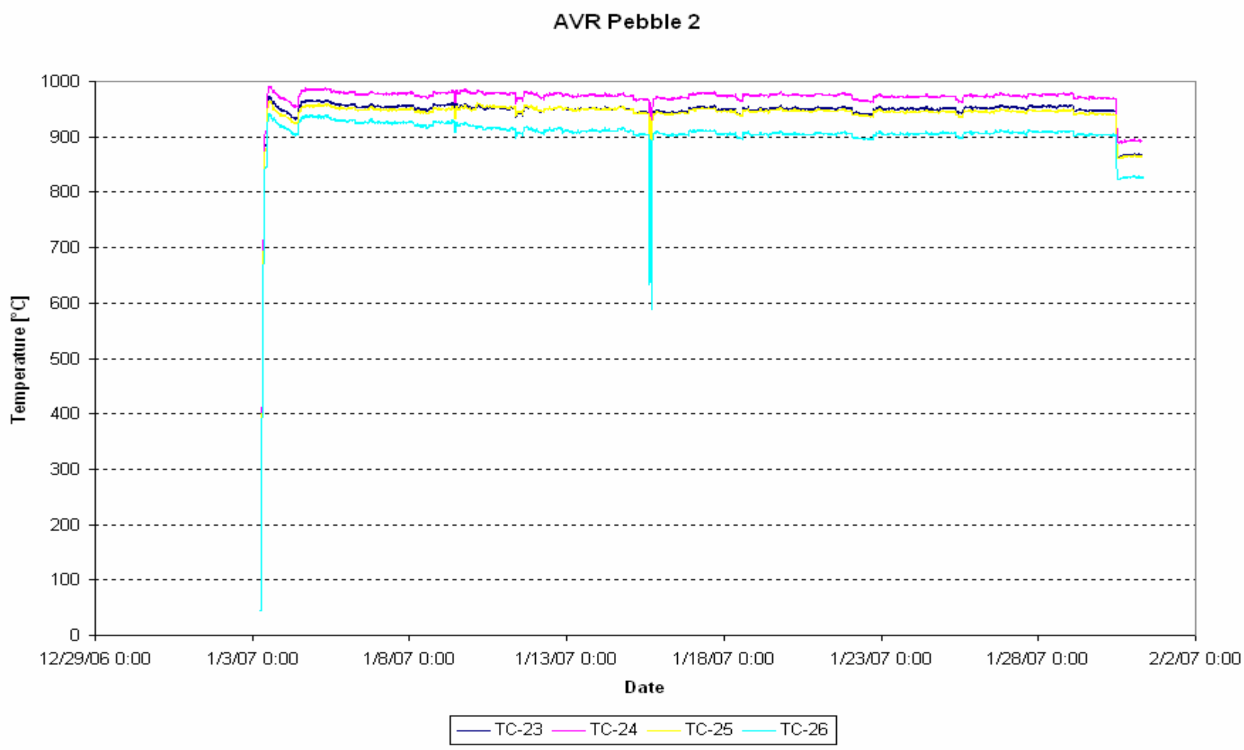

Figure 58: Temperatures pebble AVR.2 (TC-23, TC-24, TC-25, TC-26)

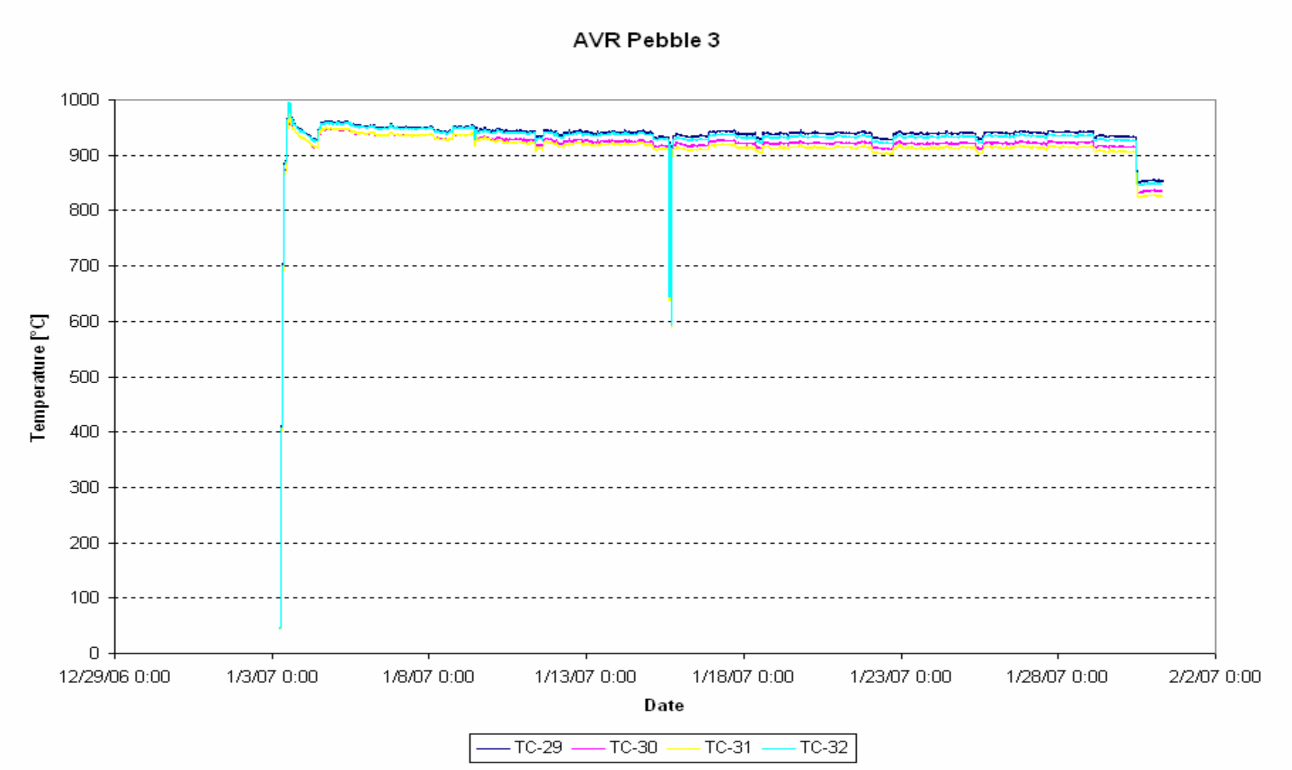

Figure 59: Temperatures pebble AVR.3 (TC-28, TC-29, TC-30, TC-31)

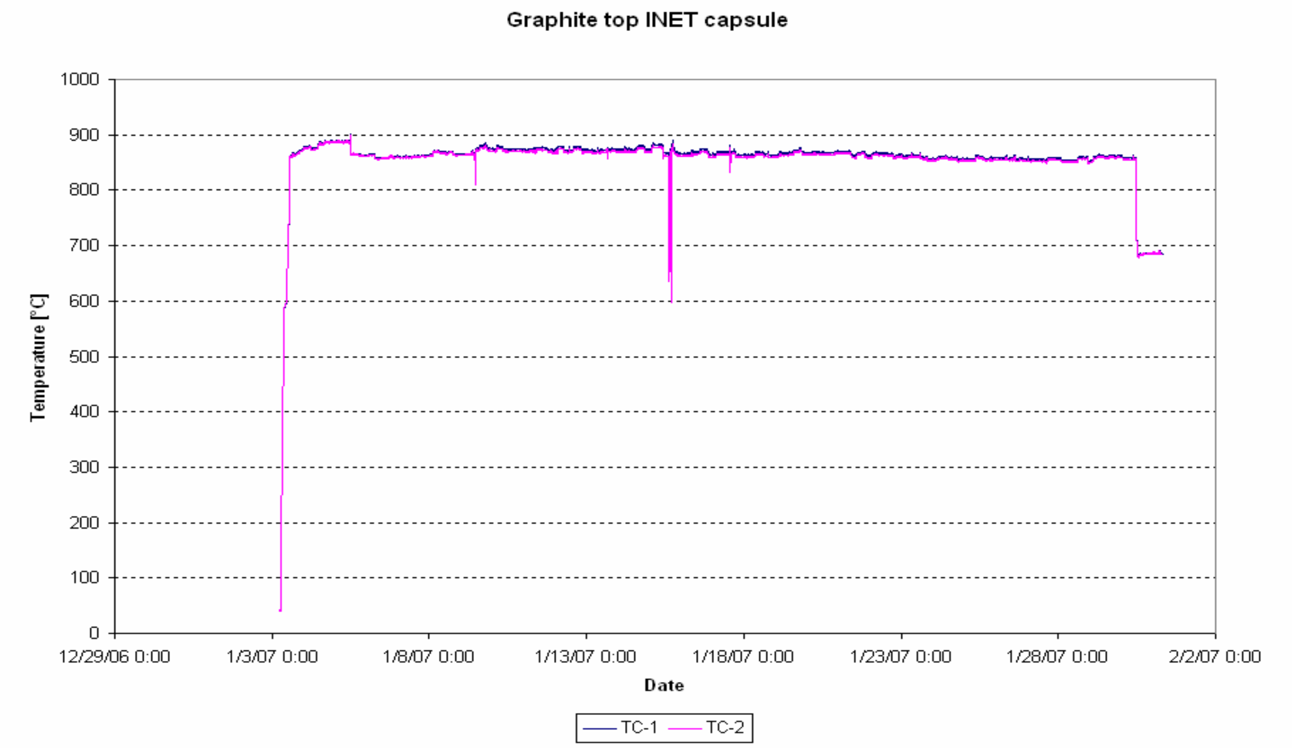

Figure 60: Temperatures top graphite INET capsule (TC-01, TC-02)

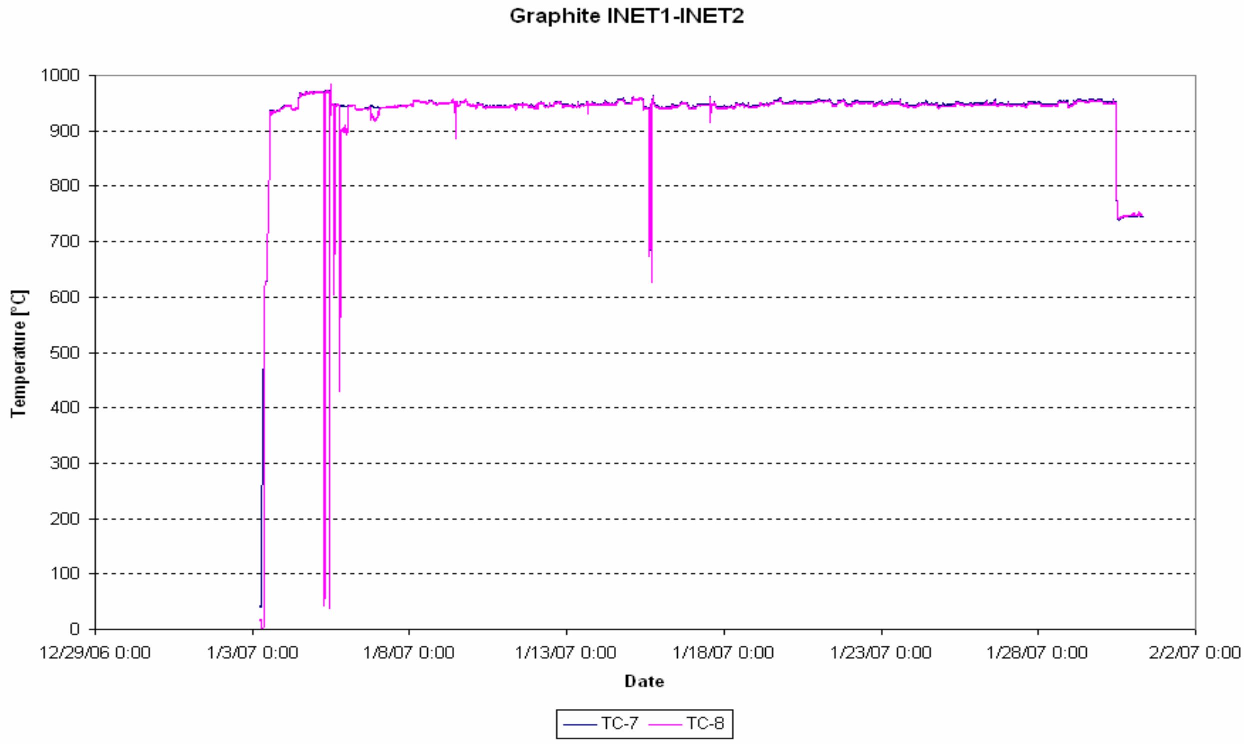

Figure 61: Temperatures graphite between INET.1 and INET.2 (TC-07, TC-08)

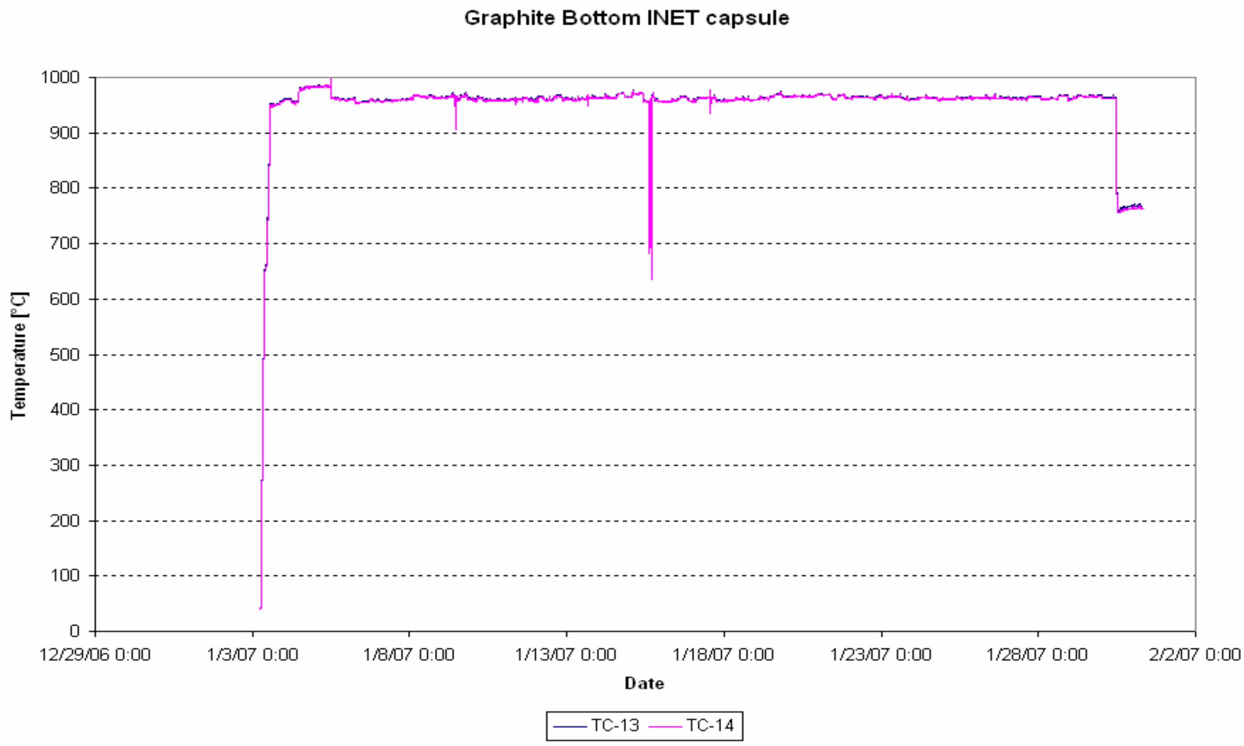

Figure 62: Temperatures bottom graphite INET Capsule (TC-13, TC-14)

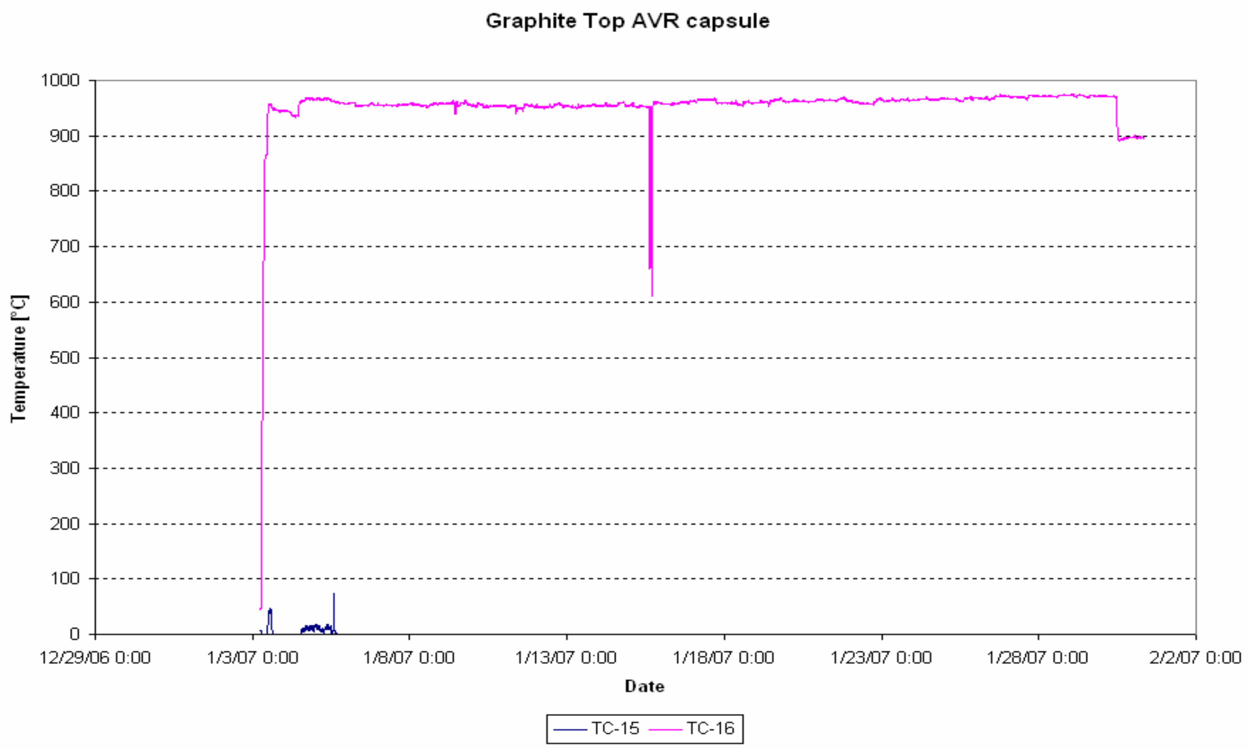

Figure 63: Temperatures top graphite AVR capsule (TC-15, TC-16)

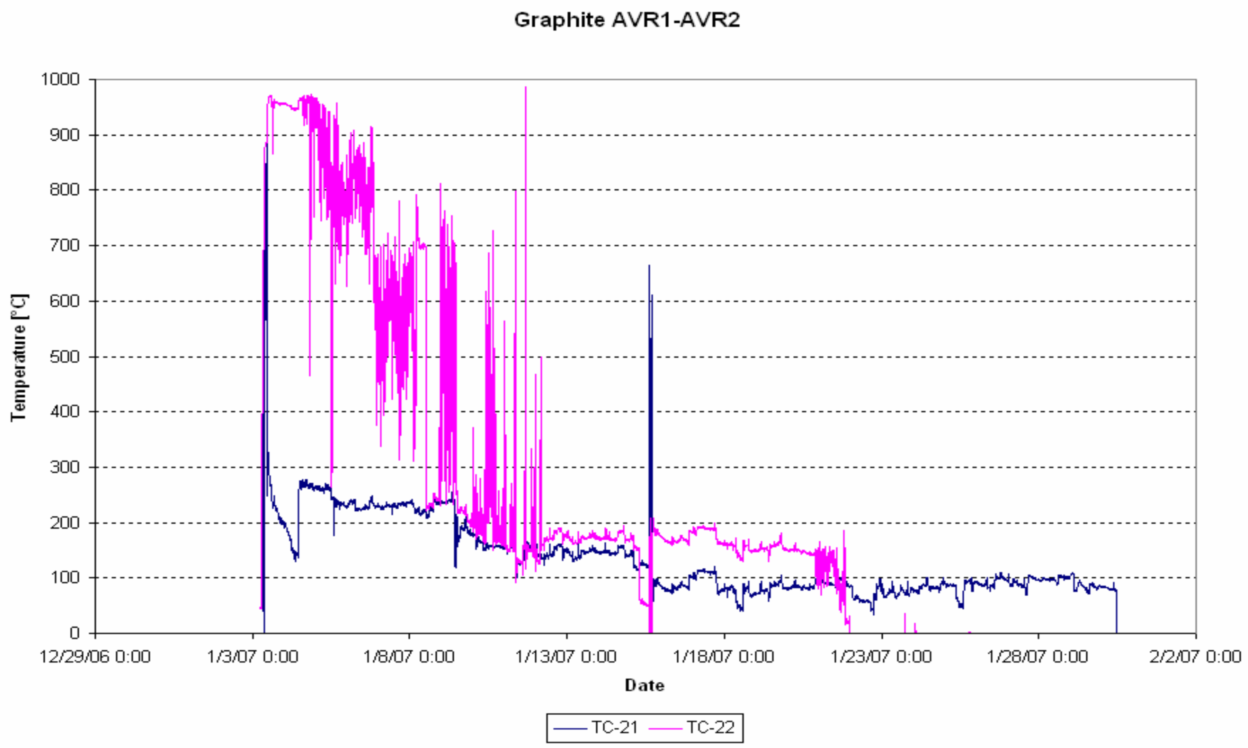

Figure 64: Temperatures graphite between AVR.1 and AVR.2 (TC-21, TC-22)

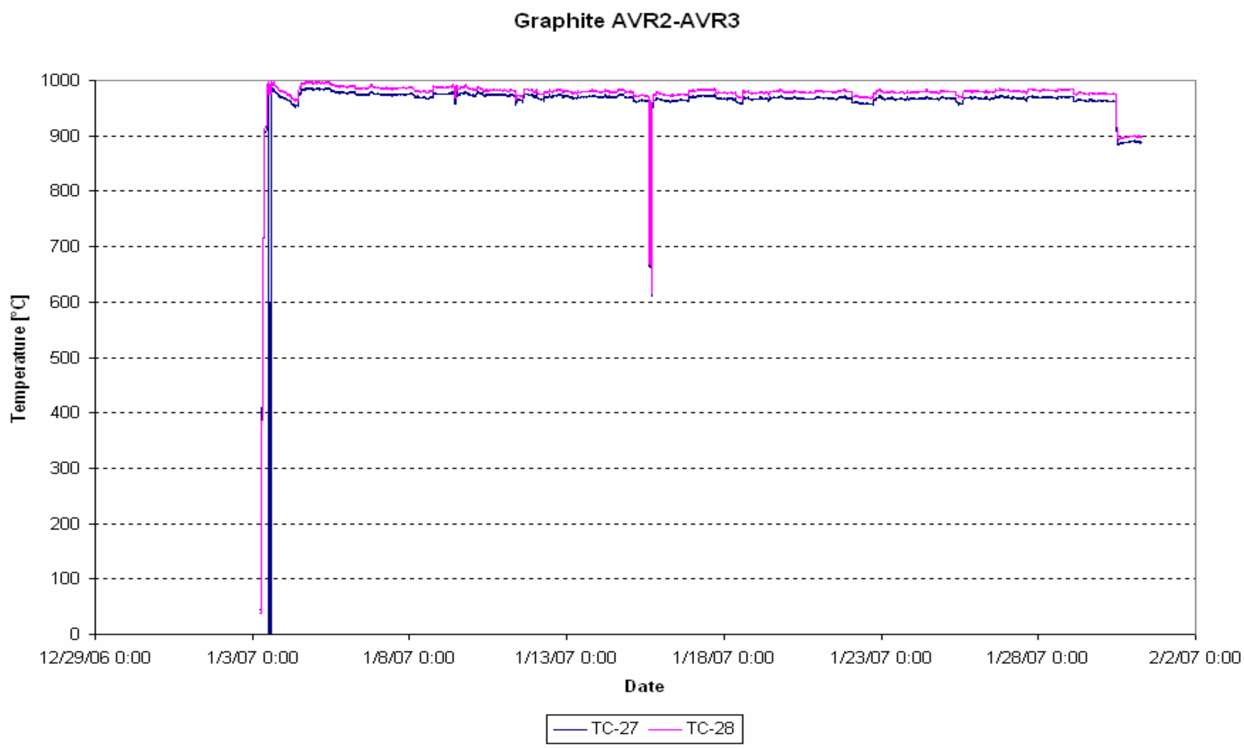

Figure 65: Temperatures graphite between AVR.2 and AVR.3 (TC-27, TC-28)

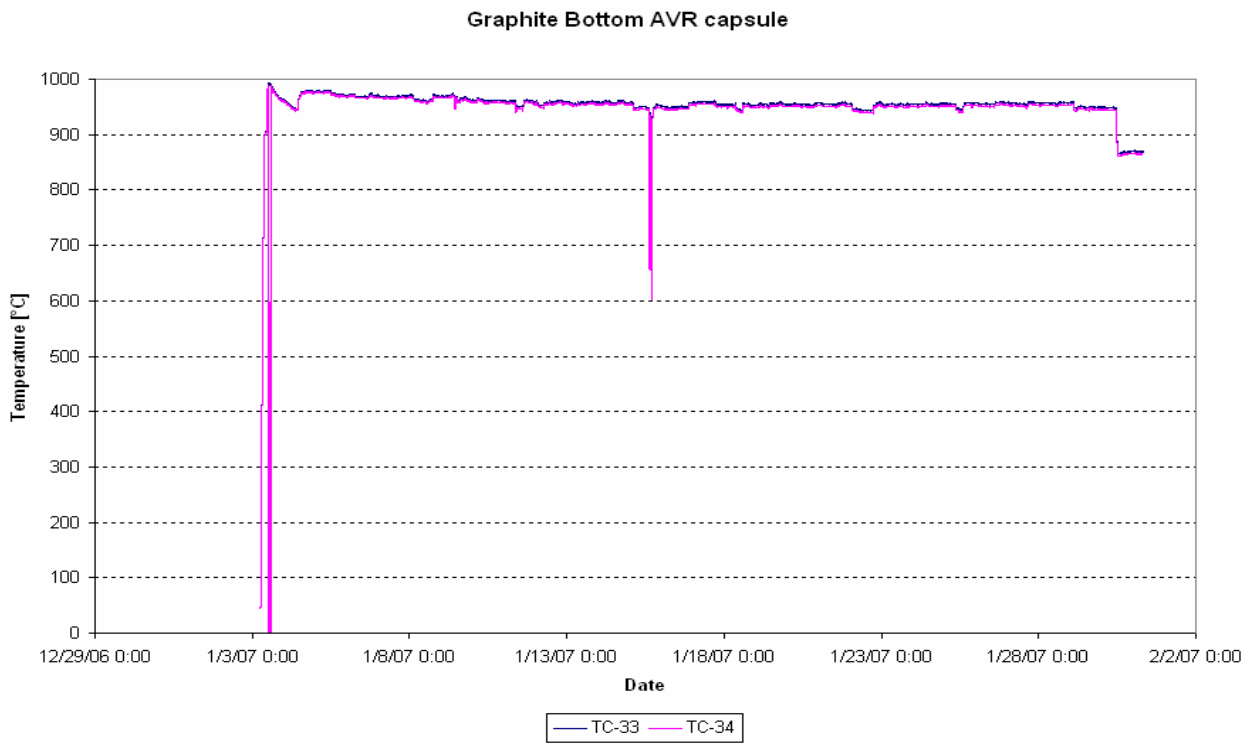

Figure 66: Temperatures bottom graphite (TC-33, TC-34)

TC number	Average temperature during full power operation [℃]	Average temperature during high temperature operation [℃]	Target temperature [℃]	Location
TC-01	859.9	866.5		Graphite
TC-02	856.8	863.3		
TC-03	850.9	857.6		INET 1
TC-04	843.7	850.2		
TC-05	840.5	847.0		
TC-06	844.4	851.2		
TC-07	941.1	948.5		Graphite
TC-08	936.7	943.9		
TC-09	936.1	943.8	940	INET 2
TC-10	933.3	940.7		
TC-11	926.7	934.2		
TC-12	935.8	943.7		
TC-13	955.9	963.0		Graphite
TC-14	954.8	962.1		
TC-15	0.6	0.5		Graphite
TC-16	957.8	960.0		
TC-17	924.1	926.6		AVR 1
TC-18	942.5	945.1		
TC-19	947.5	949.8	950	
TC-20	890.5	892.8		
TC-21	129.8	131.9		Graphite
TC-22	230.7	233.7		
TC-23	948.0	950.7		AVR 2
TC-24	971.5	974.1		
TC-25	943.9	946.5		
TC-26	908.4	911.0		
TC-27	966.3	968.9		Graphite
TC-28	977.3	979.9		
TC-29	938.5	941.2		AVR 3
TC-30	922.0	924.7		
TC-31	916.6	919.3		
TC-32	934.0	936.5		
TC-33	954.9	957.5		Graphite
TC-34	947.9	953.3		

Table 15: Time averaged temperature readings during cycle 07-01

7 Temperature Compensation

The experiment compraises 34 thermocouples connected in the rig-head to copper wires for data transmission to the temperature control unit and the data acquisition system of the HFR. These joints (Nisil/Nicrosil to copper wires) induce new thermocouples that might be influenced by temperature changes next to the plug and thus modify thermocouples values. As a matter of fact, three valves for capsule insulation are present in the rig-head close to the plug. They develop enough power to heat the thermocouple plug by approx. 30 K and could thus modify the readings. To avoid such systematic errors (that might vary with time depending on the use of the magnetic valves) four thermocouples were placed on the plugs to measure the real thermocouple signal deformations and thus deduce it from the readings.

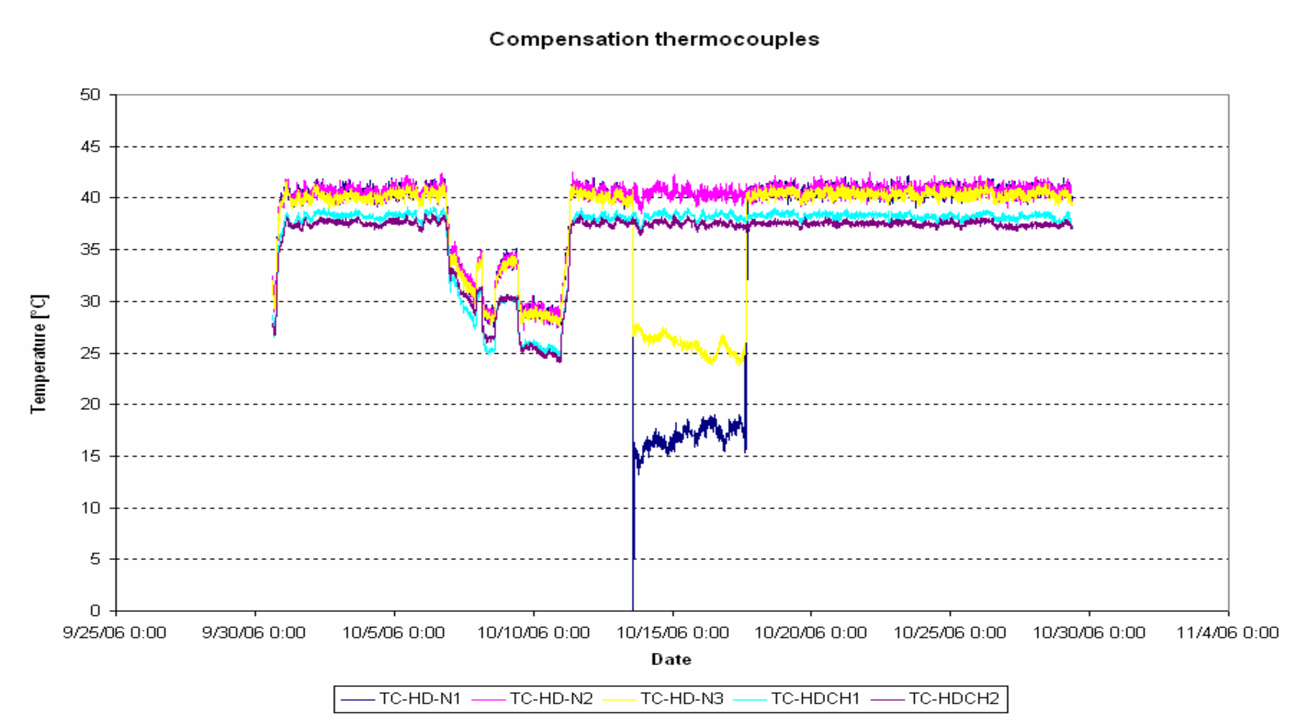

Figure 67: Reference thermocouples for temperatures compensation cycle 06-08 (TC-HD-N1, TC-HD-N2, TC-HD-N3, TC-HDCH1, TC-HDCH2)

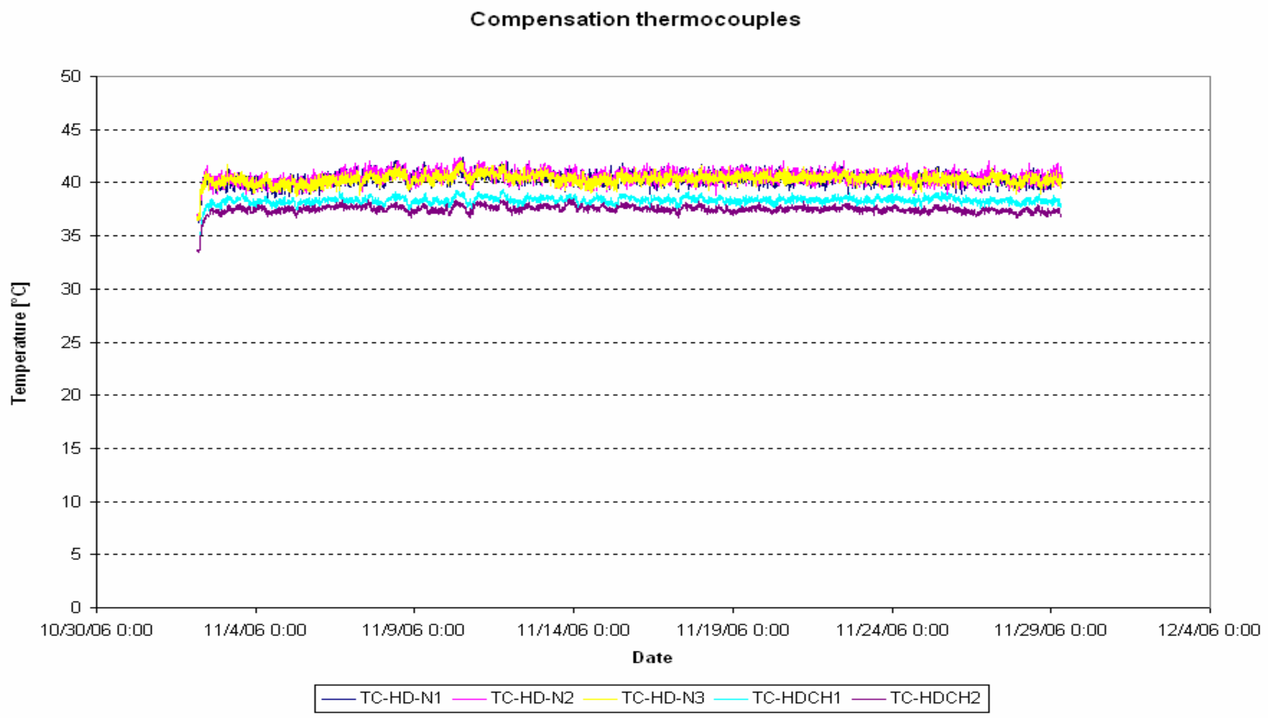

Figure 68: Reference thermocouples for temperatures compensation cycle 06-09 (TC-HD-N1, TC-HD-N2, TC-HD-N3, TC-HDCH1, TC-HDCH2)

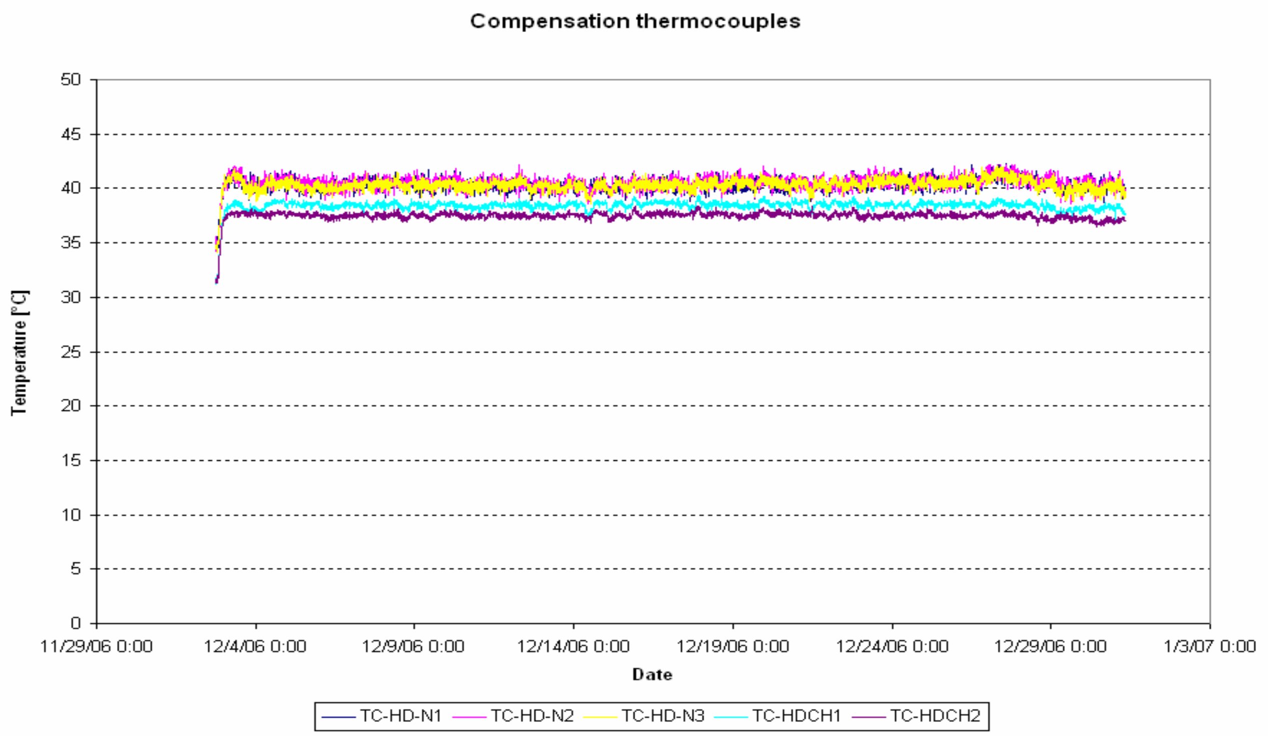

Figure 69: Reference thermocouples for temperatures compensation cycle 06-10 (TC-HD-N1, TC-HD-N2, TC-HD-N3, TC-HDCH1, TC-HDCH2)

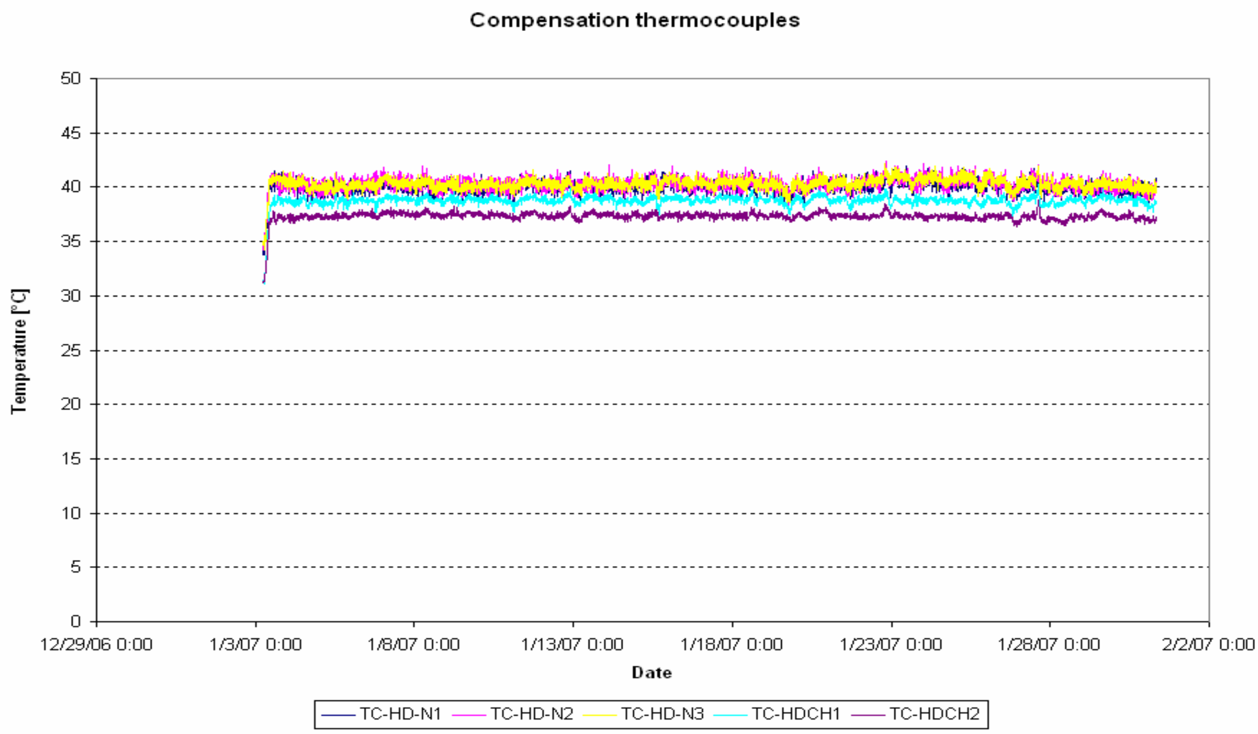

Figure 70: Reference thermocouples for temperatures compensation cycle 07-01 (TC-HD-N1, TC-HD-N2, TC-HD-N3, TC-HDCH1, TC-HDCH2)

8 Fission Gas Release Measurements

In HFR-EU1 the fission gas release was measured according to the following procedure:

A continuous gas flow (50 ml/min) was maintained throughout the cycles and the He/Ne mixture was adjusted to attain the target temperatures of TC-9 and TC-19 as the reference thermocouples. The gas sampling procedure can be resumed to:

1. Check if the selected capsule temperature remained constant over a significant time (minimum one hour).
2. Isolate manually the selected capsule by closing GA-MV1 or GA-MV2 and GA-MV13 and switch the gas flow through the filter station by closing SP I.X-MV5 and opening SP I.X-MV6 to avoid perturbation in the capsule.
3. Read GA-Pt1, the reference temperature, the gas mixture content and the sampling time and note these data.
4. Manually remove the tank from the glove box and replace it by another one for the following gas sample.
5. Open GA-MV1 or GA-MV2, depending on which capsule will be sampled and GA-MV13, switch the flow of the capsule to be purged from the filter station to the gas analysis glove box and proceed to the gamma spectrometry of the sample taken.

8.1 Evaluation of R/B

A good indication of particle health is the fraction between fission gas release rate (R) and fission gas birth rate (B) as a function of accumulated burn-up. For this reason, the following formula out of [5] was investigated:

$$\ln \frac{R}{B} = const1. - n \ln \lambda$$

From the measured concentration of 3 Kr and 2 Xe isotopes (statistical error 4 - 10% for Kr-85m, Kr-87, Kr-88 and Xe-135 and up to 20% for Xe-133), the gas pressure and the He flow-rate, the release rate R can be determined.
The birth rate B is calculated using the nominal number of fissions on the date of sampling.

The burn-up is the one pre-calculated for the experiment. Later adjustments will be made once the analysis of the burn-up measurements of the pebbles, the gamma scan wires and the fluence detectors are available.

Due to the HEU/LEU conversion of the HFR and the move of the experiment to another position, the value B has to be recalculated (activity underway). These values will be communicated later. This prevents us at this point in time from presenting release over birth vs burn-up results. Figure 71 and Figure 72 display release vs. time for the two capsules.

Nevertheless, the quality of the R/B measurement (steady-state R/B) can still be evaluated. Indeed, $\ln \frac{R}{B} = \ln \frac{R}{fission\_rate * yield} = \ln \frac{R}{yield} - \ln fission\_rate$ leading to:

$$\ln \frac{R}{yield} = const2. - n \ln \lambda$$

Considering ln R/yield instead of ln R/B for a fixed (even unknown) fission rate does not affect the plots inclination (characteristic of the measurement quality). For this reason, Figure 77 to Figure 84 display ln R/yield vs. ln λ_{ef} instead of ln R/B vs. ln λ_{eff}. R.

Note the activity peaks in Figure 71 and Figure 72. These five measurements were made with the same sampling container which proved to be contaminated and which will not be used any longer. Figure 73 and Figure 74 present the same results, without measurement taken with this gab sample.

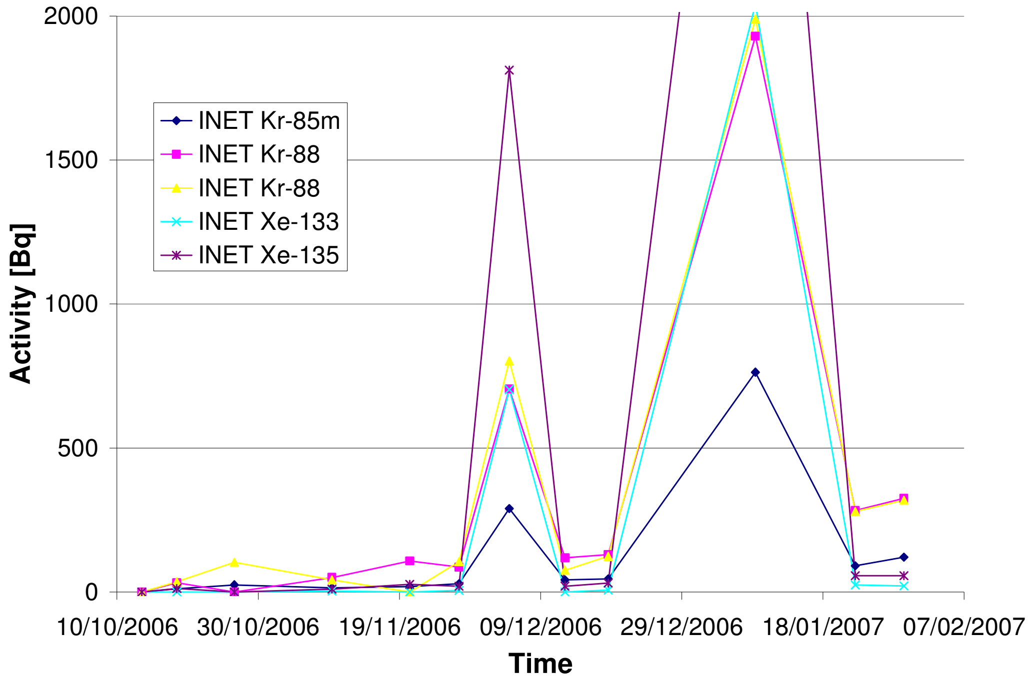

Figure 71: Release measurement vs. time for INET pebbles

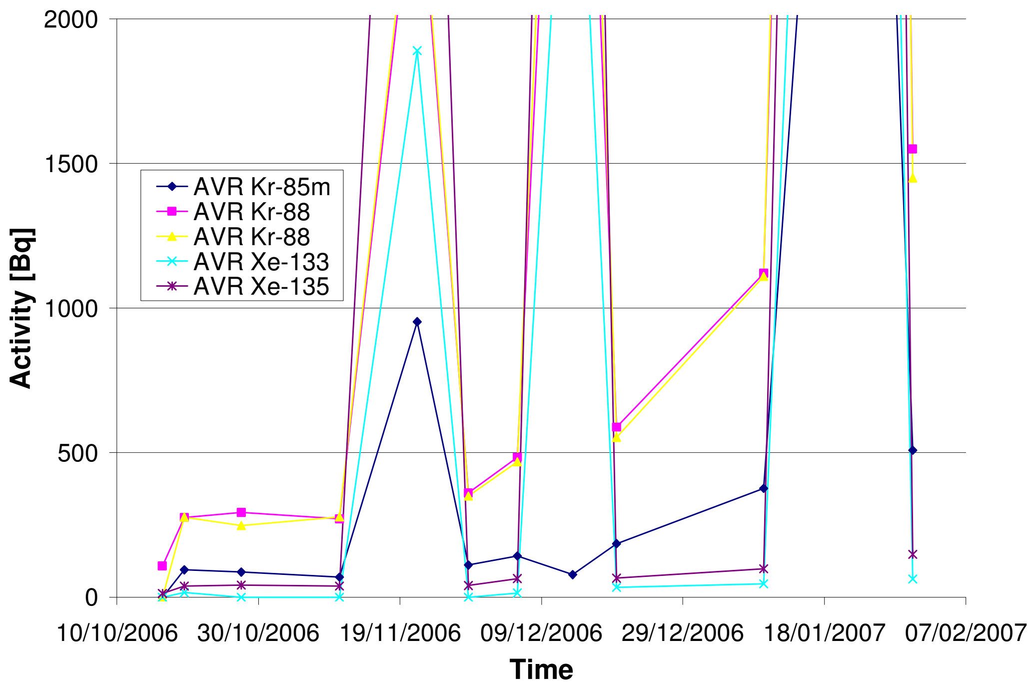

Figure 72: Release measurement vs. time for AVR pebbles

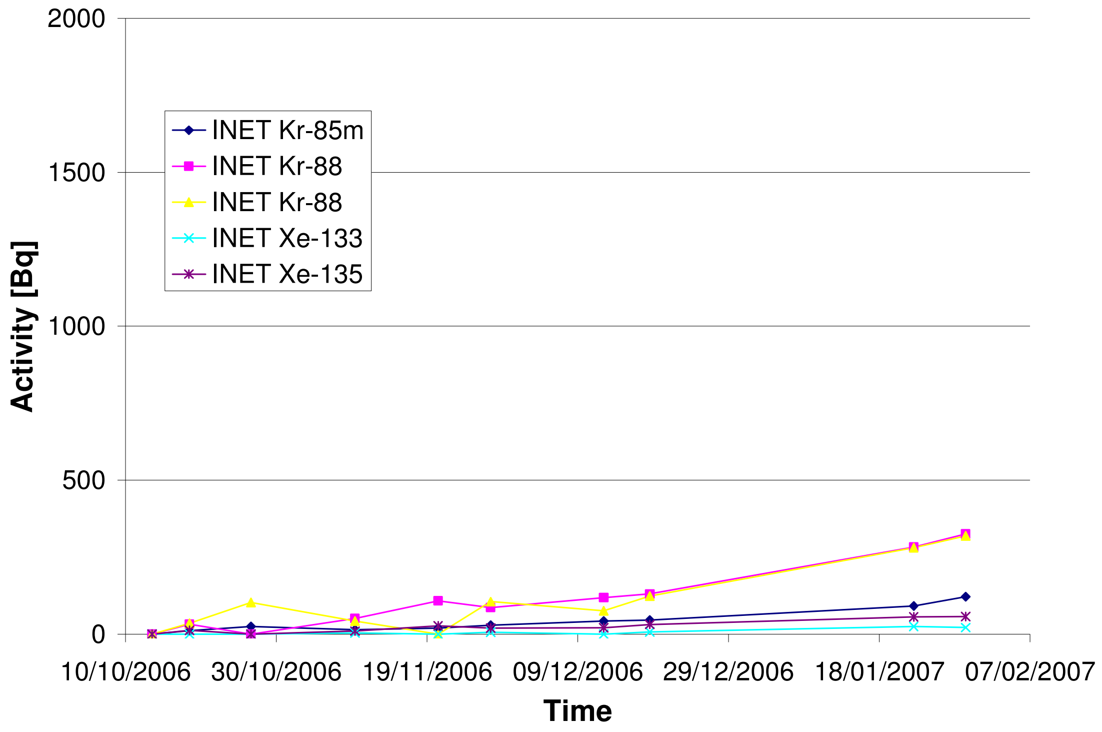

Figure 73: Purged release measurement vs. time for INET pebbles

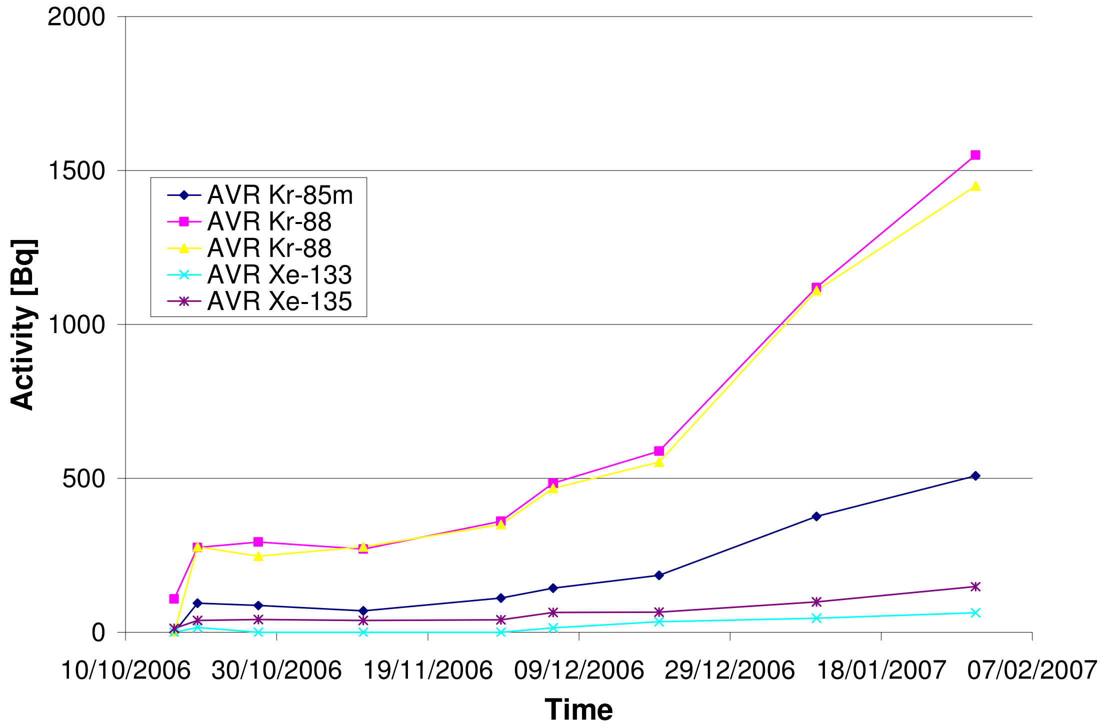

Figure 74: Purged release measurement vs. time for AVR pebbles

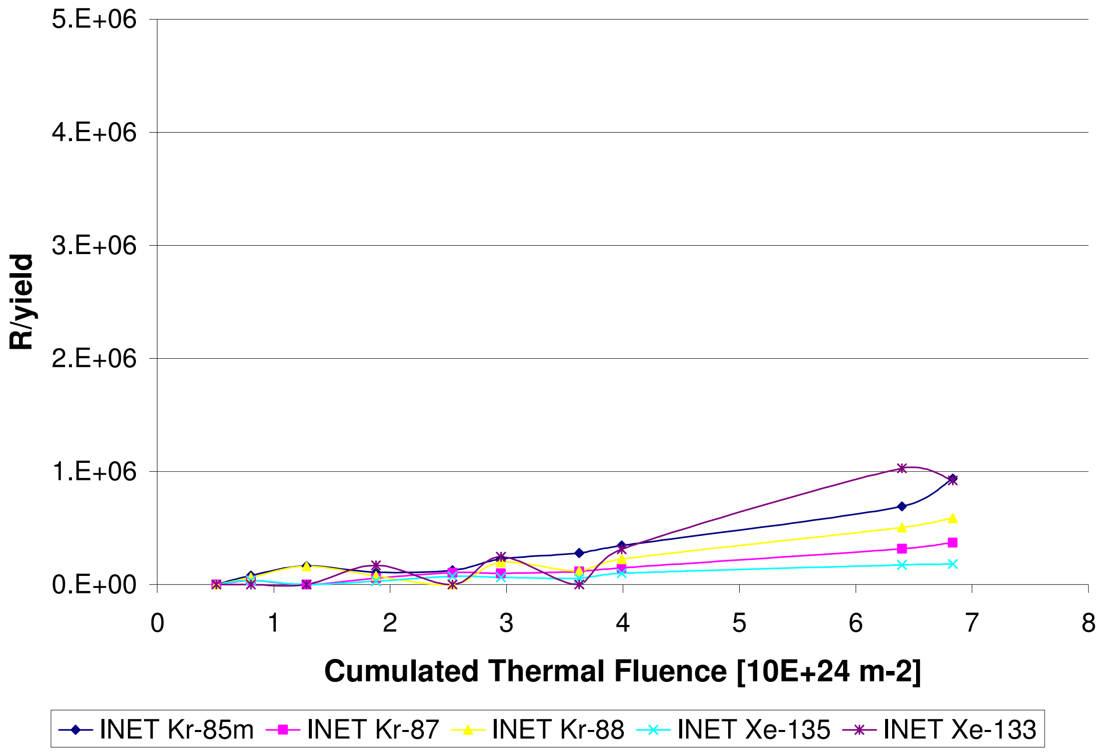

Figure 75: Release over yield vs. cumulative thermal fluence for INET pebbles

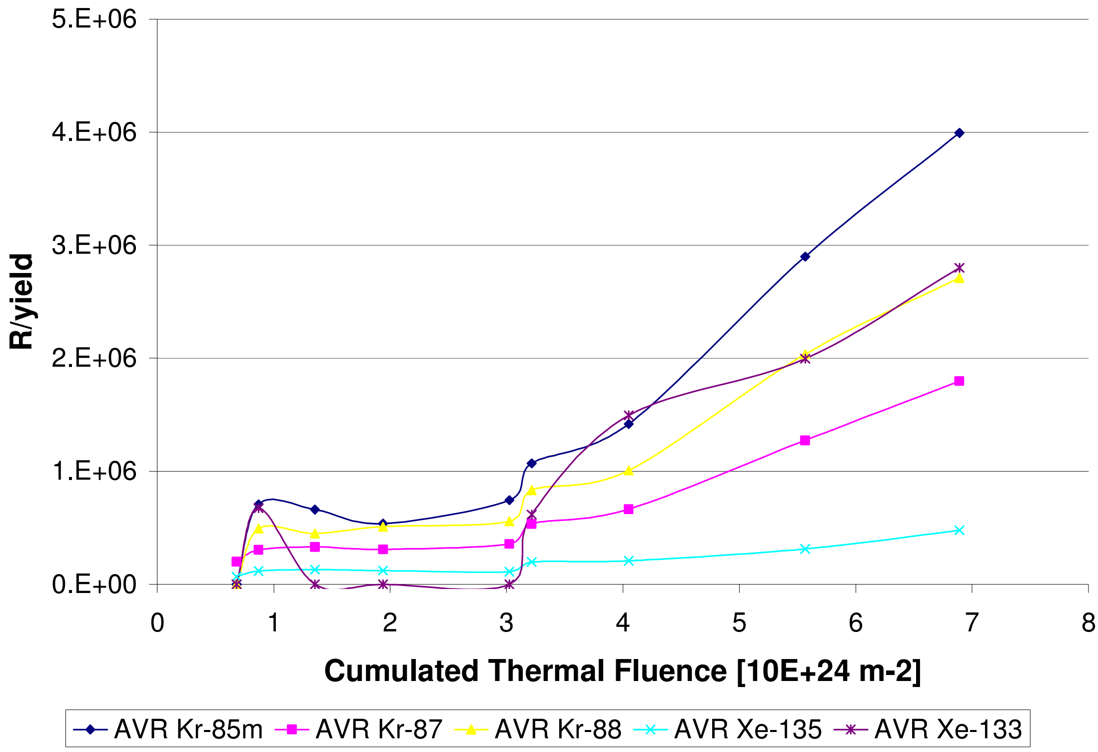

Figure 76: Release over yield vs. cumulative thermal fluence for AVR pebbles

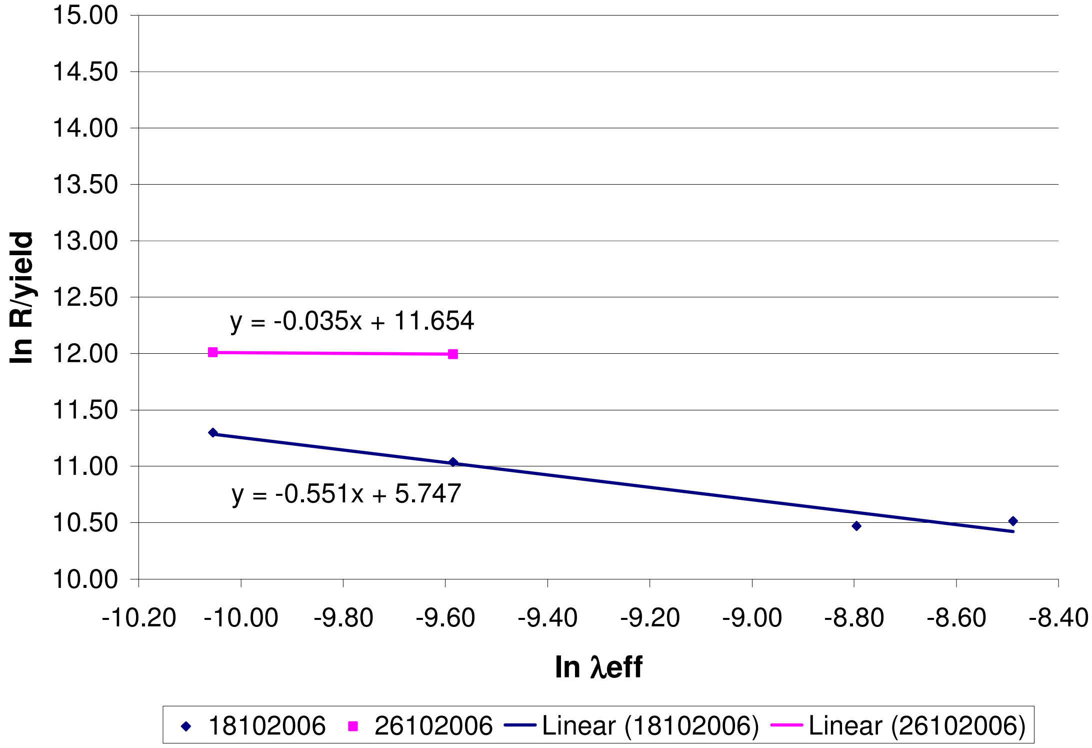

Figure 77: ln R/yield vs. ln λ_{eff} plots for gas release measurements of INET pebbles 06-08

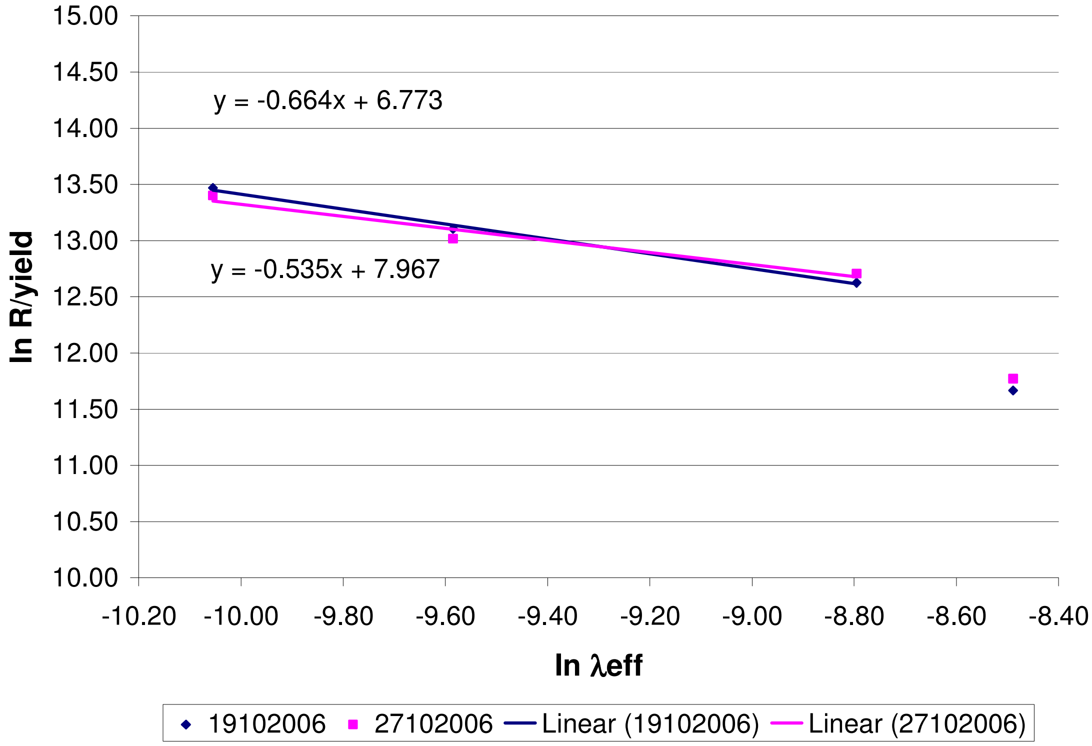

Figure 78: ln R/yield vs. ln λ_{eff} plots for gas release measurements of AVR pebbles 06-08

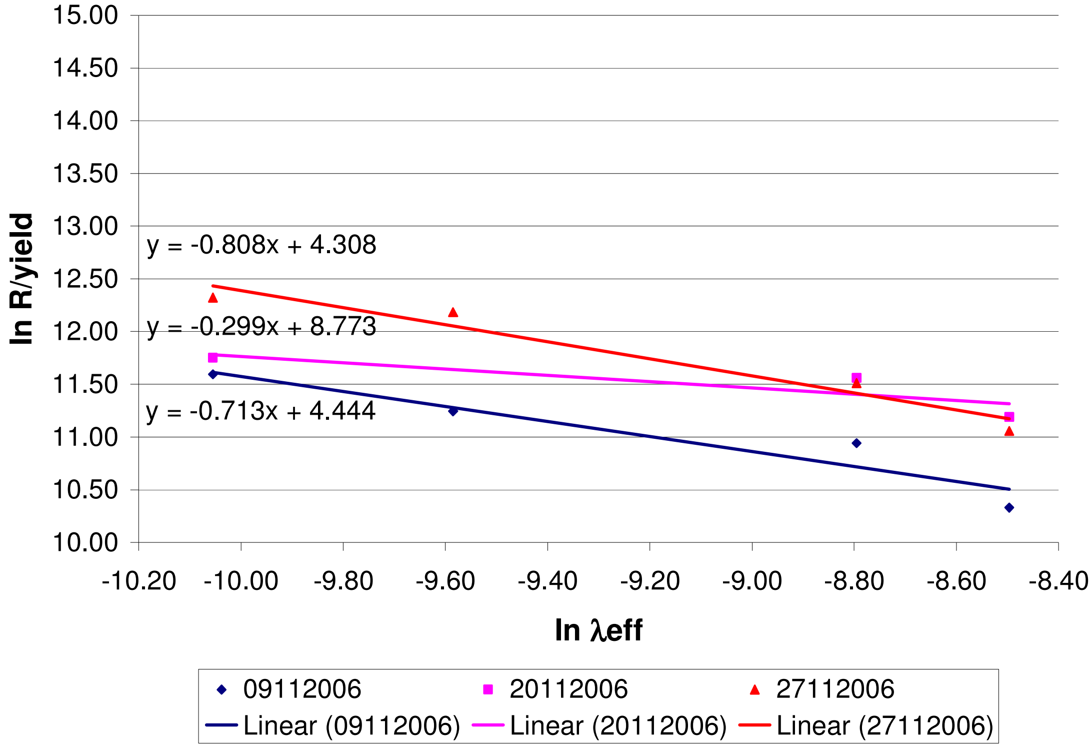

Figure 79: ln R/yield vs. ln λ_{eff} plots for gas release measurements of INET pebbles 06-09

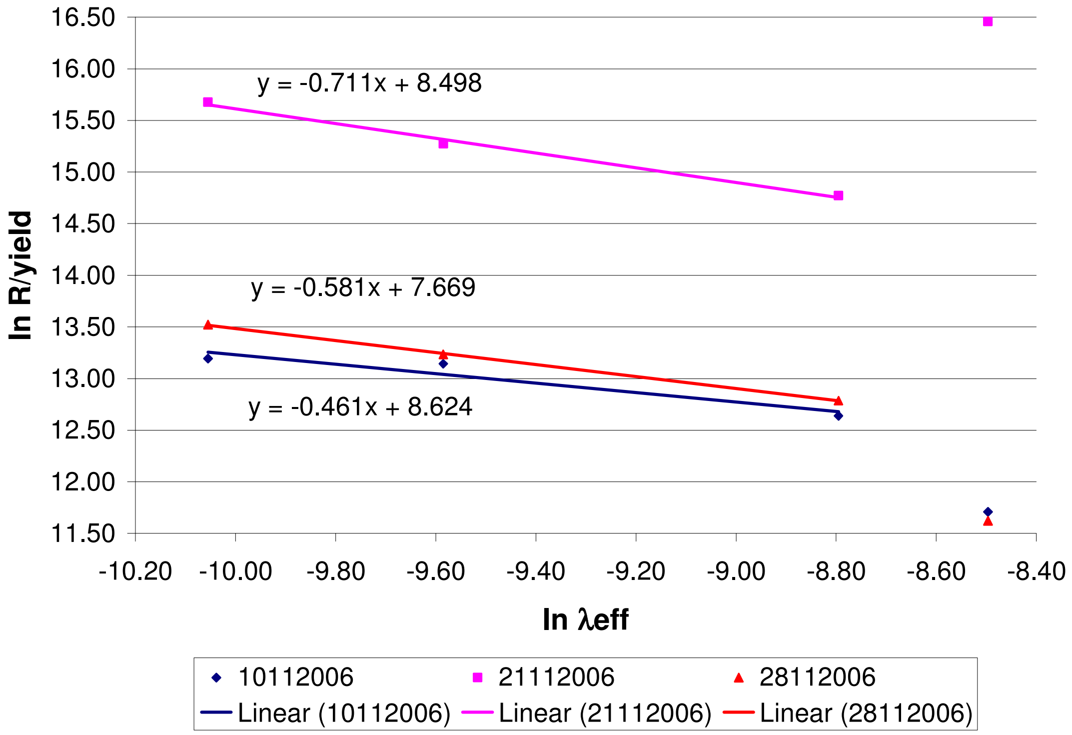

Figure 80: ln R/yield vs. ln λ_{eff} plots for gas release measurements of AVR pebbles 06-09

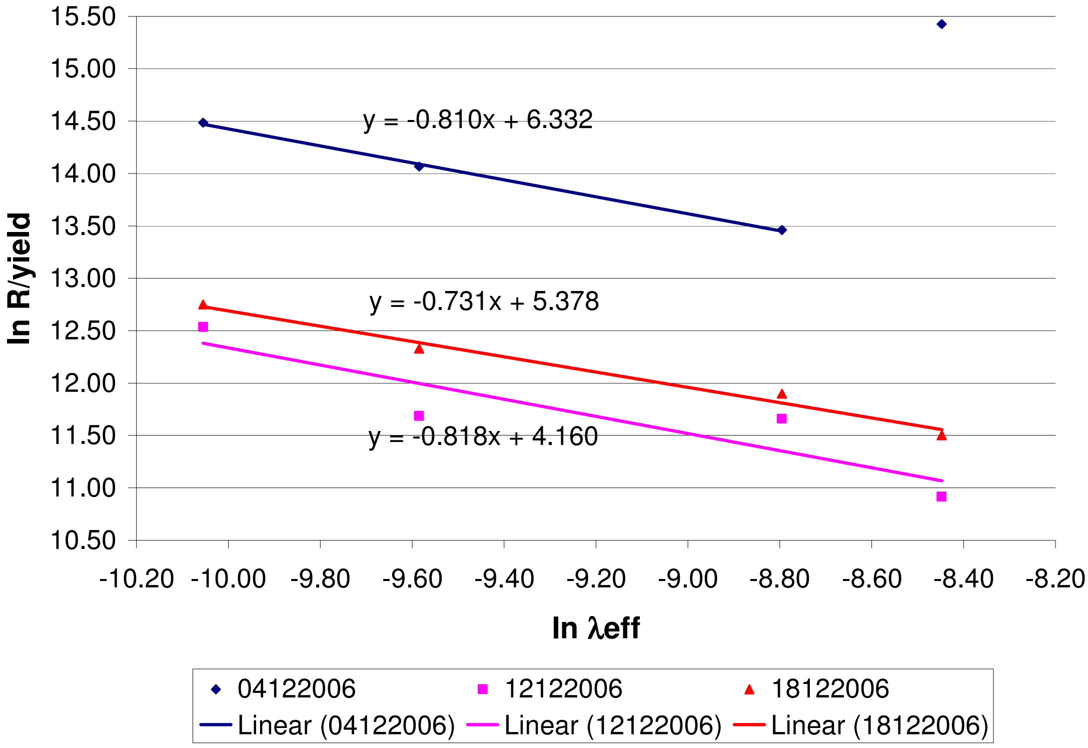

Figure 81: ln R/yield vs. ln λ_{eff} plots for gas release measurements of INET pebbles 06-10

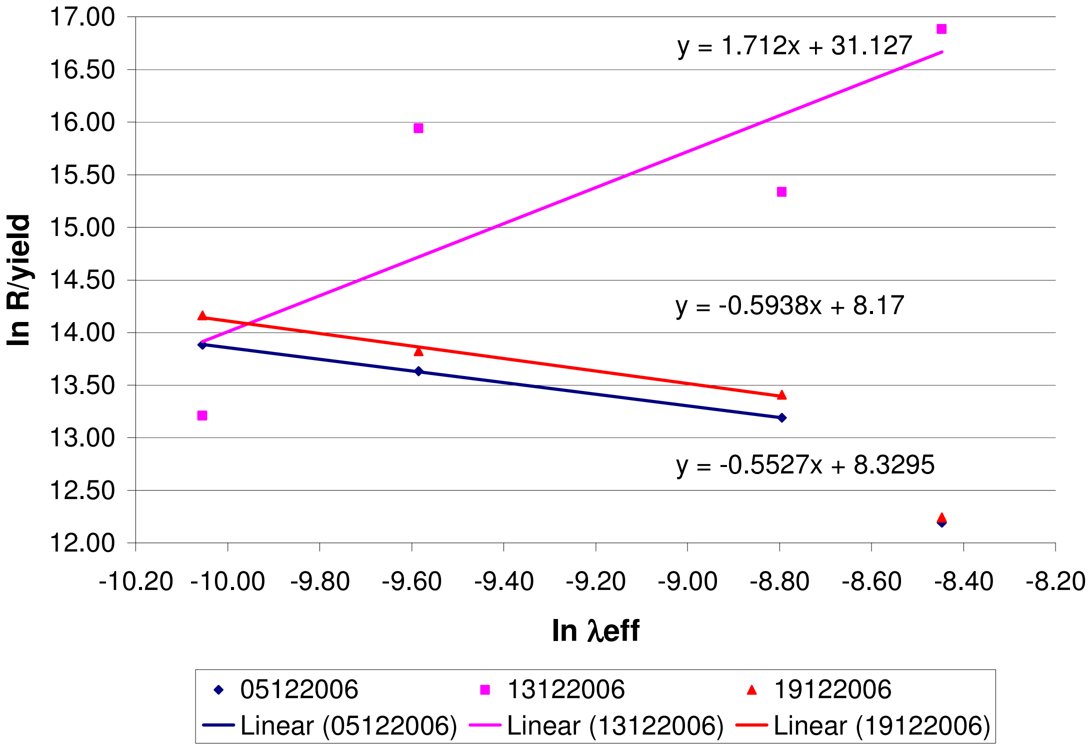

Figure 82: ln R/yield vs. ln λ_{eff} plots for gas release measurements of AVR pebbles 06-10

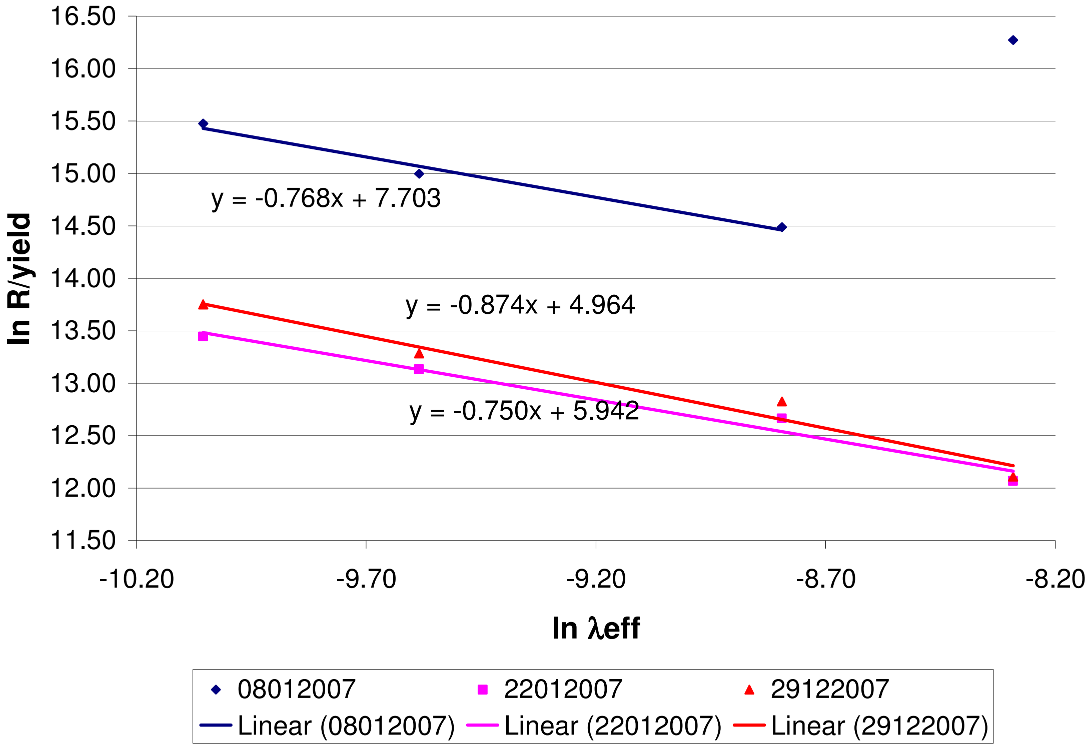

Figure 83: ln R/yield vs. ln λ_{eff} plots for gas release measurements of INET pebbles 07-01

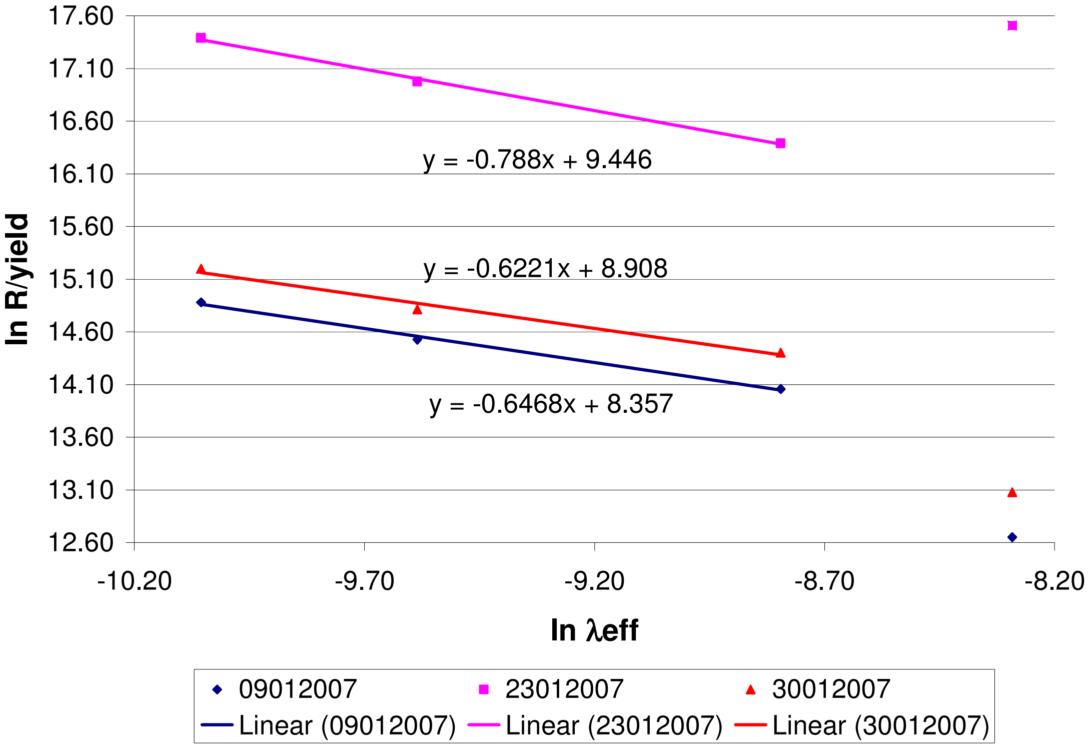

Figure 84: ln R/yield vs. ln λ_{eff} plots for gas release measurements of AVR pebbles 07-01

8.2 R/yield graph interpretation:

Concerning the INET pebbles, there is an acceptable fit between the Xe-135 measurement and the linear regression for Krypton isotopes. We can notice two exceptions: Measurement of 04/12/2006 and 08/01/2007 performed with the contaminated grab sample. Here, the measurements of Xe-135 are much higher than the expected position on the linear regression.

Concerning AVR pebbles, Xe-135 measurements cannot be fitted to the linear regression from the Krypton isotopes. In most cases, measurements are significantly lower than the expected position on the linear regression. Here again, we can notice three exceptions: Measurement of 21/11/2006, 13/12/2006 and 23/01/2007 where measurements of Xe-135 are much higher than the expected position on the linear regression. These were also performed with the contaminated grab sample.

To fit on the Kr linear regression, release over yield value for Xe-135 in the AVR case needs to be increased. This stresses that AVR pebbles retains better Xe-135 isotopes than INET ones.

8.3 NaI and Gamma spectrometry correlation

The Sweep Loop Facility was designed to perform online gas measurements. Therefore all first containment lines were foreseen with NaI scintillation detectors. These detectors were configured on the 196 keV peak of Kr-88 with the minimum bandwidth of 20 keV.

Figure 85 and Figure 86 display activity measurements performed with NaI and gamma spectrometry. Both figures underline the difficult correlation between both processes.

This can be partly explained by two phenomena:

- The values measured by the NaI detectors are still rather low. The detectors are placed in the HFR basement and were influenced by background noise. This is why the lead shielding of the instruments was improved.
- The selected peak being below 440 keV, NaI are sensitive to Ne-23 [7]. This could be evidenced by activity measurements of He/Ne mixtures from the 2nd containment which is irradiated but not in contact with the fuel. Increasing the total flow while keeping the mixture proportion led to an activity increase on the concerned NaI.

Figure 87 and Figure 88 evidence the latter phenomenon, leading to the conclusion that NaI detectors in the current configuration are of little use for gas release measurements.

This situation will be corrected for the next cycles by the following measures:

- test of multi-channel analysis with NaI detectors
- test of multi-channel analysis with HP Ge detectors

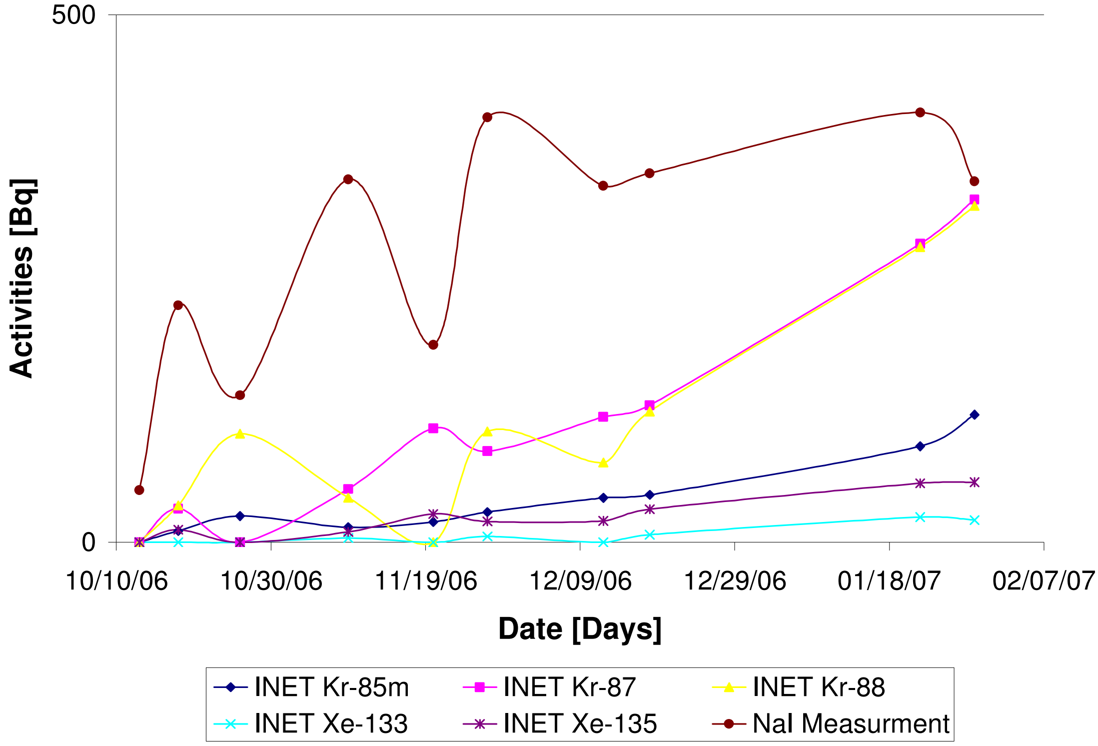

Figure 85: NaI and Gamma spectrometer measurements correlation for INET pebbles

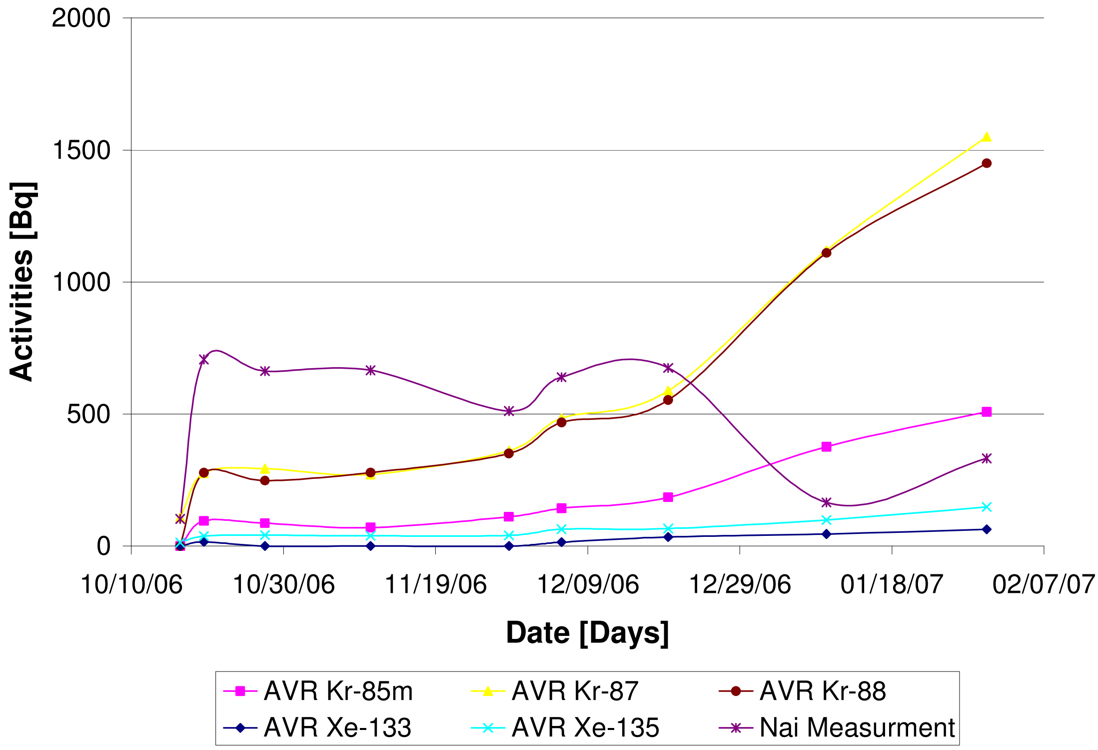

Figure 86: NaI and Gamma spectrometer measurements correlation for AVR pebbles

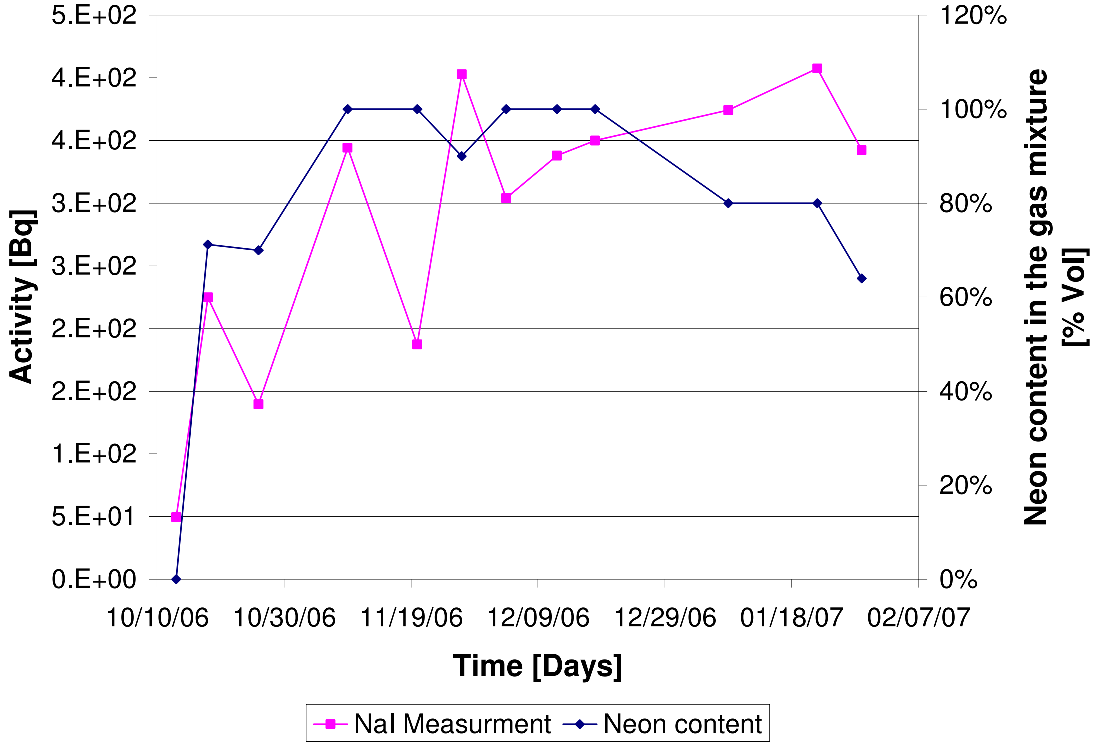

Figure 87: Correlation of NaI and Neon content in gas mixture for INET pebbles

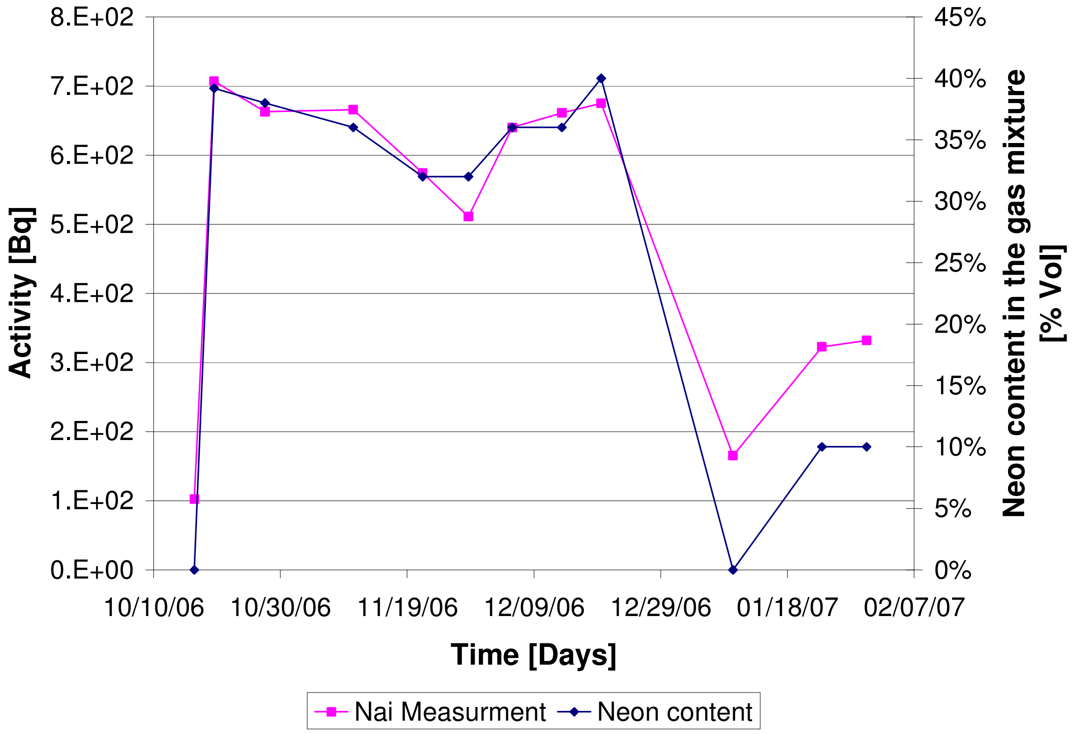

Figure 88: Correlation of NaI and Neon content in gas mixture for AVR pebbles

9 References

[1] J.A. Hendriks, Post Cycle Report, Cycle 200608, NRG technical report. 25138/07.77897/I, 09 February 2007

[2] J.A. Hendriks, Post Cycle Report, Cycle 200609, NRG technical report. 25138/07.77898/I, 09 February 2007

[3] J.A. Hendriks, Post Cycle Report, Cycle 200610, NRG technical report. 25138/07.81353/I, 09 February 2007

[4] J.A. Hendriks, Post Cycle Report, Cycle 200701, NRG technical report. 25138/07.81354/I, 14 February 2007

[5] M. A. Fütterer, HFR-EU1bis: Irradiation Progress Report, Cycles 05-03, 05-04, 05-06, 05-07, rev. B, Technical Memorandum HFR/05/4812, D(05)19257, 1 November 2005.

[6] A. Marmier, HFR-EU1bis irradiation: Refined Monte-Carlo Neutronics Calculations, Technical Memorandum, HFR / 04 / 4786, 08th of April 2005.

[7] E-Mail from Gerard Ducros 068492 CEA from 7 April 2006.

10 List of Tables

11 List of Figures